CoreConferences 2018

Batch A

By
Core Conferences LLC

Architecture and Civil Engineering

Business, Finance and Economics

Climate Change Adaptation and Multidisciplinary Issues

Cyber Security and Connected Technologies

Education, Transportation and Disaster Management

Flood Risk Management and Water Pollution

Language Teaching and Religious Studies

Universities and Women's Studies

08 – 09, March 2018
Holiday Inn Golden Mile, Hong Kong

Editor-in-Chief
Dr. A Senthilkumar

Editors:

Daniel James

Published by

Association of Scientists, Developers and Faculties
Address: RMZ Millennia Business Park, Campus 4B, Phase II, 6th Floor, No. 143, Dr. MGR Salai, Kandanchavady, Perungudi, Chennai – 600 096, India.
Email: admin@asdf.org.in || www.asdf.org.in

CoreConferences 2018

Batch A

Editor-in-Chief: **Dr. A Senthilkumar**
Editors: **Daniel James**

Disclaimer:

No responsibility is assumed by the CoreConferences 2018 Organizers/Publisher for any injury and/ or damage to persons or property as a matter of products liability, negligence or otherwise, or from any use or operation of any methods, products or ideas contained in the material herein. Contents, used in the papers and how it is submitted and approved by the contributors after changes in the formatting. Whilst every attempt made to ensure that all aspects of the paper are uniform in style, the CoreConferences 2018 Organizers, Publisher or the Editor(s) will not be responsible whatsoever for the accuracy, correctness or representation of any statements or documents presented in the papers.

ISBN-13: 978-81-933584-5-0
ISBN-10: 81-933584-5-7

PREFACE

The CoreConferences 2018 held on 08th – 09th March, 2018, in collaboration with Association of Scientists, Developers and Faculties (ASDF), an International body, at Holiday Inn Golden Mile, Hong Kong.

CoreConferences 2018 provides a chance for Academic and Industry professionals to discuss the recent progress in the area of Multiple. The outcome of the conference will trigger for the further related research and future technological improvement. This conference highlights the novel concepts and improvements related to the research and technology.

The technical committee consists of experts in the various course subfields helped to scrutinize the technical papers in various fields, support to maintain the quality level of the proceedings of conference which consist of the information of various advancements in the field of research and development globally and would act as a primary resource of researchers to gain knowledge in their relevant fields.

The constant support and encouragement from Dr. S. Prithiv Rajan, ASDF Global President, Dr. Julie Rue Bishop, ASDF International President and Dr. K. Kokula Krishna Hari, ASDF International General Secretary helped a lot to conduct the conference and to publish the proceedings within a short span. I would like to express my deep appreciation and heartfelt thanks to the ASDF team members. Without them, the proceedings could not have been completed in a successful manner. I would like to express my sincere thanks to our management, student friends and colleagues for their involvement, interest, enthusiasm to bring this proceeding of the conference in a successful way.

Dr. A Senthilkumar,

Editor in Chief,

Google Inc., Australia

Organizing Committee

Conference Super Chair

Dr A Senthilkumar, Google Inc., Australia

Conference Co-Chair

Dr Julie Rue Bishop, Australia Research Council

TECHNICAL REVIEWERS

- Sunil Chowdhary, Amity University, Noida, India
- Nasrul Humaimi Mahmood, Universiti Teknologi Malaysia, Malaysia
- P Tamizhselvan, Bharathiyar University, India
- Md Nur Alam, Pabna university of Science & Technology, Bangladesh
- N Suthanthira Vanitha, Knowledge Institute of Technology, India
- Krishnan J, Annamalai University, Chidambaram, India
- T Subbulakshmi, VIT University, Chennai, India
- O L Shanmugasundaram, K S R College of Engineering, Thiruchengode, India
- Moniruzzaman Bhuiyan, University of Northumbria, United Kingdom
- Abdelnaser Omran, Universiti Utara Malaysia, Malaysia
- Hareesh N Ramanathan, Toc H Institute of Science and Technology, India
- R Ragupathy, Annamalai University, Chidambaram, India
- Nida Iqbal, Universiti Teknologi Malaysia, Malaysia
- G Ganesan, Adikavi Nannaya University, India
- Vignesh Ramakkrishnon, Association of Scientists, Developers and Faculties, India
- S Shahil Kirupavathy, Velammal Engineering College, Chennai, India
- Rajesh Deshmukh, Shri Shankaracharya Institute of Professional Management and Technology, Raipur
- Zahurin Samad, Universiti Sains Malaysia, Malaysia
- S Ramesh, KCG College of Technology, India
- R Suguna, SKR Engineering College, Chennai, India
- S Selvaperumal, Syed Ammal Engineering College, Ramanathapuram, India
- Sarina Sulaiman, Universiti Teknologi Malaysia, Malaysia

- Tom Kolan, IBM Research, Israel
- T V P Sundararajan, Bannari Amman Institute of Technology, Sathyamangalam, India
- Arumugam Raman, Universiti Utara Malaysia, Malaysia
- Anirban Mitra, VITAM Berhampur, Odisha, India
- Hardeep Singh Saini, Indo Global College of Engineering, Mohali, Punjab
- Md Haider Ali Biswas, Khulna University, Khulna, Bangladesh
- Mohan Awasthy, Chhattisgarh Swami Vivekanand Technical University, Bhilai, Chhattisgarh
- R Nallusamy, Principal, Nandha college of Technology, Erode, India
- Mohd Helmy Abd Wahab, Universiti Tun Hussein Onn, Malaysia
- A Kavitha, Chettinad College of Engineering & Technology, Karur, India
- A Ayyasamy, Annamalai University, Chidambaram, India
- Mohamed Najeh Lakhoua, ENICarthage, Tunisia
- M K Kavitha Devi, Thiagarajar College of Engineering, Madurai, Tamil Nadu
- Somasundaram Sankaralingam, Coimbatore Institute of Technology, India
- Muhammad Iqbal Ahmad, Universiti Malaysia Kelantan, Malaysia
- Asha Ambhaikar, Rungta College of Engineering & Technology, Bhilai, India
- Pethuru Raj, IBM Research, India
- N Rajesh Jesudoss Hynes, Mepco Schlenk Engineering College, Sivakasi, Tamilnadu, India
- Hari Mohan Pandey, Amity University, Noida, India
- Nor Muzlifah Mahyuddin, Universiti Sains Malaysia, Malaysia
- Sheikh Abdul Rezan, Universiti Sains Malaysia, Malaysia
- Jia Uddin, BRAC University, Bangladesh
- Abdelbasset Brahim, University of Granada, Spain
- R Ashokan, Kongunadu College of Engineering and Technology, India
- Uvaraja V C, Bannari Amman Institute of Technology, Sathyamangalam, India
- E Bhaskaran, Government of Tamilnadu, Chennai, India
- Badruddin A. Rahman, Universiti Utara Malaysia, Malaysia
- Chitra Krishnan, VIT University, Chennai, India
- Sundar Ganesh C S, PSG College of Technology, Coimbatore, India
- S Balamuralitharan, SRM University, Chennai, India

- Balasubramanie Palanisamy, Professor & Head, Kongu Engineering College, India
- Ang Miin Huey, Universiti Sains Malaysia, Malaysia
- G Subbaraju, Shri Vishnu Engineering College for Women, India
- Yu-N Cheah, Universiti Sains Malaysia, Malaysia
- S R Kumbhar, Rajarambapu Institute of Technology, India
- Sunita Daniel, Amity University, Haryana
- P Kumar, K S R College of Engineering, Thiruchengode, India
- Shankar S, Kongu Engineering College, Perundurai, India
- V Mohanasundaram, Vivekanandha Institute of Engineering and Technology for Women, India
- Deepali Sawai, Director - MCA, University of Pune (Savitribai Phule Pune University), India
- S Vengataasalam, Kongu Engineering College, Perundurai, India
- Laila Khedher, University of Granada, Spain
- S Jaganathan, Dr. N. G. P. Institute of Technology, Coimbatore, India
- V Sathish, Bannari Amman Institute of Technology, Sathyamangalam, India
- S Nithyanandam, PRIST University, India
- B Paramasivan, National College of Engineering, Tirunelveli, India
- M Shanmugapriya, SSN College of Engineering, Chennai, India
- Syed Sahal Nazli Alhady, Universiti Sains Malaysia, Malaysia
- K Parmasivam, K S R College of Engineering, Thiruchengode, India
- V Akila, Pondicherry Engineering College, Pondicherry, India
- Mohd Hashim Siti Z, Universiti Teknologi Malaysia, Malaysia
- Zainuddin Bin Zakaria, Universiti Teknologi MARA, Dungun Campus, Terengganu
- Mansoor Zoveidavianpoor, Universiti Teknologi Malaysia, Malaysia
- Guobiao Yang, Tongji University, China
- Abhishek Bajpai, SRM University, Lucknow, India
- N Malmurugan, Mahendra Group of Institutions, India
- K Latha, Anna University, Chennai, India
- Uma N Dulhare, Muffkham Jah College of Engineering & Technology, Hyderabad, India
- M Karthikeyan, Knowledge Institute of Technology, India
- Razauden Mohamed Zulkifli, Universiti Teknologi Malaysia, Malaysia

- Chokri Ben Amar, University of Sfax, Tunisia
- V E Nethaji Mariappan, Sathyabama University, India
- Arniza Ghazali, Universiti Sains Malaysia, Malaysia
- Veera Jyothi Badnal, Osmania University, India
- Hidayani Binti Jaafar, Universiti Malaysia Kelantan, Malaysia
- Pasupuleti Visweswara Rao, Universiti Malaysia Kelantan, Malaysia
- Hanumantha Reddy T, RYM Engneering College, Bellary, India
- M Thangamani, Kongu Engineering College, India
- Marinah Binti Othman, Universiti Sains Islam Malaysia, Malaysia
- M Suresh, Kongu Engineering College, Perundurai, India
- N Meenakshi Sundaram, PSG College of Technology, Coimbatore, India
- P Raviraj, Kalaignar Karunanidhi Institute of Technology, Coimbatore, India
- R Sudhakar, Dr. Mahalingam College of Engineering and Technology, India
- K Suriyan, Bharathiyar University, India
- Mohamed Moussaoui, ENSA of Tangier Abdelmalek Essaadi University, Morrocco
- C Poongodi, Bannari Amman Institute of Technology, Sathyamangalam, India
- Reza Gharoie Ahangar, University of North Texas, USA
- Itebeddine GHORBEL, INSERM, France
- M G Sumithra, Bannari Amman Institute of Technology, Sathyamangalam, India
- L Ashok Kumar, PSG College of Technology, Coimbatore, India
- S Anand, V V College of Engineering, Tirunelveli, India
- T K P Rajagopal, Kathir College of Engineering, Coimbatore, India
- Suganthi Appalasamy, Universiti Malaysia Kelantan, Malaysia
- Rathika P, V V College of Engineering, Tirunelveli, India
- S Geetha, VIT University, Chennai, India
- D Sheela, Tagore Engineering College, Chennai, India
- Fadhilah Mat Yamin, Universiti Utara Malaysia, Malaysia
- K Nirmalkumar, Kongu Engineering College, Perundurai, India
- Mohammed Ali Hussain, KL University, India
- S Balamurugan, Kalaignar Karunanidhi Institute of Technology, Coimbatore, India
- Mohd Murtadha Mohamad, Universiti Teknologi Malaysia, Malaysia
- A Kumaravel, KSR College of Technology, India

- Roesnita Ismail, USIM: Universiti Sains Islam Malaysia, Malaysia
- Vikrant Bhateja, Shri Ramswaroop Memorial Group of Professional Colleges (SRMGPC), India
- P Thamilarasu, Paavai Engineering College, Namakkal, India
- Vijayalakshmi V, Pondicherry Engineering College, Pondicherry, India
- S Senthilkumar, Sri Shakthi Institute of Engineering and Technology, Coimbatore, India
- Nithya Kalyani S, K S R College of Engineering, Thiruchengode, India
- P Shunmuga Perumal, Anna University, Chennai, India
- Sathish Kumar Nagarajan, Sri Ramakrishna Engineering College, Coimbatore, India
- S Natarajan, Karpagam College of Engineering, Coimbatore, India
- M Ayaz Ahmad, University of Tabuk, Saudi Arabia
- C Vivekanandan, SNS College of Engineering, Coimbatore, India
- D Gracia Nirmala Rani, Thiagarajar College of Engineering, Madurai, Tamil Nadu
- Zamira Zamzuri, Universiti Kebangsaan Malaysia, Malaysia
- S Albert Alexander, Kongu Engineering College, Perundurai, India
- K P Kannan, Bannari Amman Institute of Technology, Sathyamangalam, India
- Alphin M S, SSN College of Engineering, Chennai, India
- Veeraswamy Ammisetty, St. Ann's College of Engineering & Technology, India
- K Thiruppathi, Valliammai Engineering College, India
- Helena Karsten, Abo Akademi University, Finland
- Mohamed Saber Mohamed Gad, National Research Center, Egypt
- Subramaniam Ganesan, Oakland University, Rochester, United States of America
- S Ramesh, Vel Tech High Tech Dr.Rangarajan Dr.Sakunthala Engineering College, India
- S Appavu @ Balamurugan, K. L. N. College of Information Technology, Madurai, India
- S Balaji, Jain University, India
- Selvakumar Manickam, Universiti Sains Malaysia, Malaysia
- Khairul Anuar Mohammad Shah, Universiti Sains Malaysia, Malaysia
- Geetha G, Jerusalem College of Engineering, Chennai, India
- Konguvel Elango, Dhanalakshmi Srinivasan College of Engineering, Coimbatore
- Yudi Fernando, Universiti Sains Malaysia, Malaysia
- Brahim Abdelbasset, University of Granada, Spain
- Sangeetha R G, VIT University, Chennai, India

- Balachandran Ruthramurthy, Multimedia University, Malaysia
- K R Ananth, Velalar College of Engineering and Technology, India
- Wan Hussain Wan Ishak, Universiti Utara Malaysia, Malaysia
- M Venkatachalam, RVS Technical Campus - Coimbatore, India
- Malathi R, Annamalai University, Chidambaram, India
- K Vijayaraja, KCG College of Technology, Chennai, India
- S Selvi, Institute of Road and Transport Technology, India
- Abdul Nawfar Bin Sadagatullah, Universiti Sains Malaysia, Malaysia
- John Augustine P, Sri Eshwar College of Engineering, Coimbatore, India
- Lakshmanan Thangavelu, SA College of Engineering, Chennai, India
- M Marikkannan, Institute of Road and Transport Technology, India
- S Poorani, Karpagam University, Coimbatore, India
- Yaty Sulaiman, Universiti Utara Malaysia, Malaysia
- A S N Chakravarthy, JNTU Kakinada, India
- P Sivakumar, K S R College of Engineering, Thiruchengode, India
- Samuel Charles, Dhanalakshmi Srinivasan College of Engineering, Coimbatore, India
- Jebaraj S, Universiti Teknologi PETRONAS, Malaysia
- David Rathnaraj Jebamani, Sri Ramakrishna Engineering College, India
- Kokula Krishna Hari Kunasekaran, Chief Scientist, Techno Forum Research and Development Center, India
- K Senthilkumar, Erode Sengunthar Engineering College, Erode, India
- Sergei Gorlatch, University of Muenster, Germany
- N Karthikeyan, SNS College of Engineering, Coimbatore, India
- Abdul Aziz Hussin, Universiti Sains Malaysia, Malaysia
- Manvender Kaur Chahal, Universiti Utara Malaysia, Malaysia
- Muhammad Javed, Cornell University, United States of America
- Venkatesh MP, Annamalai University, Chidambaram, India
- Djilali IDOUGHI, University of Bejaia, Algeria
- Geetha V, Pondicherry Engineering College, Pondicherry, India
- P Ganesh Kumar, K. L. N. College of Information Technology, Madurai, India
- R Muthukumar, Shree Venkateshwara Hi-Tech Engineering College, India
- Qais Faryadi, USIM: Universiti Sains Islam Malaysia, Malaysia

- K Thamizhmaran, Annamalai University, Chidambaram, India
- Ashish Chaurasia, RGPV, Bhopal, Madhya Pradesh
- Sanjeevikumar Padmanaban, Ohm Technologies, India
- Asrulnizam Bin Abd Manaf, Universiti Sains Malaysia, Malaysia
- Ahmed Salem, Old Dominion University, United States of America
- Mukesh Negi, TechMahindra Ltd, India
- A Amsavalli, Paavai Engineering College, Namakkal, India
- Mohd Zulkifli Bin Mohd Yunus, Universiti Teknologi Malaysia, Malaysia
- Shamshuritawati Sharif, Universiti Utara Malaysia, Malaysia
- Radzi Ismail, Universiti Sains Malaysia, Malaysia
- Smriti Agrawal, Chiatanya Bharathi Institute of Technology, Hyderabad
- Kamal Imran Mohd Sharif, Universiti Utara Malaysia, Malaysia
- Roselina Binti Sallehuddin, Universiti Teknologi Malaysia, Malaysia
- Zul Ariff Abdul Latiff, Universiti Malaysia Kelantan, Malaysia
- S Karthik, SNS College of Technology, India
- Ganesan Kanagaraj, Thiagarajar College of Engineering, Madurai, Tamil Nadu
- V Vijayakumari, Sri Krishna College of Technology, Coimbatore, India
- Khurram Saleem Alimgeer, COMSATS Institute of Information Technology, Islamabad
- Mehdi Asadi, IAU (Islamic Azad University), Iran
- Mukesh D Patil, Ramrao Adik Institute of Technology, India
- R Sundareswaran, SSN College of Engineering, Chennai, India
- T Krishnakumar, Tagore Engineering College, Chennai, India
- Mohd Helmy A. Wahab, Universiti Tun Hussein Onn, Malaysia
- Sivakumar Ramakrishnan, Universiti Sains Malaysia, Malaysia
- Rohaizah Saad, Universiti Utara Malaysia, Malaysia
- Kathiravan S, National Ilan University, Taiwan
- Vaiyapuri Govindasamy, Pondicherry Engineering College, Pondicherry, India
- P Sengottuvelan, Bannari Amman Institute of Technology, Sathyamangalam, India
- Subash Chandra Bose Jeganathan, Professional Group of Institutions, India
- T Ramayah, Universiti Sains Malaysia, Malaysia
- Abhishek Shukla, U.P.T.U. Lucknow, India
- M Chandrasekaran, Government College of Engineering, Bargur, India

- J Karthikeyan, SSM Institute of Engineering and Technology, India
- Wei Ping Loh, Universiti Sains Malaysia, Malaysia
- Abhay Prabhakar Kulkarni, Director - IICMR, Pune
- Daniel James, Senior Researcher, United Kingdom
- Jinnah Sheik Mohamed M, National College of Engineering, Tirunelveli, India
- Ariffin Abdul Mutalib, Universiti Utara Malaysia, Malaysia
- N Senthilnathan, Kongu Engineering College, Perundurai, India
- Yerra Rama Mohana Rao, Dr. Pauls Engineering College, India
- Sanjay Singhal, Founder, Strategizers, India
- P Ramasamy, Sri Balaji Chockalingam Engineering College, India
- Tamilarasi Angamuthu, Kongu Engineering College, Perundurai, India
- Mohd Hanim Osman, Universiti Teknologi Malaysia, Malaysia
- G A Sathish Kumar, Sri Venkateswara College of Engineering, India
- D Deepa, Bannari Amman Institute of Technology, Sathyamangalam, India
- V Ramesh, Mahatma Gandhi Institute of Technology, Hyderabad
- Dewi Nasien, Universiti Teknologi Malaysia, Malaysia
- R Dhanasekaran, Syed Ammal Engineering College, Ramanathapuram, India
- Singaravel G, K. S. R. College of Engineering, India
- Rathinam Maheswaran, Mepco Schlenk Engineering College, Sivakasi, Tamilnadu, India
- S Prakash, Nehru Colleges, Coimbatore, India
- Aede Hatib Musta'amal, Universiti Teknologi Malaysia, Malaysia
- Ahmed Mohammed Kamaruddeen, University College of Technology Sarawak, Malaysia
- A C Shagar, Sethu Institute of Technology, India
- J Sadhik Basha, International Maritime College, Oman
- Choo Ling Suan, Universiti Utara Malaysia, Malaysia
- Mohammad Ayaz Ahmad, University of Tabuk, Saudi Arabia
- G Arunkumar, Saveetha University, Chennai, India
- Ruba Soundar K, P. S. R. Engineering College, Sivakasi, India
- Norma Binti Alias, Universiti Teknologi Malaysia, Malaysia
- V C Sathish Gandhi, University College of Engineering Nagercoil, India
- Shazida Jan Mohd Khan, Universiti Utara Malaysia, Malaysia
- Zailan Siri, University of Malaya, Malaysia

- Raghvendra Kumar, LNCT College, Jabalpur
- Seddik Hassene, ENSIT, Tunisia
- Ravindra W Gaikwad, Pravara Rural Engineering College, Loni
- Anand Nayyar, KCL Institute of Management and Technology, Punjab
- Alwardoss Velayutham Raviprakash, Pondicherry Engineering College, Pondicherry, India
- Mora Veera Madhava Rao, Osmania University, India
- S Rajkumar, University College of Engineering Ariyalur, India
- Sathishbabu S, Annamalai University, Chidambaram, India
- Aziah Daud, Universiti Sains Malaysia, Malaysia
- Saratha Sathasivam, Universiti Sains Malaysia, Malaysia
- Ali Berkol, Baskent University & Space and Defence Technologies (SDT), Turkey
- Vijayan Gurumurthy Iyer, Entrepreneurship Development Institute of India
- Kannan G R, PSNA College of Engineering and Technology, Dindigul, India
- J Baskaran, Adhiparasakthi Engineering College, Melmaruvathur, India
- Aruna Anil Deoskar, IICMR, Pune, India
- S Senthamarai Kannan, Kalasalingam University, India
- A Padma, Madurai Institute of Engineering and Technology, Madurai, India
- Yousef FARHAOUI, Moulay Ismail University, Morrocco
- Cristian-Gyozo Haba, Technical University of Iasi, Romania
- Mariem Mahfoudh, MIPS, France
- Yongan Tang, Oakland University, Rochester, United States of America
- Chandrasekaran Subramaniam, Professor & Dean, Anna University, India
- M Vimalan, Thirumalai Engineering College, Kanchipuram, India
- Mathivannan Jaganathan, Universiti Utara Malaysia, Malaysia
- Jebaraj S, Universiti Teknologi PETRONAS (UTP), Malaysia
- Anbuchezhiyan M, Valliammai Engineering College, Chennai, India
- P Dhanasekaran, Erode Sengunthar Engineering College, Erode, India
- K Mohamed Bak, Ilahia School of Science and Technology, India
- P Sudhakar, M Kumarasamy College of Engineering, Karur, India
- Doug Witten, Oakland University, Rochester, United States of America
- Dzati Athiar Ramli, Universiti Sains Malaysia, Malaysia

- Shilpa Bhalerao, Acropolis Institute of Technology and Research, Indore, India
- Ata Elahi, Southern Connecticut State University, USA
- Sri Devi Ravana, University of Malaya, Malaysia
- Kumaratharan N, Sri Venkateswara College of Engineering, India
- N Shanthi, Nandha Engineering College, Erode, India
- Julie Juliewatty Mohamed, Universiti Malaysia Kelantan, Malaysia
- A Tamilarasi, Kongu Engineering College, Perundurai, India

Table of Content

Volume	01	ISBN	978-81-933584-5-0
Month	March	Year	2018

CoreConferences 2017

International Conference on Architecture and Civil Engineering 2018

ISBN	978-81-933584-5-0		**VOL**	01
Website	www.coreconferences.com		**eMail**	mail@coreconferences.com
Received	10 – January – 2018		**Accepted**	28 - January – 2018
Article ID	CoreConferences001		**eAID**	CoreConferences.2018.001

Book Wall - Adaptive and Integrated Urban Shared Reading Space

Di Ai[1], Xin Ge[2]
[1]Architecture Design Centre, Architects & Engineers Co.,Ltd. of Southeast University, Nanjing, China
[2]Department of Architecture, Southeast University, Nanjing, China

Abstract: *The reading level of Chinese urban inhabitants is backward compared with that of the developed countries, so it is an important aspect of the cultural and ethical progress to improve the reading habits of citizens. Plenty of researches have revealed the significant relationship between human behaviour in the public space and characteristics of the built environment. As the common spatial element in Chinese cities, walls, which mostly act as urban barriers, lead to the formation of numerous negative boundaries, hinder the openness, accessibility and continuity of urban public space, and set a strong limitation on people 's activities and cognitions in the urban space. The design project, 'Book Wall', is a small-scale intervention that answers directly to the problems mentioned above. Through the redesign of existing walls, they are no longer the pure urban barriers, but available, accessible and flexible reading places in daily life with their level of permeability adapting to the changing needs and conditions. The article starts with a brief introduction including the reading conditions of Chinese urban inhabitants, the influence of urban exterior space on people's reading behavior and the spatial characteristics of Chinese cities. After that, the aim of this article that is to promote paper reading and build up shared reading space in the city is illustrated and interpreted. Then the article analysed the distribution and operational mode of 'book wall', together with its innovative tectonic design and multiple ways of utilization. 'Book wall' won the first prize of Zijin Design Competition in 2016. Shortly after that, a 1:1 scale model has been built and tested in use which showed great feasibility and potential of improving public reading.*

International Conference on Architecture and Civil Engineering 2018

ISBN	978-81-933584-5-0		**VOL**	01
Website	www.coreconferences.com		**eMail**	mail@coreconferences.com
Received	10 – January – 2018		**Accepted**	28 - January – 2018
Article ID	CoreConferences002		**eAID**	CoreConferences.2018.002

The Influence of Pore Air Pressure on Slope Stability Under Various Rainfall Patterns

Cheng Qingchao[1], Tong Fuguo[2], Wang Mengmeng[3], Liu Gang[4]

[1,2,3,4]College of Hydraulic and Environmental Engineering, China Three Gorges University, Yichang 443002, Hubei, China

Abstract: *Rainfall is the most important factor to induce landslide, of which rainfall pattern is the main influence parameter. Generally, during the analysis of slope stability under different rainfall patterns, the influence of pore water pressure in saturated zone is mostly considered, while the influence of pore air pressure in unsaturated zone is seldom analyzed from the angle of water-air coupling. Based on the theory of water-air two-phase flow, this paper calculated and simulated the variation of pore air pressure changing with the rainfall time under three typical rainfall patterns (weakened, concentrated and enhanced), and combined the slope stability analysis model of considering pore air pressure to study the influence of pore air pressure on slope stability. The results show that the influence of pore air pressure on slope stability is detrimental under the three rainfall patterns. And the response duration of the pore air pressure is the longest under the weakened rainfall pattern, the concentrated pattern is the second, and the enhanced pattern is the shortest. The influence of pore air pressure on the safety factor of slope stability is the greatest under the weakened rainfall pattern, which can easily lead to the instability of the slope. Thus, we shall take the necessary engineering measures in advance in the event of such rainfall pattern prediction.*

Keywords: Rainfall Patterns; Slope Stability; Pore Air Pressure; Rainfall Infiltration; Water-air two-Phase Flow

Introduction

Rainfall is the most important factor to induce landslide, of which rainfall pattern is the main influence parameter [1]. The variation of slope seepage field under different rainfall patterns is quite different, which will affect the change of moisture content and pore pressure in slope. The increase of pore pressure is one of the key factors leading to the instability of the slope. The pore pressure in the slope can be divided into the pore water pressure in the saturated zone and the pore air pressure in the unsaturated zone [2]. The existing numerical simulation of rainfall infiltration and the test of rainfall and landslide [3-6] show that the migration of pore air in slope has an important influence on slope stability when the slope is relatively closed. In the past, the researches on the variation of pore water pressure caused by different rainfall patterns and the influence of the pore water pressure on the slope stability had been relatively mature [7-9], what's more, it is difficult to monitor and simulate the gas phase pressure and the researches on the influence of gas pressure on slope stability is relatively few in unsaturated zone under the different rainfall patterns. Therefore, based on the theory and method of water-air two-phase flow, this paper established the model of water-air two-phase flow then calculating and simulating the distribution of pore pressure in the seepage field under three different rainfall patterns (weakened, concentrated and enhanced), and combined the shear strength theory of unsaturated soil, considered slope stability analysis model of pore air pressure to study the influence of pore air pressure on slope stability.

1 Mathematical Model of Water-Air Two-Phase Flow

1.1 Basic Control Equation

The basic control equation of water-air two-phase flow contains the liquid and air flow equations, and the coupling of water-air two-phase flow is realized through the correlation of many parameters, such as matrix suction, saturation, porosity, pore pressure and so on [10]. The slope can be regarded as a porous continuous medium composed of solid, liquid and gas phases and it conforms to the law of conservation of continuous medium. The principle of conservation of mass is applied to the calculation of seepage flow in porous media so that the basic control differential equations of water and gas can be deduced, that is,

$$\phi\frac{\partial S_{\mathrm{r}}}{\partial t}+\nabla\cdot\left[-\frac{k_{\mathrm{r}}^{\mathrm{w}}k}{\mu_{\mathrm{w}}}(\nabla p_{\mathrm{w}}+\rho_{\mathrm{w}}g)\right]-\frac{Q_{\mathrm{w}}}{\rho_{\mathrm{w}}}=0 \quad (1)$$

where S_{r} is the water saturation; ϕ is the soil porosity; k is the intrinsic permeability associated with porosity, m^2; $k_{\mathrm{r}}^{\mathrm{w}}$ is the relative water permeability; μ_{w} is the viscosity coefficient of water phase，Pa·s; p_{w} is the pore water pressure, Pa; Q_{w} is the internal source term of the liquid phase; ρ_{w} is the water density, kg / m3; g is the acceleration of gravity, N / kg.

$$-\phi\frac{\partial S_{\mathrm{r}}}{\partial t}+\nabla\cdot\left[-\frac{k_{\mathrm{r}}^{\mathrm{a}}k}{\mu_{\mathrm{a}}}(\nabla p_{\mathrm{a}}+\rho_{\mathrm{a}}g)\right]-\frac{Q_{\mathrm{a}}}{\rho_{\mathrm{a}}}=0 \quad (2)$$

where $k_{\mathrm{r}}^{\mathrm{a}}$ is the gas relative permeability; μ_{a} is the viscosity coefficient of gas phase, Pa·s; p_{a} is the pore air pressure, Pa; Q_{a} is the internal source term of gas phase; ρ_{a} is the gas phase density, kg/m^3.

The unbalanced force exited in the interface of water and air, caused by the unequal air pressure and water pressure is called matrix suction. The expression is:

$$p_{\mathrm{c}}\equiv p_{\mathrm{a}}-p_{\mathrm{w}} \quad (3)$$

1.2 Calculation of Equation Solving

For the above water-air two-phase flow control differential equations, there are five unknown parameters in the formula, and another three constitutive relations need to be introduced. A large number of experiments and theoretical analysis show that there is a strong correlation between soil matrix suction and saturation, that is, there is a strong correlation between the soil-water characteristic curve and saturation, it is the relative permeability curve, which can be divided into aqueous relative Permeability Coefficient Curve and Gas Relative Permeability Coefficient Curve. These three relative curves are three important constitutive relations in water-air two-phase flow [11]. In this paper, the van Genuchten model [12] (Eq. (4))was used to characterize the relationship between substrate suction and saturation, the water-saturation relationship was expressed by van Genuchten-Mualem model [13] (Eq. (5)), the air-saturation relationship was expressed by van Brooks-Corey model [14] (Eq. (6)).

$$p_{\mathrm{c}}=p_0\left[(S_{\mathrm{e}})^{-1/\lambda}-1\right]^{1-\lambda} \quad (4)$$

$$k_{\mathrm{r}}^{\mathrm{w}}=S_{\mathrm{e}}^{\;0.5}\left[1-(1-S_{\mathrm{e}}^{\;1/m})^{m}\right]^2 \quad (5)$$

$$k_{\mathrm{r}}^{\mathrm{a}}=(1-S_{\mathrm{e}})^2(1-S_{\mathrm{e}}^{\;2}) \quad (6)$$

where S_{e} is the effective water saturation, $S_{\mathrm{e}}=\left(S_{\mathrm{r}}-S_{\mathrm{rw}}\right)/\left(1-S_{\mathrm{rw}}\right)$, S_{rw} is the residual saturation; p_0、λ is the parameters related to material properties; In accordance with relevant information, this calculation is taken $p_0=1.33$， $\lambda=0.449$， $m=0.9$，

$S_{\mathrm{rw}} = 0.3$.

2 Slope Stability Calculation Considering Pore Air Pressure

2.1 Shear Strength Formula of Unsaturated Soil

For unsaturated soils, the commonly used stress state variables are the effective stress and matrix suction. The early representative single-stress state variable formula was proposed by Fredlund et al. [15] (1978).

Fredlund formula for shear strength of dual-stress state variables, which considers the shear strength of unsaturated soils composed of the effective cohesion, the net normal stress and the strength caused by the matrix suction. The net normal stress-induced strength is related to the effective internal friction angle , The intensity caused by the matrix suction is related to another angle, can be expressed as:

$$\tau_{\mathrm{f}} = c' + (\sigma - p_{\mathrm{a}})\tan\varphi' + (p_{\mathrm{a}} - p_{\mathrm{w}})\tan\varphi^{\mathrm{b}} \tag{7}$$

where τ_{f} is the shear strength; σ is the normal positive stress; c' is the effective cohesion; φ' is the effective internal friction angle; $\tan\varphi^{\mathrm{b}}$ is the shear strength increases with the substrate suction rate $(p_{\mathrm{a}} - p_{\mathrm{w}})$.

2.2 Analysis Model of Slope Stability Considering Pore Air Pressure

Rainfall infiltration of slopes and rainfall intensity are different under different rainfall patterns. When the surface of the slope is saturated, a partial sealed space is formed, and the pore air in the slope migrates with the infiltration of rainwater, resulting in the formation of pressure gradient of air to act on the slide. Due to the inhomogeneity of slope at the bottom of the landslide strip, the air pressure between the landslides cannot be neglected in accordance with the internal force of the slope. And properties of the pore air pressure and pore water pressure are the same, they can be considered in accordance with the isotropic ball pressure, and if we assumed that each soil are vertical, pore air pressure are perpendicular to the boundary direction of the soil strips, and the size of pore air pressure is equal, direction is opposite between the two soil strips, the calculated diagram of the residual thrust method considering the pore air pressure is shown in figure 1.

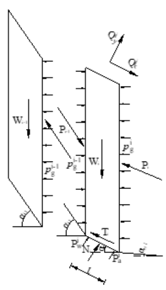

Fig 1: Residual thrust method considering the pore air pressure.

On the sliding surface, the direction of the remaining thrust is parallel to the sliding surface of the upper soil strips, and the effective normal force and tangential force meets the Fredlund shear strength criterion. For the i (i = 1, 2, ..., n) soil strip, we established a local coordinate system along the parallel and perpendicular to the direction of the bottom surface of the soil strip. According to the force balance, the thrust between the soil strips is:

$$P_i = W_i \sin\alpha_i - \left[c_i l_i + \left(W_i \cos\alpha_i - p_a^i l_i\right)\tan\varphi_i + l_i\left(p_a^i - p_w^i\right)\tan\varphi^b\right]/F_s + \left(P_{i-1} + \Delta p_i\right)\psi_i \qquad (8)$$

$$\psi_i = \left[\cos(\alpha_{i-1} - \alpha_i) - \frac{\tan\varphi_i}{F_s}\sin(\alpha_{i-1} - \alpha_i)\right]$$

where P_i is the remaining sliding force of the ith, that is, the thrust of the next soil strip; W_i is the gravity of ith soil strip; α_i is the slippery angle at the bottom of the ith soil strip; F_s is the current safety factor; p_a^i is the pore air pressure at the bottom surface of the ith soil strip; p_w^i is the pore water pressure at the bottom surface of the ith soil strip; c_i is the cohesion force at the bottom slip surface of the ith soil strip; l_i is the length of slippery surface at the bottom slip surface of the ith soil strip; φ_i is the internal friction angle at the bottom slip surface of the ith soil strip; ψ_i is the thrust transfer coefficient of the ith bar; Δp_i is the lateral air pressure gradient of the ith soil strip $\Delta p_i = p_g^{i-1} - p_g^i$; p_g^i is the air pressure between the ith soil strip.

When calculating the safety factor of slope stability, we shall first assume an initial value and then pushing downwards along the sliding strip from the first soil strip at the top of the slide body until the thrust of the last soil strip is deduced. When the safety factor is equal to zero, the safety factor is the required safety factor, otherwise we would repeat the above steps.

3 Analysis and Discussion of Engineering Case

3.1 Model and Program of Calculation and Analysis

The Tanjiahe landslide is located in Shazhenxi Town, Zigui County, Hubei Province. It is 56km away from the Three Gorges Dam with a landslide width of 400m, a vertical length of 1000m, an average thickness of 40m, an area of about 400,000 m2, a total volume of about 1600 × 104m3 and a main slip direction of 340 °[16]. The rainfall pattern was selected by the analysis of meteorological historical records. The average annual rainfall in the three gorges reservoir ranged from 996.7 to 1204.3mm. The maximum annual rainfall has reached 1752.6mm, and the maximum daily rainfall has reached 358.0mm. In order to make the typical rainfall process more representative and ensure that the total rainfall under different rainfall patterns and the maximum rainfall intensity is consistent, we have simulated the once-in-hundred-year rainfall in the three gorges reservoir: the total rainfall is 358.0mm and the maximum rainfall intensity is 40mm/h, continuing 24h, three typical rainfall patterns were shown in Figure 2. In this calculation model, the typical main sliding surface in Tanjiahe landslide is selected as the calculation section with the horizontal length of 1160m and the vertical height of 450m. Sub-grid in Tanjiahe landslide was shown in Figure 3.

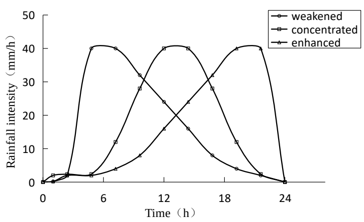

Fig.2. Three typical rainfall patterns

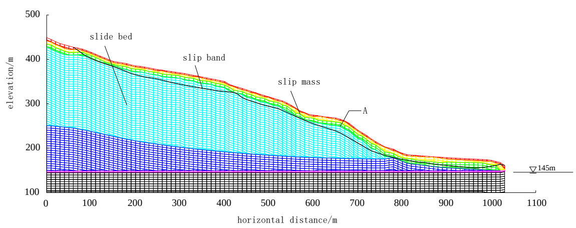

Fig.3. Sub-grid in Tanjiahe landslide

3.2 Boundary Conditions and Calculation Parameters

The boundary conditions for the calculation model are divided into the following: the lateral and bottom of the trailing edge are impervious to water; the water pressure below the water level in the leading edge of the model is the known water pressure boundary (Dirichlet boundary condition). The numerical value depends on the elevation of the water level in the reservoir (145m). When simulating rainfall infiltration process under different rainfall patterns, rainfall infiltration boundary exists above the slope in front of the model, and the rainfall infiltration boundary is the flow boundary of the known boundary element (Neumann boundary condition). In order to reduce the influence of the initial state of the slope on the analysis, the calculation is based on the initial saturated saturation of the slope to the seepage field, which is regarded as the initial condition of rainfall infiltration. When the rainfall intensity is less than the maximum infiltration rate of slope, no runoff occurs on the slope table. When the rainfall intensity is greater than the maximum infiltration rate of the slope body, the slope table produces runoff. Given that the slope head runoff is smaller than the atmospheric pressure, it can be negligible.

The main parameters involved in the calculation parameters of the landslide test data statistics, analogy and inverse calculation analysis, equation (1), (2) are $\varphi = 0.4$, $\rho_w = 1\times10^3 \mathrm{kg/m^3}$, $\rho_a = 1.29 \mathrm{kg/m^3}$, $g = 9.8 \mathrm{N/kg}$, $\mu_w = 1.0\times10^{-3} \mathrm{N\cdot s/m^2}$, $\mu_a = 1.0\times10^{-5} \mathrm{N\cdot s/m^2}$ .The main mechanical parameters are listed in table 1.

Table 1 The main mechanical parameters

layer	dry density ρ_d /g·cm^{-3}	poisson ratio μ	porosity n	saturated infiltration coefficient k_s /m·s^{-1}	The intrinsic permeability coefficient k /m^2
slip mass	1.53	0.21	0.36	1.7×10^{-5}	4.0×10^{-13}
slip bed	1.68	0.28	0.30	5.0×10^{-6}	2.0×10^{-13}

3.3 Analysis of Calculation Results

3.3.1 Water Head change of Pore Air Pressure

The maximum pore air pressure head in the weakened, concentrated and enhanced rainfall patterns was 4.40, 3.99 and 3.64m at A node, the maximum difference value is 0.76m, response duration of pore air pressure was 12.5, 10.3, 7.2 h, the maximum difference value is 5.3 h;

The weakened rainfall pattern resulted in a large amount of rainfall in the early period, thus resulting in the rapid formation of transient saturated zone on the slope. The relative permeability coefficient of the surface soil decreased to 0, and the air in the slope was hard to escape from the slope surface. In the concentrated and enhanced rainfall patterns, the air escapes from the slope before the slope expresses to the local saturation during the pre-rainfall growth, which makes the pore air pressure response duration is shorter than weakened type.

When the rainfall intensity weakened below the rainfall infiltration intensity, the slope surface changed from saturated infiltration to unsaturated infiltration, and the pore air pressure rapidly dissipated through the unsaturated seepage voids (the viscosity of the air was far less than water viscosity), the peak value of pore air pressure of slope changed after the maximum rainfall intensity, which corresponded with the actual cases.

3.3.2 Analysis of Slope Stability

The curve of the safety factor on the sliding surface under different rainfall patterns changing with time was shown Figure 5. The curve of the safety factor of slope stability considering the pore air pressure is represented by weakened Q, concentrated Q and enhanced Q respectively. The influence of pore air pressure on the safety factor of slope is the largest in the weakened rainfall patterns, followed by the concentrated and the enhanced patterns, the overall impact is the smallest. The minimum value of safety factor of slope without considering the pore air pressure in the weakened rainfall pattern is 1.25, the minimum value of the slope safety factor considering the pore air pressure reaches 1.11, which is lower than the value of safety factor reserve (F_{s0} =1.20).

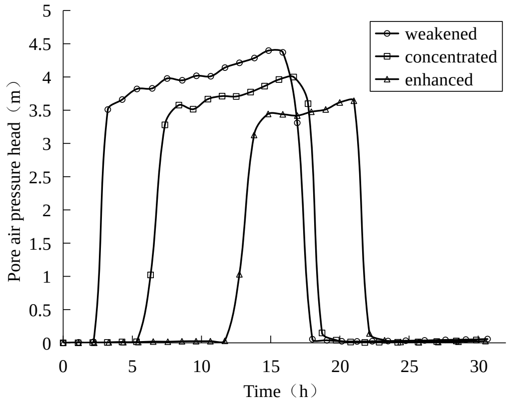

Fig.4. A node pore air pressure head

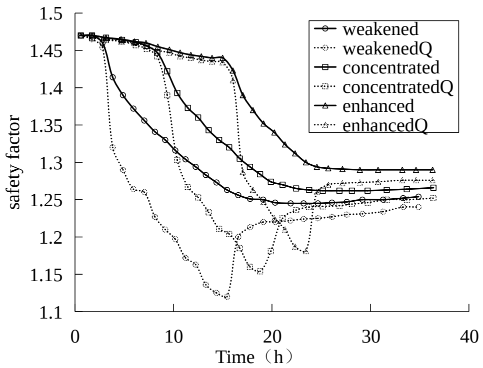

Fig.5.The curves of slope safety factor

4 Conclusion

Based on the theory and method of water-air two-phase flow method, this paper calculates the variation law of pore air pressure on the slope during rainfall infiltration and combines the shear strength theory of unsaturated soil and the slope stability analysis model considering pore air pressure. Taking landslide as an example, the influence of pore air pressure on slope stability under different rainfall patterns was simulated. The results show that: (1) The pore air pressure has an adverse influence on the slope stability under different rainfall patterns. And the influence of pore air pressure on the safety factor slope stability is the largest for the weakened rainfall pattern, followed by the concentrated and enhanced patterns. (2) The response time and the intensity of the change of the pore air pressure under the weakened rainfall patterns are the largest, followed by the concentrated and the enhanced patterns. (3) After experiencing three rainfall patterns with a total rainfall of 358mm and a duration of 24h, the stability and safety factor of the Tanjiahe landslide are all decreased. The weakened rainfall pattern was most likely to induce landslide considering the influence of pore air pressure. And if we encountered this type of rainfall pattern, the necessary engineering measures should be taken in advance (such as piling support, at the same time, embedded the vent pipe into the slope to increase the release channel of pore air, thereby reducing the influence of pore air pressure).

References

1. Rahimi A, Rahardjo H, Leong E. Effect of Antecedent Rainfall Patterns on Rainfall-Induced Slope Failure[J]. Journal of Geotechnical and Geoenvironmental Engineering, 2011,137(5):483-491.
2. Cheng Qingchao, Tong Fuguo, Liu Gang, Xue Song. Pore air pressure effect-considered analysis on slope stability[J]. Water Resources and Hydropower Engineering, 2017(07):136-143.
3. Han Tongchun，Ma Shiguo，Xu Riqing. Research on delayed effect of landslides caused by air pressure under heavy rainfall[J]. Rock and Soil Mechanics, 2013(05):1360-1366.
4. Wang Jicheng, Yu Jianlin, Gong Xiaonan, Ma Shiguo. Research on effect of closed air pressure on slope stability under intense rainfall[J]. Rock and Soil Mechanics, 2014(11):3157-3162.
5. Sun Dongmei, Zhu Yueming, Zhang Mingjin, Zeng Hongfeng. Analysis of rainfall infiltration process considering influence

of pore air pressure[J]. Rock and Soil Mechanics, 2008(09):2307-2313.

6. Liu Gang, Tong Fuguo, Xi Niannian. Impact Test of Rainfall on Clay Soil Infiltration Rate,Moisture Content and Pore Pressure under Aeration and Gas Sealing Condition[J]. Water Resources and Power, 2015(12):19-21.
7. Wu L Z, Xu Q, Zhu J D. Incorporating hydro-mechanical coupling in an analysis of the effects of rainfall patterns on unsaturated soil slope stability[J]. Arab J Geosci, 2017,10(17):1-11.
8. Qiu Zhanhong，He Chunmu，Zhu Bingjian. Investigations of water transport in valley-type MSW landfills and their stabilities subjected to various rainfall patterns[J]. Rock and Soil Mechanics, 2012(10):3151-3155.
9. S M A, J I, J L H. Influence of Rainfall Patterns on the Instability of Slopes[J]. Civil Engineering Dimension, 2013,15(2):120-128.
10. Tong F, Niemi A, Yang Z. A Numerical Model of Tracer Transport in a Non-isothermal Two-Phase Flow System for CO_2 Geological Storage Characterization[J]. Transport in Porous Media, 2013,98(1):173-192.
11. Xue Song, Tong Fuguo, Hao Shuang, Wang Jun. Effects of initial degree of saturation of soil on rainfall infiltration[J]. Advances in Science and Technology of Water Resources, 2016(04):31-35.
12. VAN GENUCHTEN M T. A closed-form equation for predicting the hydraulic conductivity of unsaturated soils[J]. Soil Science Society of America Journal, 1976,12(3):513-522.
13. Mualem Y. A new model for predicting the hydraulic conductivity of unsaturated porous media[J]. Water Resources Research, 1976,12(3):513.
14. Corey A T. The interrelation between gas and oil relative permeability[J]. Producers Monthly, 1954,19(11):38-41.
15. Fredlund D G, Morgenstern N R, Widger R A. The shear strength of unsaturated soils[J]. Canadian Geotechnical Journal, 1978,15(3):313-321.
16. Zhang Guodong，Tan Taixi，Xu Zhihua. Analysis for deformation monitoring of Tanjiahe landslide in the Three Gorges Reservoir area[J]. Journal of Natural Disasters, 2017(03):185-192.

International Conference on Architecture and Civil Engineering 2018

ISBN	978-81-933584-5-0		**VOL**	01
Website	www.coreconferences.com		**eMail**	mail@coreconferences.com
Received	12 – January – 2018		**Accepted**	25 - January – 2018
Article ID	CoreConferences003		**eAID**	CoreConferences.2018.003

Economic Excavator Configuration for Earthwork Scheduling

Hyoung-Chul Lim[1], Hong-Chul Lee[2], Dong-Eun Lee[3]
[1]Professor, School of Architectural Engineering, Changwon National University, Korea
[2]PhD Candidate, School of Architecture & Civil Engineering, Kyungpook National University, Korea
[3]Professor, School of Architecture & Civil Engineering, Kyungpook National University, Korea

Abstract- *Excavating processes performed frequently in building, civil and infrastructure projects are critical and costly. To define a cost-effective excavator configuration, an earthwork planner depends mostly on experience and intuition. This paper presents a computational system called the Economic Excavator Configuration System, which selects the most favorable configuration of a heavy-duty excavator according to the earthwork package and its job conditions. This system instructs the earthwork manager in the best-fit excavator configuration for profitable operation by considering the implicit constraints and conditions exhaustively. The system identifies the best-fit PDFs of the process completion time and that of the total profit, given an excavator configuration. A test case, which was performed at a building basement excavating project, confirmed the usability and validity of the method.*

I. Introduction

Excavating, which initiates processing entity (i.e., a rock-earth volume) in an earthwork operation, requires hydraulic heavy-duty excavators. They include front shovel, back shovel (or hoe, backhoe), loader, and specialty which need a great financial investment. A backhoe is used for digging below track level such as pits for basement. It is a boom and stick downward swing machine mounted on either crawler or pneumatic-tire with many different working attachments and engine configurations. Eco-economic performance of a hoe varies with the configuration of machine attributes given an earthwork package. The best-fit configuration of machine attributes which maximize the total profit of the excavating process can be identified by considering the work package information and other attributes involved in soil, job site, and management all together. In order to assure the most favorable cost productivity, the cash inflow and outflow items, which are subject to the transitory nature of operating conditions on a job site, should be considered.

Fuel and oil consumption take up a big portion of the cost in excavating jobs. For sure, saving fuel consumption is an important issue for reducing process completion cost and alleviating environmental burden. Identifying the most favorable machine configuration involves many different source of data, and sophisticated and repetitive computations using these sources. They include the earthwork control account information under study; excavator database of which each record maintains a maximum digging depth, a maximum dumping height, engine capacity, and a set of buckets attachable; the historical performance data of each equipment including its fuel and oil consumption amount; job site conditions; and work characteristics, etc. Indeed, it is time consuming, error prone, and expensive to collect this entire information from many different sources in time and to identify the optimal solution by manual basis depending on intuitive gut feeling. It may take easily several hours for a well experienced earthwork manager to complete the entire data compiling and decision process.

In order to increase the eco-economic performance, the values of the attributes that influence an excavator's cost productivity should be determined and analyzed in real time. Earthwork management tools can be strengthened by introducing a computational method that collects and analyses the values of the attributes that influence an excavator's internal and external system variables that influence an excavator's eco-economic performance negatively records the data into a database; computes swiftly the cycle time and the time, cost and profit performance of each excavator configuration of engine, maximum digging depth, and bucket configuration; identifies the optimal machine configuration; and handles the variability of the process completion time and that of the process completion profit with the configuration. Thus, such a method may provide a tool to control economic excavating and fuel efficiency.

II. Economic Excavator Configuration System

The system implements the stochastic time-profit tradeoff analysis into its system. The method described below was coded by using MATLAB for improving the usability of the computational method in eco-economic excavator operation practice. The method identifies the most favorable combination of maximum digging depth, engine capacity (HP), bucket size, and the timing when fuel saving mode should start. It implements an excavating operation plan which maximizes expected profit by using the optimal configuration.

2.1 Defining Work Package, Excavator, and Attachment Attributes

The system reads the earthwork package's control account information (i.e., the unit price commissioned in \$/M^3-BM(C_u), target duration in days (D_T), daily working hours (H_D), average digging depth in feet (H_A), soil type (S_T), and total volume of work in bank measure M^3 (V_T)) from a matrix W_P. The C_u, D_T, H_D, and V_T are obtained from contract documents; the H_A and the S_T are from earthwork manager. The S_T, which is associated with the bucket fill factor (f_F), is classified according to Das (2011).

$$W_p = |30 \quad 5 \quad 8 \quad 5 \quad 'Common\ earth' \quad 2{,}000| \qquad (1)$$

Given the value of soil type S_T (i.e., *Common Earth*), the value of f_F is obtained from matrix M_S shown in Eq.2 of which each column denotes soil type (S_T) and the range of bucket fill factor (i.e., [100; 110]). Then, system sets its probability density function (i.e., f_F=*uniform (100,110)*).

$$Ms = \begin{vmatrix} Bank\ clay & 100{:}110 \\ Common\ Earth & 100{:}110 \\ Rock - Earth\ mixture & 105{:}115 \\ Rock - poorly\ blasted & 85{:}100 \\ Rock - well\ blasted & 100{:}110 \\ Shale & 85{:}100 \\ Sandstone & 85{:}100 \\ Standing\ bank & 85{:}100 \end{vmatrix} \qquad (2)$$

Given the excavator name (E_N), maximum digging depth (H_M), and maximum loading height (H_{ML}), system creates a query in structured query language (SQL), queries the equipment database, and retrieves the available excavators' attributes (i.e., equipment ID (E_{ID}), engine type (E_T; 1=gasoline, 2=diesel), average hourly fuel consumptions in idle(A_F^i), low(A_F^l), medium(A_F^m), high(A_F^h), and accelerated (A_F^a) states (l/hour), hourly cost of owning(C_F), hourly cost of operating(C_V) (\$/hour), maximum digging depth(H_M), maximum loading height(H_{ML}), engine capacity(HP), and the series of buckets (B_s) attachable to each and every backhoe along with their hourly cost). For example, given that E_N, H_M, and H_{ML} are 'Backhoe', '13ft', and '14ft', respectively, the method executes the SQL statement shown in Eq.3. Then, it saves the returned dataset (i.e., E_{ID}, E_T, A_F^i, A_F^l, A_F^m, A_F^h, A_F^a, C_F, C_V, H_M, H_{ML}, and *HP*) in equipment matrix E_q and the buckets with hourly cost in matrix B_s. Each backhoe may attach a bucket from different size of buckets. For example, the buckets of CAT 320 come in various sizes, ranging from 0.72cy to 2.08cy nominal capacity. The number of backhoes available (i.e., n=*length* (E_q)) and the number of buckets attachable to a backhoe (i.e., m=*length* (B_s)) are 8 and 6, respectively. Given the easiness to load the material (E_L) by the equipment operator in the percentage value of [30:50%], which may be a lower value for easy-to-load materials (i.e., loam, sand, or gravel, etc.); a higher value for hard-to-load materials (i.e., sticky clay or blasted rock, etc.) according to Nunnally (2006), system saves the values of E_L into computer memory.

$$\begin{array}{lc} SELECT & E_{ID}, E_T, A_F^i, A_F^l, A_F^m, A_F^h, A_F^a, C_F, C_V, H_M, H_{ML}, HP \\ FROM & 'ExcavatorTable' \\ WHERE & 'E_N = Backhoe' \ \&\& \ 'H_M \geq 13m' \ \&\& \ 'H_{ML} \geq 14m' \end{array} \qquad (3)$$

2.2 Defining Job Site and Work Characteristics

The job efficiency factor involves job conditions (C_J) (i.e., the haul road, the loading floor, the surface and weather condition in the cut, the variability in the depth of cut, and truck spotting on one or both sides, topography etc.) and management conditions (C_M). The method either makes use of the job efficiency factor matrix E_F provided by Nunnally (2000) and Peurifoy et al. (2006) or the fuzzy inference system (FIS) which effectively handles the vagueness, fuzziness, and uncertainty of the input variables. Each column and row of E_F represents excellent, good, fair, and poor job conditions and management conditions, respectively.

Given the soil type (S_T) defined the value of earth volume conversion factor (f) is obtained from the matrix M_f provided by Peurifoy et al. (2006). For example, when clay in compacted measure is converted to loosen measure, the f is 1.41.

The index of maximum digging depth i and that of bucket size j are set to one (i.e., $i = 1$ *and* $j = 1$), respectively, in Step 10. After retrieving the maximum digging depth (H_M^i) of the i^{th} excavator from the equipment matrix $E_q(i,10)$, the method computes the optimum depth of cut (H_O^i), which is the depth of cut resulting in a full bucket in one pass, by multiplying H_M^i and E_L as shown in Eq.4.

$$H_O^i = E_L \times H_M^i \quad (4)$$

The vector of optimum depth of cut (H_O) is appended to the last column of E_q (i.e., E_q=[E_q H_O]) in Step 12. The swing-depth factor (f_1^i) is computed by using A_S, H_O^i, and H_A defined in previous Steps. The cycle time (C_m) is determined by average value of entire cycle time (i.e., mean (E_t (:, 8) as shown in Eq.5.

$$C_m = mean\big(E_t(:,8)\big) \quad (5)$$

The hourly production amount (P_i^j) of the i^{th} excavator (i.e., i=*1: n*) and j^{th} bucket size (i.e., j=*1:m*), which has ($n\times m$) order, is computed enumerative for all available bucket j (i.e., j==*m?*) using the general output formula shown in Eq.6 (Peurifoy 2006). The method initializes the values of C_m, A_S, and R_P are obtained from the corresponding elements of E_F. The value of C_m is the historical cycle time which was performed by the same excavator and operator in a nearby excavating pit at the same job site. Where, P_i^j is hourly production in bank measure M^3, Q_j is the j^{th} bucket capacity in loose measure M^3, f is earth volume conversion factor, f_F is bucket fill factor, f_1^i is swing-depth factor of i^{th} excavator, f_2 is efficiency factor which represent the combining effect of job and management factors, t is operating time factor, and C_m is the cycle time in seconds.

$$P_i^j = \frac{3{,}600 \times 0.76 \times Q_j \times \mathrm{f} \times f_F \times f_1^i \times f_2 \times t}{\mathrm{C_m}} \quad (6)$$

The method checks if the series of Step 11-15 are computed for each and every excavator (i.e., i=*1: n*) and buckets (j=*1:m*) available under study (i.e., i==*n?*).

2.3 Identifying the Most Favorable Excavator Configuration

The method identifies the most favorable combination of maximum depth of cut (i), bucket size (j), and engine capacity (HP) which accomplishes the maximum hourly production. It is found by returning the inverse of function P_i^j (i.e., finverse(max(P_i^j))) as shown in Eq.7. The method retrieves the engine capacity (HP) of the excavator having E_{ID}.

$$[i, j, HP] = max(P_i^j)^{-1} \quad (7)$$

2.4 Computing the Time, Cost, and Profit Performance

Given the optimal best-fit excavator configuration of the maximum digging depth (i), bucket size (j), and engine capacity (HP), the time, cost, and profit performance is computed as follows: In next step, the number of simulations (k) and the iteration counter (*iter*) are set to 120 and zero, respectively, assuming a 99% confidence level (Lee and Arditi 2006). Then, using the random variates of C_m generated by system, the hourly production amount (P) is computed by reusing Eq.7. The total job completion hours (T_T^{ij}) of the excavator having i^{th} maximum depth of cut and j^{th} bucket size is computed by dividing the total volume of work in bank measure (V_T) by the hourly production amount P_i^j as shown in Eq.8.

$$T_T^{ij} = \frac{V_T}{P_i^j} \quad (8)$$

The working hours (H_L^{ij}) remained at the last working day and the volume of work to be performed at the last working day (V_L) are computed by calculating the remainder after division by using *rem* (T_T^{ij}, H_D) and by multiplying the P_i^j and H_L^{ij} as shown in Eqs.9 and 10, respectively. The H_D is the daily working hours (i.e., 8 hours/day) defined in Step 1.

$$H_L^{ij} = rem\big(T_T^{ij}, H_D\big) \quad (9)$$

$$V_L = P_i^j \times H_L^{ij} \quad (10)$$

With the working hours (H_L^{ij}) remained at the last working day, two options are available. The one (O_T=*1*) is to reduce the total job completion days by distributing H_L^{ij} to previous working days as night-work hours. When employing night shift, the quotient is computed by dividing T_T^{ij} by H_D (i.e., D^{ij} =*fix*(T_T^{ij}/H_D)) and no fuel saving strategy is used to expedite the job completion. Noteworthy is that reducing one working day (C_I) saves its corresponding indirect cost, but a percentage (α) of surcharge (e.g., α % of the excavator's hourly operating cost C_H) incurs. The other (O_T=2) is to perform the operation for the working hours H_L^{ij} which is the reminder at the right next working day after D^{ij}. In this case, an extra cost (C_E), which is a windfall profit (or easy money) to the equipment operator, occurs as shown in Eq.11.

$$C_E = \begin{cases} (\alpha+1)\times C_H \times H_L^{ij} & if\ O_T = 1 \\ 0 & if\ O_T = 2 \end{cases} \quad (11)$$

Depending on the option selected, the total job completion cost (C_T^{ij}) of the excavator having i^{th} maximum depth of cut and j^{th} bucket size is computed either by multiplying the hourly owning and operating cost (C_H=C_F+C_V) and the rounded down value of T_T^{ij}/H_D (i.e., T_T^{ij}=$floor(T_T^{ij}/H_D)$) to the nearest integer and adding the extra cost (C_E, where O_T=1.) as shown in Eq.12 or by multiplying C_H and the rounded up value of T_T^{ij}/H_D (i.e., T_T^{ij} = ceil(T_T^{ij}/H_D)) to the nearest integer and adding the extra cost (C_E, where O_T=2.) as shown in Eq.13. Note that the value of T_T^{ij}/H_D is either rounded down or rounded up depending on whether the night shift is used or the equipment contract is based on day (not hour), respectively. The system checks which option is more favorable for maximizing the expected total profit by comparing $C_T^{ij}(1)$ and $C_T^{ij}(2)$ shown in Eqs.12 and 13, respectively.

$$C_T^{ij}(1) = floor\left(\frac{T_T^{ij}}{H_D}\right) \times \left(C_H^{ij} \times H_D + C_I\right) + C_E;\ O_T = 1 \quad (12)$$

$$C_T^{ij}(2) = ceil(T_T^{ij}/H_D) \times \left(C_H^{ij} \times H_D + C_I\right);\ \ O_T = 2 \quad (13)$$

The expected total profit (P_T^{ij}) of an excavator having i^{th} maximum depth of cut and j^{th} bucket size is computed by subtracting the total job completion cost (C_T^{ij}) from the contract amount commissioned as shown in Eq.14.

$$P_T^{ij} = C_u \times V_T - C_T^{ij} \quad (14)$$

2.5 Implementing Stochastic Time-Profit Tradeoff Analysis

The method computes the Eqs.8 to 14, for the maximum number of simulation (i.e., *iter==nSim?*) by iterating the simulation counter (i.e., *iter=iter+1*). After these iterations, the data cube of the hourly production, which maintains the values of *iter,* i, j, P_j, T_T^{ij}, C_T^{ij}, P_T^{ij}, $\tilde{\imath}$, and $\tilde{\jmath}$ in (n×m×$iter$) dimension, is generated in the stochastic mode and proceeds to Step 24. Noteworthy is that C_m is random variates generated. From this data cube, the most favorable set of maximum depth of cut ($\tilde{\imath}$) and bucket size ($\tilde{\jmath}$) that maximizes the expected total profit is identified by using the max function (i.e., max(P_T^{ij})), and the inverse of function P_T^{ij} shown in Eq.15. The method retrieves the engine capacity (HP) of the excavator having E_{ID} as well.

$$[\tilde{\imath}, \tilde{\jmath}, HP] = find(max(P_T^{ij})) \quad (15)$$

The probability to complete the job by a user-queried deadline T_U and a user-queried profit margin P_U are computed using the data cube, given an excavator of which configuration is the set of (i, j) or ($\tilde{\imath}$, $\tilde{\jmath}$). The normal distribution of T_T with mean (μ) and standard deviation (σ) is transformed to a standard normal distribution by changing variables to Z= (T_T- μ)/σ as shown in Eqs.16 and 17.

$$Pr(T_T \le T_U) = \emptyset(\frac{T_U - \mu}{\sigma}) \quad (16)$$

$$Pr(P_T \le P_U) = \emptyset(\frac{P_U - \mu}{\sigma}) \quad (17)$$

The system prompts an excavator which has the optimal configuration of maximum digging depth, bucket size, and HP with its T_T, C_T, and P_T. The stochastic mode defines the motions' times using their respective probability density functions (PDFs), computes the general output formula for a user-defined iteration, and compiles the sets of hourly productions and that of total profits. The historical data of each motion time, angle of swing, and rpm are processed to estimate their best-fit-PDFs and parameters.

III. Case Study

The earthwork of which the area, the average digging depth, the soil type, the job description, and the unit price of the job are 600m, 5ft, 'hard tough clay', 'placing the foundation of a large office building', and the owner's estimate of $1.0/bank measure M3. The hourly owning and operating costs (CH) of these backhoes are assumed to be equivalent to market rental costs even if it may not be true. They are maintained in a database. The equipment database administering hydraulic excavators having various range of bucket size (i.e., 2-10 CY) was implemented and used for a case study which was carried out for an earthwork contractor in Korea. The work package indicates the average depth of cut, the average angle of swing, job condition, management condition, the bucket fill factor, and the operating time are 3.0 ft, 120 degree, good, good, 75%, and 55 minutes/hour, respectively.

According to the contract information, the earthwork's control account parameters in matrix W_P is [1; 6; 8; 5; 'Hard tough clay'; 12,000] each of which denotes the unit price commissioned is $1/bank measure M^3; the target duration is 6 days; the working hours per day is 8; the average digging depth is 5 ft; the soil type is 'hard tough clay'; and the total volume of work is 12,000 bank measure M^3. Given the name of 'Back shovel' and the maximum digging depth of '22.1 ft', the method identifies the bucket fill factor (f_F) from matrix M_S (i.e., uniform (100, 110)) and retrieves the available excavators and their corresponding series of buckets from equipment database using Eq.3. Then, it gets the easiness to load the material of 30% which is corresponding value of the hard-to-load materials.

After computing the hourly production amounts for all excavators having different maximum digging depth, HP, and bucket size enumerative, the method, in deterministic mode, confirms that the optimal combination of maximum digging depth, HP, and bucket size are *19.4 ft, 168 HP, and 2.5*CY, respectively. In addition, the method computes that the maximum hourly production amount (P_l^j) of 310.533 bank measure m3/hr is achieved when the excavator having the optimal configuration is used. Given the maximum depth of cut of 19.4 ft and the bucket size of 2.5 CY, the total job completion hours (T_T^{ij}), the working hours (H_L^{ij}) remained at the last working day (H_L^{ij}), and the earth volume to be excavated at the last working day (V_L) were computed as 50.54 hours, 2.54 hours, and 788.75 bank measure m^3, respectively. Then, the method computes the set of the hourly production amount (P_l^j), and the expected total profit (P_T^{ij}) of each and every excavator which has many combinations of the maximum depth of cut (i), HP, and the bucket size (j), respectively. It appears that the biggest bucket out of the series is always the most favorable choice to each and every excavator.

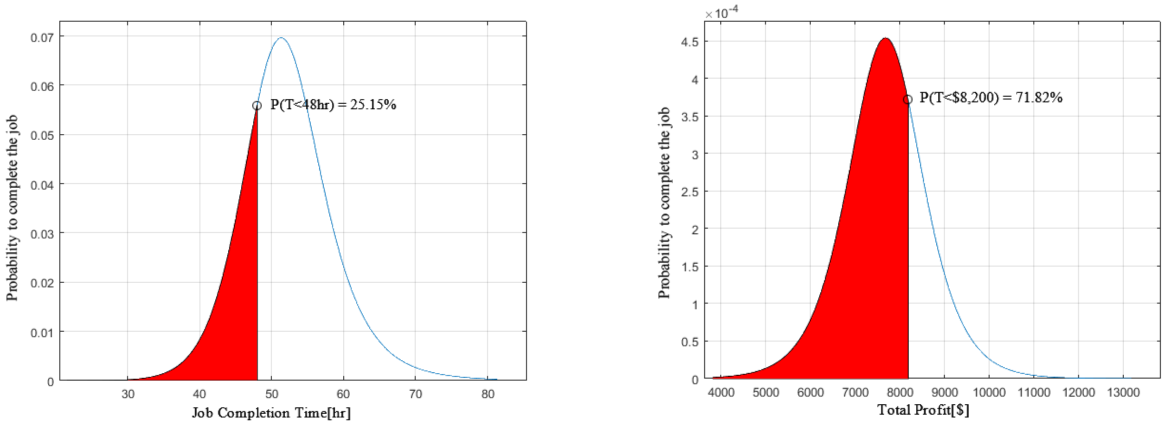

(a) (b)

Figure 1. Job Completion Time(a) and Total Profit(b)

In stochastic mode, system identifies the most favorable combination of the maximum depth of cut ($\tilde{i}$) and its corresponding bucket size ($\tilde{j}$) which results in the maximum expected total profit of $ 7,610. Finally, it computes the probability of completing the job by a user-queried deadline of 48 hours or a user-queried profit margin of $ 8,200 to 25.15% and 71.82% as shown in Figure 1, respectively. The probability distribution of the total job completion time and that of the total profit margin is negatively and positively skewed, respectively.

IV. Conclusion

This paper presents an easy-to-use computerized system that identifies the best-fit combination of the maximum digging depth, the engine size (HP), and the bucket size for eco-economic excavation, given an earthwork package, excavators' machine attributes, and operational constraints, etc. This study advances the body of knowledge relative to excavator selection, because it identifies the most favorable excavator configuration that minimizes the total excavating cost, and/or the fuel consumption before and during the excavating operation, hence, achieving the maximum total profit expeditiously. In addition, it provides the most favorable option and the right time when the fuel saving mode starts. Indeed, this tool allows collecting many input data expeditiously, implementing the deterministic and stochastic time-profit tradeoff analysis modes jointly and independently. The system allows earthwork managers to make more informed decisions with the exact global solution(s) found after searching the entire solution space enumerative and exhaustively. The comprehensive mathematical formulas relative to system contribute to expedite the excavating process by trading off the multi-objectives. It features the automatic configuration of excavator engine and its attachments and the automatic fuel saving mode initiation for smart excavating operation.

References

1. Das, B.M. (2011). Principles of Geotechnical Engineering, 7th ed. CENGAGE Learning. CT. USA.
2. Nunnally, S.W. (2000). Managing Construction Equipment. Prentice Hall, 2nd ed. Upper Saddle River, New Jersey.
3. Peurifoy, R. L., Schexnayder, C. J., and Shapira, A. (2009). Construction planning, equipment, and methods, 7th Ed., McGraw-Hill, New York.

CORE CONFERENCES

International Conference on Architecture and Civil Engineering 2018

ISBN	978-81-933584-5-0
Website	www.coreconferences.com
Received	12 – January – 2018
Article ID	CoreConferences003

VOL	01
eMail	mail@coreconferences.com
Accepted	25 - January – 2018
eAID	CoreConferences.2018.003

A Mixed Integer Linear Programming (MILP) model for Advanced Earthwork Allocation Planning

Dae-Young Kim[1], Han-Seong Gwak[2], Sang-Hun Kang[3], Dong-Eun Lee[4]

[1]Assistant Professor, Department of Architectural Engineering, Pusan National University, Korea
[2]Research Fellow, School of Architecture & Civil Engineering, Kyungpook National University, Korea
[3]Undergraduate, Department of Architectural Engineering, Pusan National University, Korea
[4]Professor, School of Architecture & Civil Engineering, Kyungpook National University, Korea

Abstract- *This paper presents a MILP model which identifies the optimal cut-fill pairs and their sequence with minimum total earthwork cost. The proposed model is of value to earthwork managers because it identifies the most favorable EAP by accounting for the rock-earth type of each and every rock-earth, the series of rock-earths occupying each and every cut and fill pits, and the moving directions (i.e., the order of cut-fill rock-earth pairs), expeditiously. A test case confirms the usability and validity of the model.*

I. Introduction

Earthwork is engineering processes to change a current ground surface into a desired surface by excavating rock-earth from cut pits and moving it to fill pits. Earthwork allocation planning (EAP) identifies the optimal cut-fill pairs and their sequence to minimize the total earthmoving cost by assigning cuts to fills economically [1,3]. Various EAP methods, which are based on either linear programing or evolutionary algorithms, have been introduced into the earthwork community to identify favorable cut-fill pairs and their sequence [4,5,6]. However, existing studies for EAP did not handle several issues discussed as follows: First, the series of rock-earth of cut pit should be excavated in top-down sequence; the series of rock-earth of fill pit should be embanked in bottom-up sequence. Second, the cut-fill pit pairs and their sequencing should be constrained by taking into account top-down sequence of cut rock-earths and bottom-up sequence fill rock-earths. Third, rock-earth type (or quality) needs to be considered to bank each fill rock-earth of fill pits. For example, a fill pit may have a subgrade, which supports the asphalt paving layer, and a road-bed. Only good quality soil (i.e., less than 100 mm particle-size) can be used to construct the subgrade. The series of cut or fill rock-earths and their soil types could be obtained from geological columnar sections of all pits. Fourth, once excavator positions into a cut pit, it is needed to dig out cut rock-earths as many as possible in order to minimize the excavator's travel distance between cut pits. Therefore, constraints about excavator movement are required to be added in the model. Fifth, when a non-conforming cut rock-earth is transported into a fill rock-earth, secondary blasting, which used to reduce the dimensions of oversized rock-earth, or disposing rock-earth should be required. It also requires additional corrective action cost or disposal cost. A justification should be confirmed by comparing if the disposal cost is smaller than the corrective action cost of the non-confirming cut rock-earth. This paper proposes a MILP model as a viable solution that considers the research gaps identified. A new MILP model which handles these issues with the least cost is presented in this paper.

II. MILP Model for Optimal EAP

2.1 Defining Earthwork Job-Site

An earthwork site is divided into pits. A pit is classified into either a cut ($i \in C$), a fill ($j \in F$), or a balanced pit according to the rock-earth volume required to achieve the planned ground level. If the amount of rock-earth needs to be moved out of the pit (i.e., cut volume: $CV(i)$), then the pit is cut pit (i). If the amount of rock-earth needs to be moved into the pit (i.e., fill volume: $FV(j)$), then the pit is fill pit (j). A cut pit (i) and a fill pit (j) are respectively sliced into a series of cut earth-block and a series of fill earth-block using user-defined earth unit size (the earth-block size). The data structure of the series of cut earth-blocks generated by slicing the i^{th} cut pit by the size is a first-in-first-out (FIFO) queue because these cut earth-blocks are excavated from their corresponding cut pit in top-down order. The data structure of the series of fill earth-blocks generated by slicing the j^{th} fill pit is a last-in-first-out (LIFO) queue because these fill earth-blocks are backfilled into their fill pit in bottom-up order. Also, a set of borrow pits (b) and disposal pits (w) are considered for the earthwork. A borrow pit (b) is an off-site source to import the scarce fill rock-earths, a disposal pit (w) is an off-site location to export the excess cut rock-earths. Each borrow pit has a maximum borrow capacity ($BC(b)$). Each disposal pit also has a maximum waste capacity ($WC(w)$).

2.2 Defining the Earthmoving Input Sets, Parameters and Variables

$X\ (i,j,t)$ is a variable that represents a cut earth-block moved from a cut pit i to a fill pit j at t^{th} earthmoving iteration. $X\ (i,w,t)$ is a variable that represents cut earth-block moved from a cut pit i to a waste pit w at t^{th} earthmoving iteration. $X\ (b,j,t)$ is a variable that represents a cut earth-block moved from a borrow pit b to a fill pit j at t^{th} earthmoving iteration. $C\ (i,j)$ is a value that represents unit earth-block moving cost from a cut pit i to a fill pit j. $c\ (i,w)$ is a value that represents unit earth-block moving cost from a cut pit i to a waste pit w. $c\ (b,j)$ is a value that represents unit earth-block moving cost from a borrow pit b to a fill pit j. This study computes the unit earth-block moving costs ($c\ (i,j)$, $c\ (b,j)$, $c\ (i,w)$) by taking into account these productivity loss factors using Gwak et al.'s [2] approach. $Ax\ (j,t)$ is used to identify if corrective action is occur in j^{th} fill pit at t^{th} earthmoving iteration. $Ac\ (j,t)$ is a value that represents corrective action cost in j^{th} fill pit at t^{th} earthmoving iteration. $Y\ (i,k,t)$ and $p\ (b,n,t)$ indicates whether the k^{th} cut rock-block of the i^{th} cut pit and the n^{th} rock-block of the b^{th} borrow pit moves at the t^{th} earthmoving iteration, respectively. $Z\ (j,k,t)$ and $q\ (w,k,t)$ denote whether the k^{th} fill rock-earth of the j^{th} fill pit and the k^{th} fill rock-earth of the w^{th} disposal pit are banked at the t^{th} earthmoving iteration, respectively.

2.3 Formulating the Objective Function and the Constraints

The MILP model with the objective function of minimizing the total earthmoving cost of rock-earth among cut pits, fill pits, disposal pits, and borrow pits and minimizing corrective action cost of nonconforming rock-earths transported into the fill pit is presented as follows:

$$\text{Minimize Z} = \sum_t \sum_i \sum_j x(i,j,t) \times c(i,j) + \sum_t \sum_i \sum_w x(i,w,t) \times c(i,w) + \sum_t \sum_b \sum_j x(b,j,t) \times c(b,j) + \sum_t \sum_j ax(j,t) \times ac(j,t)$$

Subject to:

$$\textstyle\sum_t \sum_j x(i,j,t) + \sum_t \sum_w x(i,w,t) = CV(i), \forall i \quad (1)$$
$$\textstyle\sum_t \sum_j x(i,j,t) + \sum_t \sum_b x(b,j,t) = FV(j), \forall j \quad (2)$$
$$\textstyle\sum_t \sum_j x(b,j,t) \leq BC(b), \forall b \quad (3)$$
$$\textstyle\sum_t \sum_i x(i,w,t) \leq WC(w), \forall w \quad (4)$$
$$\textstyle\sum_t \sum_j x(i,j,t) + \sum_t \sum_w x(i,w,t) + \sum_b \sum_j x(b,j,t) = 1, \forall t \quad (5)$$
$$\textstyle\sum_t y(i,n,t) = 1, \forall i, \forall n \in N(i) \quad (6)$$
$$\textstyle\sum_t p(b,n,t) = 1, \forall b, \forall n \in Q(b) \quad (7)$$
$$\textstyle\sum_t z(j,n,t) = 1, \forall j, \forall n \in M(j) \quad (8)$$
$$\textstyle\sum_t q(w,n,t) = 1, \forall w, \forall n \in R(w) \quad (9)$$
$$\textstyle\sum_t y(i,n-1,t) \times t \leq \sum_t y(i,n,t) \times t, \forall i, n = 2,3,..,N(i) \quad (10)$$
$$\textstyle\sum_t p(b,n-1,t) \times t \leq \sum_t p(b,n,t) \times t, \forall b, n = 2,3,..,Q(b) \quad (11)$$
$$\textstyle\sum_t z(j,n-1,t) \times t \leq \sum_t z(j,n,t) \times t, \forall j, n = 2,3,..,M(j) \quad (12)$$
$$\textstyle\sum_t q(w,n-1,t) \times t \leq \sum_t q(w,n,t) \times t, \forall w, n = 2,3,..,R(w) \quad (13)$$
$$\textstyle\sum_i \sum_{n \in N(i)} y(i,j,t) + \sum_b \sum_{n \in Q(b)} p(b,n,t) = 1, \forall t \quad (14)$$
$$\textstyle\sum_j \sum_{n \in M(j)} z(j,n,t) + \sum_w \sum_{n \in R(w)} q(w,n,t) = 1, \forall t \quad (15)$$
$$\textstyle\sum_j x(i,j,t) + \sum_w x(i,w,t) = \sum_{n \in N(i)} y(i,n,t), \forall t, \forall i \quad (16)$$
$$\textstyle\sum_j x(b,j,t) = \sum_{n \in Q(b)} p(b,n,t), \forall t, \forall b \quad (17)$$
$$\textstyle\sum_i x(i,j,t) + \sum_b x(b,j,t) = \sum_{n \in M(j)} z(j,n,t), \forall t, \forall j \quad (18)$$
$$\textstyle\sum_i x(i,w,t) = \sum_{n \in R(w)} p(w,n,t), \forall t, \forall w \quad (19)$$
$$ax(j,t) \leq \textstyle\sum_i x(i,j,t) + \sum_b x(b,j,t) + \frac{1}{3}\left(\sum_i \sum_{n \in N(i)} y(i,n,t) \times N(i,n) + \sum_j \sum_{n \in M(j)} z(j,n,t) \times M(j,n)\right) + \frac{1}{6}, \forall j, \forall t \quad (20)$$

$$ax(j,t) \geq \sum_i x(i,j,t) + \sum_b x(b,j,t) + \frac{1}{3}\left(\sum_i \sum_{n\in N(i)} y(i,n,t) \times N(i,n) + \sum_j \sum_{n\in M(j)} z(j,n,t) \times M(j,n)\right) - \frac{5}{6}, \forall j, \forall t \quad (21)$$

Required number of rock-earth block to achieve the planned elevation is constrained by Eqs. (1) and (2). Maximum capacity of borrow (or waste) pit is constrained by Eqs. (3) and (4). The transportation of the rock-earth block is constrained by Eqs. (5) to (9). The excavating order of cut rock-earths from a cut pit (i) and that from a borrow pit are constrained by Eqs. (10) and (11), respectively. The backfilling order of fill rock-earths to a fill pit (j) and that to a disposal pit (w) are constrained by Eqs. (12) and (13), respectively. The index of a rock-earth in a cut pit (or borrow pit) and that in a fill pit (or disposal pit) are constrained by Eqs. (14) to (19). Moving a rock-earth which is nonconforming to a fill rock-earth is prohibited by the constraints shown in Eqs. (20) to (21).

III. Case Study

The earthmoving project shown in Fig. 1 was reproduced from existing studies (i.e., [6]) to verify the usability of the OPS method in the context of a land clearing earthwork. The earthwork consists of rough grading on a small office building site. The land size, earthwork volume, grid (or pit) spacing, and total number of grids (pits) are 90 m× 105 m, 43,770 m3, 15 m× 15 m, and 42 pits (=6× 7), respectively. The volume of a rock-earth block is set to 450 m3 (=length (15 m) × width (15 m) × depth (2 m)). The cut and/or fill volume of each pit required to accomplish the planned ground level are computed as shown in Table 1 using the current and planned elevations, which are denoted by dotted and solid lines, respectively.

A total of 96 rock-earth blocks are moved from cut pits to their corresponding fill pits. The optimal rock-earth types and the number of rock-earth blocks to move from a cut pit to its corresponding fill pit and the most economical cut-fill rock-earth block pairs satisfying the quality requirements of their fill pits are computed. However, the results are not presented due to lack of space. The total earthmoving cost is $11,111.02. The corrective action cost incurred by nonconforming rock-earths is $0 because those rock-earth blocks which do not conform to the fill rock-earth blocks are moved to their corresponding fill pits.

To minimize the earthmoving cost, the cut rock-earths in cut pits should be moved to the fill rock-earths of the nearest fill pits (i.e., 2, 5, 9, 12, 17, 24, 27, 32, 34, 39, and 42.). The optimal cut-fill pairs are denoted by the dash red lines; the excavator's repositioning sequences are [3 →10 →11 →18 →19 → 11→ 25→ 26→ 33 →40 →41] as denoted by the straight blue lines in Fig. 2.

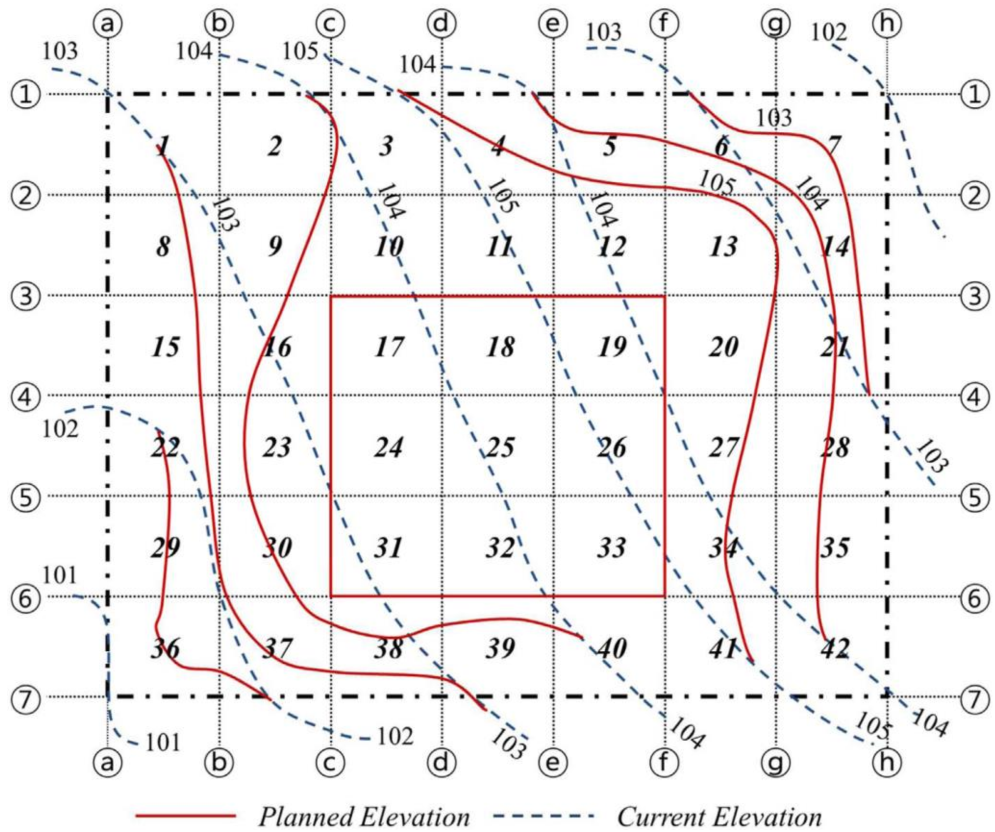

Figure 1. Earthwork job site grid plan

Table 1. Cut and fill worksheet

Pit ID	Cut amount(m^3)			Fill amount(m^3)			Pit ID	Cut amount(m^3)			Fill amount(m^3)		
	n_i=0	n_i=1	CV_i	m_j=0	m_j=1	FV_j		n_i=0	n_i=1	CV_i	m_j=0	m_j=1	FV_j
1	0	0	0	0	0	0	22	0	0	0	450	550	1,000
2	0	0	0	0	188	188	23	0	0	0	1,350	463	1,813
3	0	166	166	0	0	0	24	0	0	0	350	900	1,250
4	0	0	0	0	0	0	25	0	546	546	0	0	0
5	0	0	0	450	800	1,250	26	525	600	1,125	0	0	0
6	0	0	0	900	850	1,750	27	0	0	0	500	706	1,206
7	0	0	0	450	488	938	28	0	0	0	536	1000	1,563
8	0	0	0	313	0	313	29	0	0	0	688	500	1,188
9	0	0	0	450	300	750	30	0	0	0	2,000	500	2,500
10	157	0	157	0	0	0	31	0	0	0	1,500	375	1,875
11	0	597	597	0	0	0	32	0	0	0	206	0	206
12	0	0	0	417	450	867	33	800	388	1,188	0	0	0
13	0	0	0	2,250	875	3,125	34	0	0	0	0	48	48
14	0	0	0	900	1,163	2,063	35	0	0	0	0	875	875
15	0	0	0	0	750	750	36	0	0	0	0	625	625
16	0	0	0	738	450	1,188	37	0	0	0	900	413	1,313
17	0	0	0	0	170	170	38	0	0	0	613	450	1,063
18	0	787	787	0	0	0	39	0	0	0	209	0	209
19	0	773	773	0	0	0	40	0	563	563	0	0	0
20	0	0	0	1,350	1,025	2,375	41	0	128	128	0	0	0
21	0	0	0	2,125	0	2,125	42	0	0	0	0	313	313

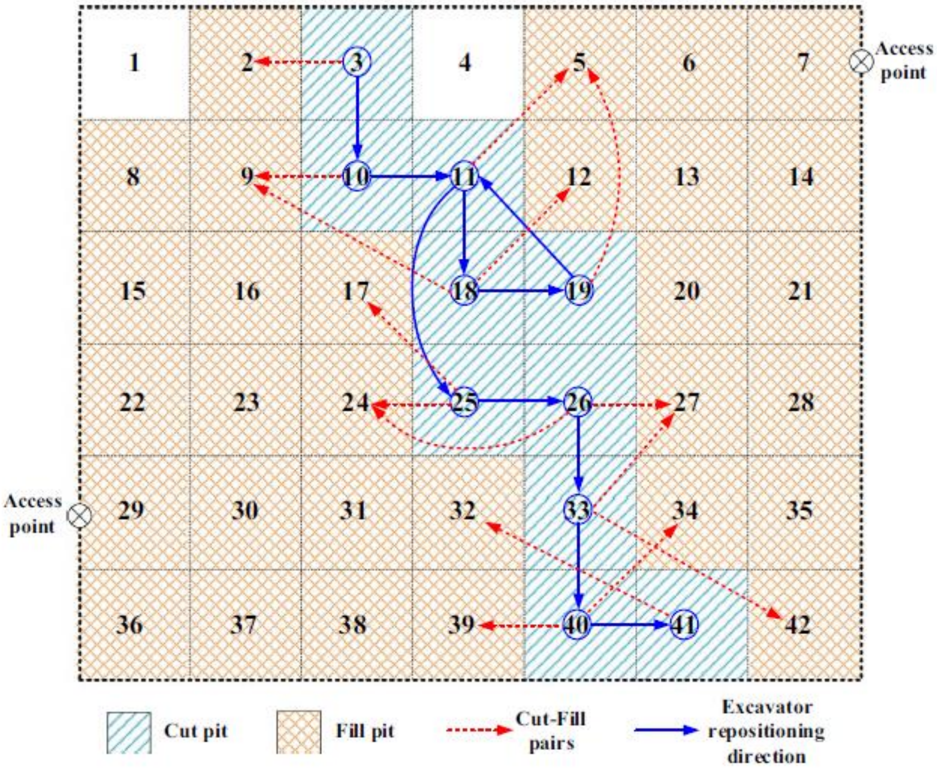

Figure 2. Graphical representation of the solution.

IV. Conclusion

This paper presents a MILP model that determines the optimal sets of cut-fill pairs and their sequence for EAP by taking into account the operational constraints. It minimizes (1) the total cost of moving the rock-earth blocks among the cut, fill, disposal, and borrow pits, (2) the additional expenses for correcting nonconforming rock-earth blocks, and (3) the excavators' repositioning cost. With the mathematical formula, an earthwork project manager may perform earthwork allocation planning by identifying the optimal cut-fill pairs and their sequence before and during the earthwork operation.

References

1. Cang Liu and Ming Lu. "Optimizing earthmoving job planning based on evaluation of temporary haul road networks design for mass earthworks projects", Journal of Construction Engineering and Management, 141(3), 04014082, 2014.
2. Han-Seong Gwak and Chang-Yong Yi, Dong-Eun. Lee. "Stochastic optimal haul-route searching method based on genetic algorithm and simulation", Journal of Computing in Civil Engineering, 30(3), 04015029, 2015.
3. Khaled Nassar and Ossama Hosny. "Solving the least-cost route cut and fill sequencing problem using particle swarm", Journal of Construction Engineering and Management, 138(8), 931–942, 2011.
4. S.M. Easa. "Earthwork allocations with linear unit costs", Journal of Construction Engineering and Management, 114(4), 641–655, 1988.
5. Sumegh Kataria and S.A. Samdani, A.K. Singh. "Ant Colony Optimization in Earthwork Allocation", International Conference on Intelligent Systems, 2005.
6. Warren L. Hare and Valentin R. Koch, Yves. Lucet. "Models and algorithms to improve earthwork operations in road design using mixed integer linear programming", European Journal of Operational Research, 215(2), 470–480, 2011.

International Conference on Architecture and Civil Engineering 2018

ISBN	978-81-933584-5-0		**VOL**	01
Website	www.coreconferences.com		**eMail**	mail@coreconferences.com
Received	11 – January – 2018		**Accepted**	30 - January – 2018
Article ID	CoreConferences005		**eAID**	CoreConferences.2018.005

An Analysis on the Safety Networks and Risk Level of Crane-related Accidents using S.N.A.

WonSang Shin[1], YoungKi Huh[2] and Changbaek Son[3]

[1]PhD Candidate, Dept. of Construction Engineering, Semyung University, Jecheon-si, South Korea

[2]Professor, Dept. of Architectural Engineering, Pusan National University, Pusan Metropolitan City, South Korea

[3]Professor, Dept. of Architectural Engineering, Semyung University, Jecheon-si, South Korea

Abstract - *In this study, crane-related safety accidents that occurred on construction sites were analyzed using the data collected by the Korea Occupational Safety and Health Agency (KOSHA), and the networks of crane-related safety accidents were analyzed using the centrality and clustering techniques of SNA analysis. Based on the results of this analysis, the following conclusions were reached. In this study, wide range of machinery and equipment types used on construction sites, only mobile and tower cranes were analyzed in this study with regard to which safety accidents frequently occurred. It is necessary to analyze the networks of safety disasters related to various machinery and equipment types, and thus to establish data for the development of management measures by occupation type through follow-up research.*

I. Introduction

As construction technologies and methods have advanced, high-rise and large-scale buildings have been constructed and a variety of construction machinery and equipment are being utilized to efficiently perform construction tasks. These have contributed to improvements in productivity, and reductions in construction duration and costs. A crane, the most basic type of heavy equipment that is commonly used on construction sites, moves most of the resources (materials, machines, etc.) used on construction sites vertically and horizontally, improving the efficiency of construction tasks.

Aside from these advantages, cranes are also involved in various forms of serious safety accidents due to their high usability. From 1997 to 2013, there were 1,171 deaths caused by crane-related accidents across all industries in the United States; approximately half of this total (544) were in the construction industry [1]. Considering these facts, cranes are clearly very dangerous on construction sites, and the damage to property and life caused by crane accidents can be very serious. On most construction sites, however, heavy equipment is still selected and utilized based only on the experience of supervisors and operators.

Many studies have been conducted with the goal of reducing safety accidents related to construction equipment and cranes, including a study on the development of real-time support systems for the safe operation of mobile cranes [1], an analysis of forecasts of the movement of workers and equipment on construction sites [2], a study on the development of systems for the improvement of the safety of earthwork equipment [3], an in-depth analysis of fatal injuries caused by crane-related accidents [4], and a study on the safety status of tower crane operators [5]. These earlier studies were performed using different methodologies, but involved analyses of less than 100 safety accidents, and did not consider the origins and causes of actual crane-related safety accidents.

Against this backdrop, this study collected data on crane-related accidents that occurred over the past 3 years with the aim of overcoming the limitations of the earlier studies, and the networks and risk level of safety accidents related to each crane type were analyzed using SNA techniques to obtain key risk factors, with the aim of suggesting management measures that can be utilized on construction sites.

II. Analysis Methodology

Social network analysis (SNA) is a methodology used to structurally visualize various types of relations (organizations, humans, knowledge, etc.) using nodes and links, analyze their attributes and predict measures to optimize the structure of analysis targets. The methodology has been utilized in various fields including military science, business administration, pedagogy, engineering science, etc. In this study, of the various SNA methods, centrality and clustering analyses that can analyze a large amount of data and extract key influential factors were carried out to develop a network of crane-related safety accidents. Centrality analysis is used to identify which node is the most important, and to determine the degree of centrality that shows how many key nodes a network is concentrated on. Clustering analysis is used to find out which groups a network is comprised of, and to identify the characteristics of the network through relations between sub-groups. These analysis methods use the following equations.

① Degree Centrality (D.C.)

$$D.C = \frac{d(ni)}{(g-1)} \quad (1)$$

d(ni) = degree of node n, g = the total number of nodes

② Betweenness Centrality (B.C.)

$$B.C = \frac{\sum_{j>k} g\, jk(ni)/gjk}{[(g-1)(g-2)/2]} \quad (2)$$

gjk = the number of geodesics between nodes j and k
gjk(ni) = the number of geodesics between nodes j and k that contain node i

③ Clustering Index (SMI)

$$SMI = \frac{Outside\ Link\ Density\ - Inside\ Link\ Density}{Inside\ Link\ Density\ - Outside\ Link\ Density} \quad (3)$$

III. Analysis of Crane-Related Safety Accidents

Prior to the analysis of the networks of crane-related safety accidents, crane-related safety accidents were analyzed to examine the level of occurrence using the data of 444 safety accidents collected by the Korea Occupational Safety and Health Agency (KOSHA) from 2013 to 2015. The data used in this study were collected from 5 metropolitan cities (Seoul Special Metropolitan City, Daejeon Metropolitan City, Gwanju Metropolitan City, Daegu Metropolitan City and Busan Metropolitan City) where many construction projects have been carried out. The number of safety accident victims by crane type is as shown in Figure 1, and the top 20 occupations that showed the largest number of safety accidents are listed in Table 1. Figure 1 shows that mobile cranes had the highest number of accident victims, followed by tower cranes, overhead travelling cranes and jib cranes; this can be attributed to the fact that mobile cranes are widely used in both small-scale construction sites and large-scale construction sites thanks to their high usability. In addition, Table 1 shows that crane-related safety accidents occurred to general workers the most, followed by construction machinery operators, machinery and equipment workers, framing carpenters and steel benders.

IV. Analysis of The Networks Crane-Related Safety Accidents

To identify the key risk factors for crane-related safety accidents, Net-Miner, a software program for SNA analysis, was utilized. Data on safety accidents related to mobile cranes (315 cases) and tower cranes (106 cases) that occurred most frequently and thus require some kind of urgent remedial response were analyzed in this study only. Risk factors, disaster types, equipment operation conditions, working conditions and workers' occupations were entered as additional variables to analyze the data in detail. Betweenness centrality and clustering techniques were used to analyze the data.

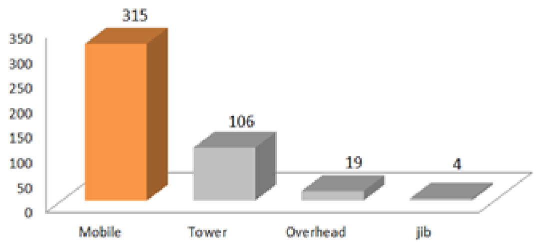

Figure 1. Number of safety accident by crane type (Unit: Person)

General worker	Construction machinery operator	Machinery & equipment worker	Framing carpenter	Steel bender
136	79	42	28	25
Steel worker	Welder	Cable workers	Scaffolder	Plumber
24	17	16	13	9
Indoor wiring electrician	Panel fitter	Construction carpenter	Painter	Foreman
8	8	6	5	4
Landscape worker	Mason	Transmission & distribution electrician	Sash worker	Steel plate worker
4	4	4	2	2

Table 1. No. of crane-related accident victims by occupation type (Unit: Person)

Figure 2 shows the results of a centrality analysis on safety accidents related to mobile cranes. A network of safety accidents was formed centering on nodes including “general worker (degree: 99),” “construction machinery operator (61)” and “steel worker (23),” and it was found that safety accidents frequently occurred while “lifting materials (131),” “installing steel frames (36)” and “leaving a crane (20).” Through clustering analysis, a total of 10 communities were obtained; among them, the modularity of the sixth community was 42.98, showing the strongest cohesion, and thus the sixth community was selected for further analysis. Figure 2 shows that 11 groups were generated within the data of mobile cranes. Groups other than G1 (0.810), G2 (0.859) and G4 (0.653) that showed the highest cohesion (SMI) were excluded from the final analysis. G1 indicates that many accidents (0.2) of being struck by steel frames (0.3) occur when steel workers use a mobile crane to install steel frames (in-out degree: 0.3), and G2 indicates that accidents of “falls (0.2)” frequently occur when machinery and equipment workers “stop (0.3)” and “leave a mobile crane (0.4).” In addition, G4 shows that general workers often experience accidents of being “caught in between (0.2)” when they use a mobile crane to “lift materials (0.3).”

Figure 3 shows the results of a centrality analysis on safety accidents related to tower cranes. A network of safety accidents was formed centering on nodes including “general works (degree: 32),” “machinery and equipment worker (22),” “framing carpenter (11),” and “steel bender (9),” and it was found that safety accidents frequently occurred while “lifting materials (61),” “dismantling (13)” and “installing (9).” Through clustering analysis, a total of 11 communities were obtained; among them, the modularity of the second community was 17.076, showing the strongest cohesion, and thus the second community was selected for further analysis. Figure 3 shows that 2 groups were generated within the data of tower cranes. Since the SMI of the two groups was higher than 0.8 (G1: 0.846, G2: 0.9), both of them were selected for the final analysis. G1 indicates that many accidents of being “caught in between (0.2)” “wire ropes (0.2)” or being “struck by an object (0.3)” occur when general workers use a tower crane to “lift materials (in-out degree: 0.4),” and that framing carpenters often experience accidents of being “hit against a mold (0.2)” when they use a tower crane to “lift materials (0.1).” It was also found that steel benders often experience accidents of being “hit (0.2)” against “a steel frame (0.5)” when they use a tower crane to “lift materials (0.1).” G2 shows that accidents of “collapses (0.4)” frequently occur when machinery and equipment workers “stop (0.5)” and “dismantle a tower crane (0.5),” and that accidents of “falls (0.2)” frequently occur when they “install a tower crane (0.3).”

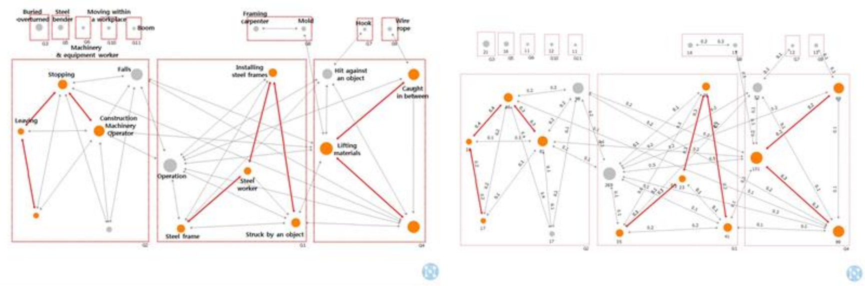

Figure 2. Centrality and Clustering of Mobile Crane

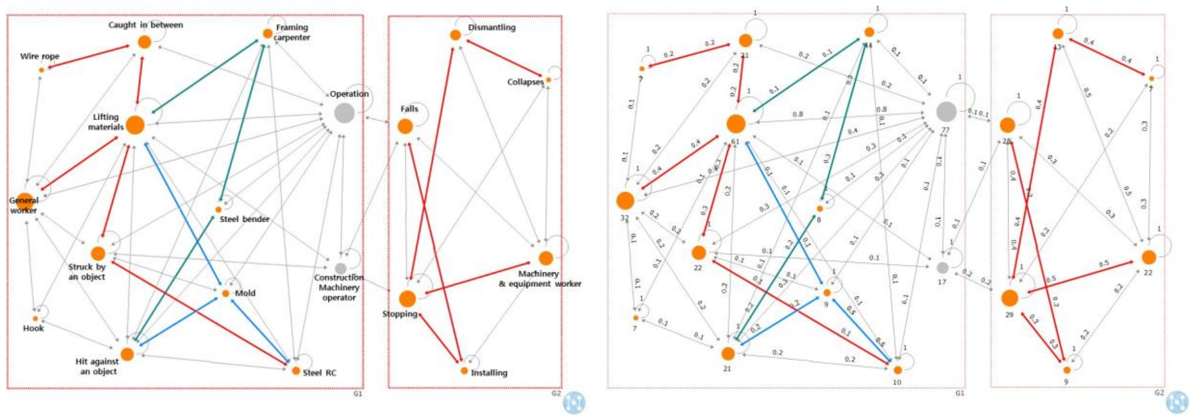

Figure 3. Centrality and Clustering of Tower Crane

V. Analysis of The Risk on Crane-Related Safety Accidents

It is important to examine to whom safety accidents on construction sites occur and due to what factors, but the risk level of the factors should also be analyzed. In this regard, the risk level of the crane-related safety accidents discussed in Chapter 4 above was also analyzed in this study. Risk analysis was performed based on a calculation method used by KOSHA. Table 2 shows that the risk level of mobile cranes and tower cranes with regard to which safety accidents frequently occur was 499.91 and 139.81, respectively. In detail, the risk level of items related to mobile cranes including "general worker," "caught in between" and "lifting materials" was high, and the risk level of items related to tower cranes including "general worker," "struck by an object" and "lifting materials" was high.

Table 2. Analysis of the risk level of crane-related safety accidents

Mobile crane				
Type		No. of victims	Disaster intensity	Risk level
Mobile crane		315	1.587	499.91
By occupation type	General worker	99	1.249	123.65
	Construction machinery operator	61	0.662	40.38
	Steel worker	23	2.012	46.28
By disaster type	Caught in between	69	0.828	57.13
	Struck by an object	41	2.770	46.28
	Falls	17	0.239	4.06
By work type	Lifting materials	131	1.498	196.24
	Installing steel frames	36	1.213	43.67
	Leaving a crane	20	0.402	8.04

Tower crane				
Type		No. of victims	Disaster intensity	Risk level
Tower crane		106	1.319	139.81
By occupation type	General worker	32	2.062	65.98
	Machinery & equipment worker	22	0.784	17.25
	Framing carpenter	11	1.822	20.04
	Steel bender	9	0.508	4.57
By disaster type	Struck by an object	22	2.873	63.21
	Hit against an object	21	0.563	11.82
	Caught in between	21	1.706	35.83
	Falls	28	0.674	18.87
	Collapses	7	1.159	8.11
By work type	Lifting materials	62	1.395	86.49
	Dismantling	13	0.841	10.93
	Installing	9	0.896	8.06

VI. Conclusion

In this study, crane-related safety accidents that occurred on construction sites were analyzed using the data collected by the Korea Occupational Safety and Health Agency (KOSHA), and the networks of crane-related safety accidents were analyzed using the centrality and clustering techniques of SNA analysis. Based on the results of this analysis, the following conclusions were reached.

1. Crane-related safety accidents that occurred on construction sites were analyzed, and it was found that the number of accidents related to mobile cranes was the highest, followed by tower cranes, overhead travelling cranes and jib cranes. The crane-related safety accidents were also analyzed by occupation type, and it was found that many crane-related accidents occurred to general workers, construction machinery operators, machinery and equipment workers, framing carpenters, and steel benders.
2. An analysis of the networks of crane-related safety accidents was conducted, and it was found that mobile cranes formed networks centering on nodes including general worker, construction machinery operator and steel worker, and that safety accidents frequently occurred while “lifting materials,” “installing steel frames” and “leaving a crane.” Tower cranes formed networks centering on nodes including general worker, machinery and equipment worker, framing carpenter and steel bender, and safety accidents frequently occurred while “lifting materials,” “dismantling” and “installing.”
3. The risk level of crane-related safety accidents was analyzed, and it was found that the risk level of items related to mobile cranes including “general worker,” “caught in between” and “lifting materials” was high, and that the risk level of items related to tower cranes including “general worker,” “stuck by an object” and “lifting materials” was high.

If management measures are developed based on the key risk factors of crane-related safety accidents above, it is expected that these can contribute to a reduction in the crane-related safety accidents that occur on construction sites.

In this study, wide range of machinery and equipment types used on construction sites, only mobile and tower cranes were analyzed in this study with regard to which safety accidents frequently occurred. It is necessary to analyze the networks of safety disasters related to various machinery and equipment types, and thus to establish data for the development of management measures by occupation type through follow-up research.

References

1. Zhenhua Zhu, M. W. Park., Christian Koch, Mohamad Soltani, Amin Hammad, Khashayar Davari, "Predicting movement of onsite workers and mobile equipment for enhancing construction site safety" Journal of Automation in Construction, vol. 68, pp. 95-101, 2016
2. Faridaddin Vahdatikhaki, Seied Mohammad Langari, Alhusain Taher, Khaled El Ammari, Amin Hammad, "Enhancing coordination and safety of earthwork equipment operations using multi-agent system" Journal of Automation in Construction, vol. 81, pp. 267-285, 2017
3. Yihai Fang, Yong K Cho, Jingdao Chen, "A Framework for real-time pro-active assistance for mobile crane lifting operation" Journal of Automation in Construction, vol. 72, pp. 367-379, 2016
4. W. C. Shin., H. W. Yeo., J. H. Kwon, K. H. Yi, "A study on Cause analyses of fatal injuries by the mobile ranes", Journal of Korea Safety Management Science, vol. 18, no. 1, pp. 9-15, March 2016.
5. D. Y. Kim, "A fundamental study on safety management for highrise building towercrane operators", Journal of Architectural Institute of Korea, vol. 29, no. 2, pp. 59-66, February 2013.

International Conference on Architecture and Civil Engineering 2018

ISBN	978-81-933584-5-0		**VOL**	01
Website	www.coreconferences.com		**eMail**	mail@coreconferences.com
Received	14 – January – 2018		**Accepted**	03 - February – 2018
Article ID	CoreConferences006		**eAID**	CoreConferences.2018.006

Drainage-Related Risks for Operation and Maintenance of Tunnelling Projects: An Overview

Yong Siang Lee[1], Farid E Mohamed Ghazali[2]

[1,2]School of Civil Engineering, Engineering Campus, University Sains Malaysia, 14300 Nibong Tebal, Penang, Malaysia

Abstract: *The importance of drainage-related risks associated with tunnelling projects requires special attention from tunnel operators to analyse and manage the risks. The optimal management of drainage-related risks in tunnelling projects involves multiple objectives such as flood management, maximisation of design capacity of drainage contamination and optimisation of overall drainage system. This paper focuses on identifying the key drainage-related risks that have great potential of occurring in highway tunnelling projects. The outcomes of this research are developed based on findings obtained from extensive literature review and several case studies that have been carried out by other researchers. The identified drainage-related risks will be reviewed in this paper. All these risks can be included as key information when drafting a new risk management plan or to be added into the existing risk management plan in order to enhance the operation and maintenance of tunnelling projects.*

International Conference on Architecture and Civil Engineering 2018

ISBN	978-81-933584-5-0
Website	www.coreconferences.com
Received	15 – January – 2018
Article ID	CoreConferences007

VOL	01
eMail	mail@coreconferences.com
Accepted	10 - February – 2018
eAID	CoreConferences.2018.007

A Development of Accident Prediction Technique based on Monitoring Data for the Area of Dense Energy Consumption

Jung Hoon Kim[1], Young Gu Kim[2], Young Do Jo[3]
[1,2,3]Institutes of Gas R&D, Korea Gas Safety Corporation, Republic of Korea

Abstract-*Accident likelihood is growing due to a correlation for gas and electricity installed in the area of dense energy consumption like traditional market and underground shopping center. In order to prevent and respond accident risks related to gas and electricity in this area, it should be monitored and predicted for risk factors of gas or electricity by developing safety management system. In this study, the method of accident prediction development related to gas risk was proposed in the area of dense energy consumption. From statistical data of risk factors in the area of dense energy consumption, temperature as risk factor except gas leak in gas use has been extracted. General aspects of temperature changes and associated theories were investigated to analyze characteristics of temperature data. In addition, to check the changes in temperature due to convection around the burner, related experiments were carried out. Through such investigations and experiments, the change characteristics in temperature data related to fire prediction were derived and algorithm was developed to apply them to the development of energy safety management systems.*

I. Introduction

The areas of dense energy consumption are traditional market and underground shopping center etc. which have a large floating population with facilities of gas and electricity. Accident risks related to gas and electricity are explosion (35.6%), leak (16.8 %) and fire (26.1 %) during the most recent 10 years [1].

In order to prevent and respond accident risks related to gas and electricity in this area, it should be needed to develop safety management system based on internet of things (IOT) which executes sensor data collection and data analysis for accident prediction and safety control etc. [2,3].

In this study, the method of fire accident prediction technique related to gas usage in the area of dense energy consumption was proposed for safety management system. From statistical data of risk factors in the area of dense energy consumption, A temperature as risk factor except gas leak in gas use has been extracted. A characteristic analysis of risk factor was carried out by temperature variation tests and related law. Accident prediction algorithms using temperature data were developed based on these characteristics for application to safety management systems.

II. Statistical Data of Risks Factor in the Area of Dense Energy Consumption

In this study, the method of fire prediction model development in the area of dense energy consumption was proposed for safety management system. Accident ranking of risk factors was analyzed by using statistical fire data in traditional market and underground shopping center of Korea during the last 9 years as Table 1 [4].

Upper risk factors are mostly electrical factor, carelessness, mechanical factor. Risk factors related to gas are carelessness (preparing food) (seventh), carelessness (adjacent position of the flame) (14th). In traditional market and underground shopping center, fire occurs near the burner but no safety management is made. To prevent from these accidents and other fires, a temperature sensor should be installed around the gas burner to avoid fire and gas-related explosion accidents.

Table 1 Statistical data of fire in Korea during the last 9 years

Accident Ranking	Upper Risk Factor	Lower Risk Factor	Traditional Market Accidents	Underground Shopping Center	Sum
1	Electrical factor	Short circuit due to deterioration of insulation	78	4	82
2	Unknown	Unknown	77	1	78
3	Electrical factor	Unidentified short circuit	75	1	76
4	Carelessness	Cigaret ends	45	8	53
5	Mechanical factor	Overheating/ Overload	40	0	40
6	Electrical factor	Overload / Over-current	34	4	38
7	Carelessness	Preparing food	31	3	34
8	Arson	Arson suspicion	29	1	30
9	Electrical factor	Etc.	20	4	24
10	Electrical factor	Short circuit due to tracking	23	0	23
11	Electrical factor	Short circuit due to compression damage	20	1	21
12	Electrical factor	Short circuit due to misconnection	18	1	19
13	Carelessness	Etc	19	0	19
14	Carelessness	Adjacent position of the flame	15	0	15

III. **Characteristic Analysis of the Risk Factor in the Area of Dense Energy Consumption**

Using the burner will increase the ambient temperature and cause a different pattern of temperature increase in the event of an accident. Therefore, it is important to consider statistical factors or characteristic factors that may reflect the pattern of temperature changes.

Most gas use facilities in the area of dense energy consumption are interior spaces. Change pattern characteristics are needed to account for the different ambient temperature changes depending on the surrounding environment (ventilation system, internal structure near the burner, number of internal personnel, heating and cooling facility, and fire power of the burner).

Accurate temperature forecasting requires long-term on-site data collection. Since the pattern of temperature changes or the magnitude is different from normal, these characteristics should be applied in the event of an accident(overheating, fire, etc.).

Temperature changes around the burner generally take place from the start of cooking to the point of boiling (①-② Figure 1). There is a boiling point from the point of boiling to the point of burning as shown in ②-③ Figure 2. Ambient temperature tends to be similar to the inner temperature in pot but is variable according to time.

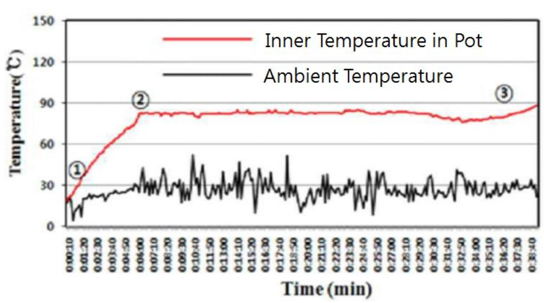

Figure 1. Changes of inner temperature in pot and ambient temperature

Newton's law of cooling enables larger time-heating energy changes depending on the size of the fire. In addition, the closer it is to the burner fire, the bigger it becomes.

$$\frac{dQ}{dt} = h \cdot A\big(T_{env} - T(t)\big) = -h \cdot A\Delta T(t)$$

Q: thermal energy, h: heat transfer coefficient, A: the area of heat transfer targets, T_{env} : ambient temperature, T: a surface temperature of heat transfer targets. If the burner and the temperature sensor are close to each other, the effect of convection directly on the changes in the temperature around the burner will benefit from temperature detection. In the case of remote distances, it is necessary to consider the installation of temperature sensor, since rapid burning or temperature change around the burner is difficult to detect.

When using the burner, the temperature will always increase, and if there is an accident, the different pattern of temperature increase will occur. These characteristics can be used to predict accidents.

IV. Experiment of Temperature Variation According to A Distance Between Fire and Steel Plate

When portable butane gas stove is operated using oversized grill, it is tested for temperature change at the top and bottom of the container, container retention cover in the burner, and butane containers in accordance with the burn time. Figure 2 shows temperature measurement location in this test.

Figure 2. Temperature measurement locations

It is required to verify the characteristics of temperature change for fire caused by overheat to check the parts related to convection. It can be seen that the temperature changes with the distance between oversized grill and portable butane gas stove cover(cover) become more variable as the distance approaches in Figure 3. We can confirm the results of these experiments are consistent with Newton's law of cooling.

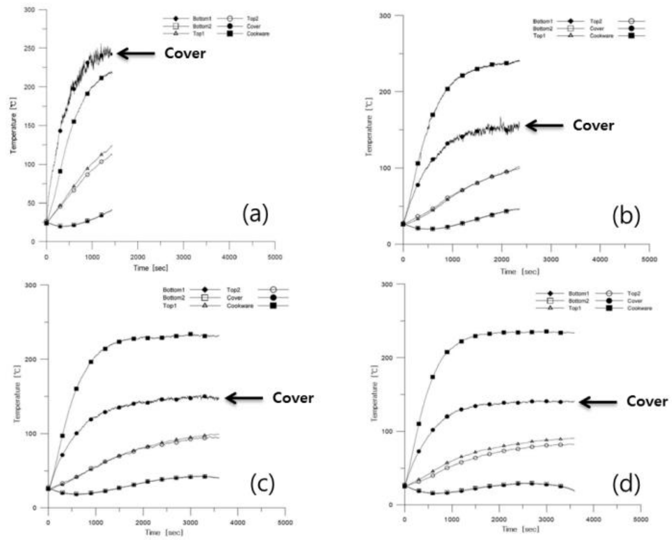

Figure 3. Experiment Temperature according to a distance between hot grill and cover: (a) 12.34 mm, (b) 24.06 mm, (c) 28.49 mm, (d) 33.59 mm

V. Development of Accident Prediction Technique Considering Experiment Results

After the analysis of the risks associated with gas use in the area of dense energy consumption using statistical data, the relevant accident risks, except gas leakage, are related to temperatures. To prevent such accident hazard, the radio temperature sensor may be installed around the burner to develop and utilize a prediction model considering the characteristics of temperature data change. A predictive method was developed using algorithms such as Figure 4, taking into account the temperature change data (slope) measured at the site, fire hazards limit temperature, temperature variability and rapid rise temperature data, etc.

Temperature data are monitored in real time from the energy safety management system server that collects data from IOT sensors and utilized as statistical characteristics values of ordinary temperature data with reference data for a given time period. Where real-time temperature data is greater than 1 step warning temperature (set value or ordinary temperature statistical value), the time to reach the limit is predicted by regression analysis, and where small, initial fire is considered.

An algorithm inform the energy safety management system that the pattern of temperature changes being monitored is in a fire indication if the pattern differs from the usual one, and if not, it is in a fire safety condition.

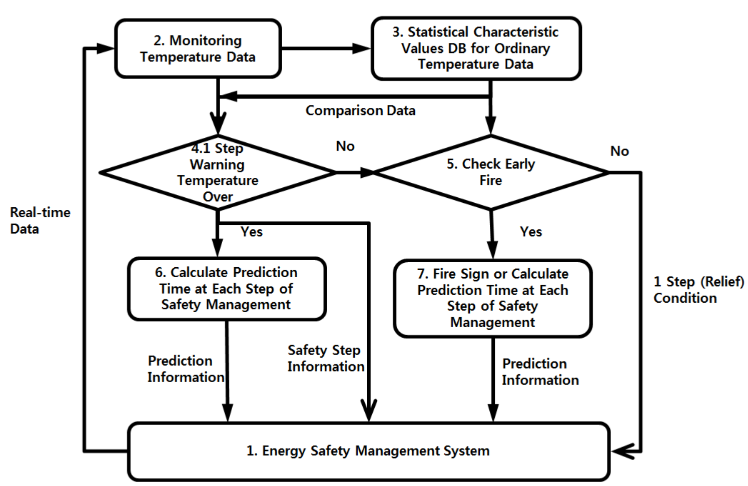

Figure 4. Accident Prediction Algorithm based on Temperature Data

VI. Conclusions

Accident likelihood is growing due to a correlation for gas and electricity installed in the area of dense energy consumption. To prevent and respond accident risks related to gas and electricity in this area, it should be needed to develop safety management system which executes sensor data collection and data analysis for accident prediction and safety control etc. In this study, the technique of fire prediction in the area of dense energy consumption was developed for safety management system. To analyze the characteristics of the temperature data, we investigated and analyzed the typical temperature changes and associated theoretical equation. In addition, the experiments were performed to verify the temperature changes caused by convection around the burner. Main characteristics of temperature data variation are linear/nonlinear relation and variability over time which can be applied to accident prediction or fire indication decision. Then, the algorithm of prediction technique was developed for safety management system. The verification test of the algorithm for accident prediction technique will work in the future.

References

1. Gas Accident Year book, Korea Gas Safety Corporation, 2015.
2. Z.L. Tan, and C.L Zhang, "Construction of the safety management system for urban underground business district with the application of IOT," *Service Systems and Service Management* (ICSSSM). Hong Kong, pp. 743-746, July 2013 [*10th International Conference on Service Systems and Service Management*, 2013].
3. C.A. Zhou, C. Chen, and H. Ren, "Comprehensive Evaluation on Multiple Constraint Elements of City Underground Space Development and Utilization Based on Analytic Hierarchy Process and Fuzzy Comprehensive Evaluation Method," Applied Mechanics and Materials. London, vol. 357-360, pp. 2754-2758, August 2013.
4. Statistical Yearbook of Emergency Management, Disaster Integration Management of Korea, 2007-2015.

International Conference on Architecture and Civil Engineering 2018

ISBN	978-81-933584-5-0
Website	www.coreconferences.com
Received	15 – January – 2018
Article ID	CoreConferences008

VOL	01
eMail	mail@coreconferences.com
Accepted	05 - February – 2018
eAID	CoreConferences.2018.008

Concrete using Coconut Fiber –An Alternative

R R Singh[1], Damandeep Singh[2]
[1]Professor in Civil Engineering Department, [2]Student of M.E. Structures, PEC University of Technology, Chandigarh, India

Abstract: *Use of Fiber is one of the vital and emerging trends in Construction Technology. Fiber can be considered as an alternative in the use of an air entraining agent providing sufficient freeze thaw protection and moreover as a reinforcing material. Fiber reinforced materials are composite materials that typically consist of strong fibers embedded in resin matrix. It is a composite obtained by adding a single type or a blend of fibers to the conventional concrete mix. The fibers provide strength and stiffness to the composite and generally carry most of the applied loads. The matrix acts to bond and protect the fibers and to provide for transfer of stress from fiber to fiber through shear stresses. Fibers can be in form of steel fibers, glass fibers, natural fibers, synthetic fibers, etc. The mechanism by which fibres produce resistance to freezing and thawing is that fibres introduction reduces water absorption of the concrete increasing penetration resistance to de-icing salts. Reduced water absorption is a function of the fibres to reduce plastic shrinkage cracking, reducing the ability of water to permeate into the bleed in a concrete. So this research paper describes experimental studies on the use of coconut fibre as enhancement of concrete.*

Introduction

In the recent times it is very difficult to point out another material which is as versatile as concrete. Moreover some studies show that it is the second most widely used material after water. It is by far, the most widely used construction material which is constantly expanding and reshaping in this booming time of development of the infrastructure. With the recent advances in concrete it has now become possible to control the various factors and to obtain a concrete of certain specific requirements.

With the quest for affordable housing system for both the rural and urban population and other infrastructure, various proposals focussing on cutting down conventional building material costs have been put forward. One of the suggestions in the forefront has been the sourcing, development and use of alternative, non-conventional local construction materials including the possibility of using some agricultural wastes as construction materials. Natural reinforcing materials can be obtained at low cost and low levels of energy using local manpower and technology. Utilisation of fibres as a form of concrete enhancement is of particular interest to less developed regions where conventional construction materials are not readily available or are too expensive. So from there comes the idea of Fibre reinforced concrete.

Fiber reinforced concrete is concrete containing cement, water, aggregate, and discontinuous, uniformly dispersed or discrete fibers. It is a composite obtained by adding a single type or a blend of fibers to the conventional concrete mix. Fibers can be in form of steel fibers, glass fibers, natural fibers, synthetic fibers, etc. Main role of fibers is to bridge the cracks that develop in concrete and increase the ductility of concrete elements. There is considerable improvement in the post-cracking behaviour of concrete containing fibers due to both plastic shrinkage and drying shrinkage. They also reduce the permeability of concrete and thus reduce bleeding of water. Some types of fibers produce greater abrasion resistance in concrete and impart more resistance to impact load.

Concrete made with Portland cement has certain characteristics: it is strong in compression but weak in tension and tends to be brittle. The weakness in tension can be overcome by the use of conventional steel bar reinforcement and to some extent by the inclusion of a sufficient volume of certain fibres. The use of fibres also alters the behaviour of the fibre-matrix composite after it has cracked, thereby improving its toughness. The overall goal for this research is to investigate the potential of using waste and low energy materials for building any type of infrastructure. The objective of this research is to experiment on the use of coconut fibres as an enhancement of concrete. Coconut fibres are not commonly used in the construction industry but are often discarded as wastes.

Coconut fibres obtained from coconut husk, belonging to the family of palm fibres, are agricultural waste products obtained in the processing of coconut oil. Coconut fibre has been used to enhance concrete and mortar, and has proven to improve the toughness of the concrete and mortar in this research.

Advantages of Fiber Reinforced Concrete

Fibre reinforced concrete has high modulus of elasticity for effective long-term reinforcement, even in the hardened concrete. Moreover it does not rust nor corrode and requires no minimum cover. Fibre reinforced concrete has ideal aspect ratio (i.e. relationship between Fiber diameter and length) which makes them excellent for early-age performance. These are easily placed, cast, sprayed and less labour intensive. Moreover they have greater retained toughness in conventional concrete mixes and higher flexural strength, depending on addition rate. They can be made into thin sheets or irregular shapes and possesses enough plasticity to go under large deformation once the peak load has been reached.

Methodology

The following materials were used for preparing the concrete mix:-

1. OPC of 53 grades
2. Fine aggregate i.e. sand
3. Coarse aggregate
4. Coconut fibers
5. Water

Ordinary Portland cement of grade 53 was used in this research. The fine aggregate was natural sand which is freely available and the coarse aggregate having a size of20mm and 10mm (smaller size aggregate as suitable for the mould used for casting).The fibres were coconut fibres with length 6mm with approximate mean aspect ratio. Coconut Coir Fibre: Fibres were collected from the local temples, cleaned, sun dried, removed dust to analyze its properties. Coconut fibres require no pre-treatment, except water treatment. Coconut Fibre has high water absorption. Due to this property, the coconut fibres were pre soaked in water for 24 hours.

Preparation and Testing of Specimen

Standard 15cm x 15cm x 15cm cubes are taken and three cubes for different % of fibers. Finally the compressive strength of concrete with and without coconut fiber is tested. The average of three results of same percentage of coconut fibers is considered and effect is seen. The different properties of ingredients are tabulated in table below.

Test Results of The Ingredients

Sr.No.	Items	Results
1.	Cement	OPC-53 GRADE
2.	Sp. Gravity of cement	3.2
3.	Sp. Gravity of coarse aggregate	2.7
4.	Sp. Gravity of fine aggregate	2.8
5.	Water absorption of coarse aggregate	1%
6.	Water absorption of fine aggregate	4%
7.	Free moisture content of coarse aggregate	-
8.	Free moisture content of fine aggregate	-
9.	Fineness modulus	3.92
10.	Zone of fine aggregate	III

The influence of coconut fiber on concrete has been studied for three different grades of concrete that are M20, M25, and M30. The coconut fiber is used of 0% (no fibres), 0.2%, 0.4%, 0.6%, 0.8% and 1.0%.

Mixing Procedure

The dry cement and aggregates were mixed for two minutes by hand. The mixing continued for further few minutes while about 80% of the water was added. The mixing was continued for another few minutes and the fibres were fed continuously to the concrete for a period of 2–3 min while stirring. Finally, the remaining water was added and the mixing was continued for an additional two minutes. This ensured a complete distribution of fibres throughout the concrete mix.

Method of Compaction

The moulds with half filled fresh concrete were vibrated vertically on the vibrated table while casting for about 30 seconds. The moulds were then fully filled with fresh concrete and vibrated further for about 60 seconds. This method of compaction was to align the fibres normal to the direction of vibration.

Curing

The specimens were stripped from the moulds 24 hours after casting and submerged in water until testing. Specimens were removed from the water after 28 days of submersion in water for testing the 28-day strength.

Testing and Result Analysis

All the cubes were tested in a 'Compressive Testing Machine' to determine the compressive strength of the cubes.

The procedure is as follows: - Compression test of cube specimen is made as soon as practicable after removal from curing pond. Place the specimen centrally on the location marks of the compression testing machine and load is applied continuously, uniformly and without shock. The rate loading is 2kN/Sec continuously. The load is increased until the specimen fails and record maximum load carried by the each specimen during the test.

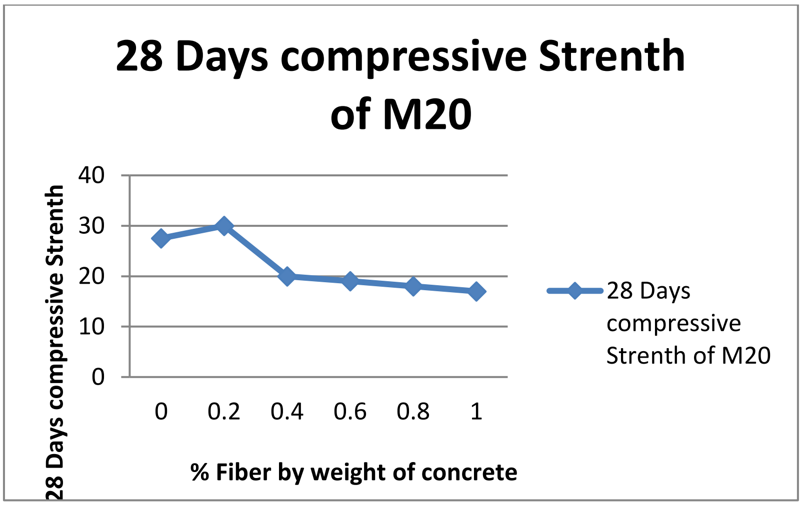

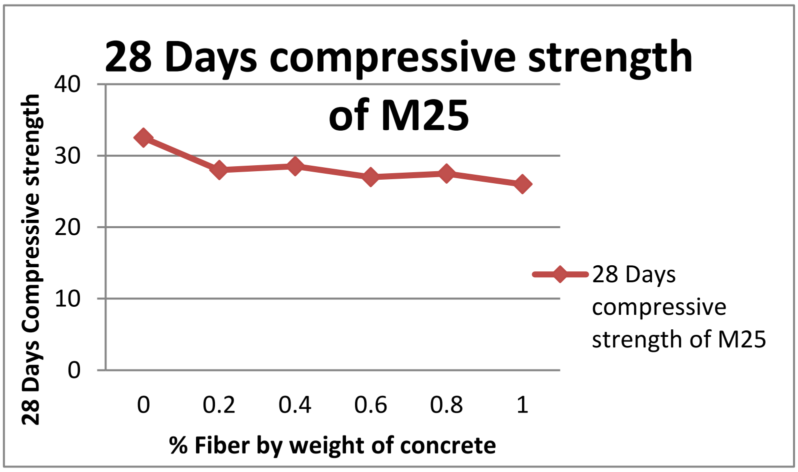

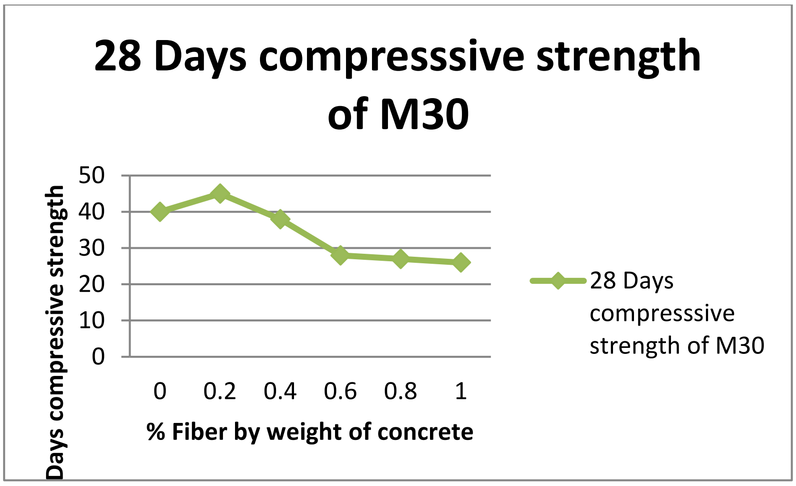

These results show that compressive strength of concrete increases just at 0.2% fibres. It is because at this fibre content it fills the voids. It is also seen that compressive strength of concrete reduces drastically when fibres content is increased beyond 0.2%. The amount of gain of compressive strength is shown in table below: -

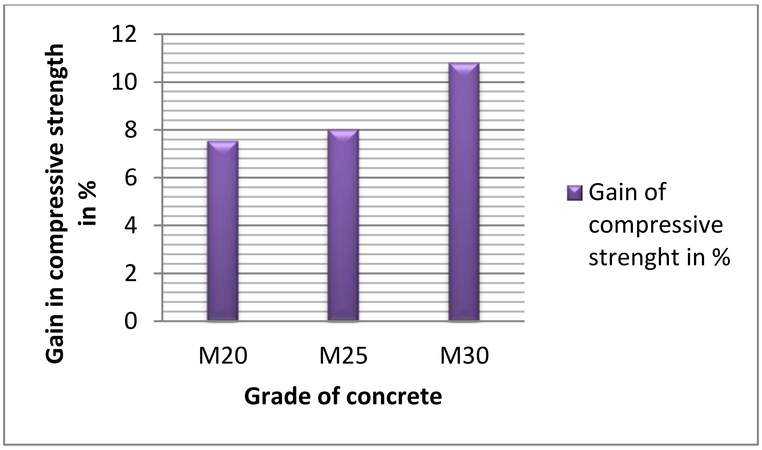

Conclusion

The compressive strength of concrete increases at certain aspect ratio of fibres and at a specific 0.2%. Compressive strength of concrete decreases beyond 0.2%. The amount of gain of compressive strength gradually increases with increase in grade of concrete and it can be concluded that addition of coconut fiber will reduces the quantity of ingredients to achieve same strength and thus it becomes economic.

References

1. Ali Majid, Anthony Liu, "Mechanical and Dynamic Properties of Coconut Fibre Reinforced Concrete." Construction and Building Materials". Reed Business Information, Inc. (US). 2012.
2. Noor Md. Sadiqul Hasan, HabiburRahmanSobuz, Md. Shiblee Sayed and Md. Saiful Islam, "The Use of Coconut fibre in the Production of Structural Lightweight Concrete".
3. Kshitija nadgouda, "coconut fibre reinforced concrete" Proceedings of Thirteenth IRF International Conference, 14th September 2014, Chennai, India .
4. Yalley, P. P. and Kwan, Alan ShuKhen. "Use of coconut fibre as an enhancement of concrete". Journal of Engineering and Technology 3, Pages 54-73. 2009.
5. Domke P. V., "Improvement in the strength of concrete by using industrial and agricultural waste". IOSR Journal of Engineering, Vol. 2(4), Pages 755-759. April 2012.
6. Paramasivam P, Nathan G. K., Das Gupta N. C., "Coconut Fibre reinforced corrugated slabs", International Journal of Cement Composites and Lightweight Concrete, Volume 6, Issue 1, Pages 19-27. 1984.

International Conference on Architecture and Civil Engineering 2018

ISBN	978-81-933584-5-0	**VOL**	01
Website	www.coreconferences.com	**eMail**	mail@coreconferences.com
Received	18 – January – 2018	**Accepted**	10 - February – 2018
Article ID	CoreConferences009	**eAID**	CoreConferences.2018.009

Experimental Analysis of Single Walled Carbon Nanotubes- Bio Composites

Mohana Priya G[1], Mythili T[2], M Anuratha[3], M Samyuktha[4]
[1,2]Assistant Professor, [3,4]Student, Third year, Department of Aeronautical Engineering,
Mahendra Engineering College, Namakkal, India

Abstract: *In this study, a technique is presented for developing constitutes models for polymer composite systems with single walled carbon nanotubes (SWNT). Because the polymer molecules are on the same size scale as the nanotubes, the interaction at the polymer/nanotube interface is highly dependent on the local molecular structure and bonding. It is proposed herein that the nanotube, the local polymer near the nanotube, and the nanotubes polymer interface can be modeled as an effective continuum fiber by using an equivalent-continuum modeling method. The effective fiber serves as a means for incorporating micromechanical analyses for the prediction of bulk mechanical properties of SWNT/polymer composites with various nanotube lengths, concentrations and orientations. This experiment results the importance of composites in aviation industry and also explains in details about carbon nanotubes composites that can be used in aircraft structures. Considerable growth has been seen in the use of biocomposites in the automotive and decking markets over the past decades. The dispersion of nanotubes in composites has been investigated as a means of deriving new and advanced engineering materials, these composite materials have been formed into fibers and thin films and their mechanical and electrical properties determined. The remarkable properties of carbon nanotubes offer the potential for fabricating conducting polymers without impairing the other desirable polymer properties. Aircraft wing is made up of SWNT-biocomposites, which is allowed to test in a wind tunnel. These results in the determination of drag force and pressure distribution. The strength of the wing can be increased by using this biocomposites materials in recent works at laboratories, SWNTs have been dispersed in polymer and pitch solutions using high energy ultrasonic probes.*

International Conference on Architecture and Civil Engineering 2018

ISBN	978-81-933584-5-0
Website	www.coreconferences.com
Received	15 – January – 2018
Article ID	CoreConferences010

VOL	01
eMail	mail@coreconferences.com
Accepted	05 - February – 2018
eAID	CoreConferences.2018.010

Resource Leveling Considering Float Consumption Impact

Dae-Young Kim[1], Byoung-Yoon Choi[2], Dong-Eun Lee[3]
[1]Professor, Dept. of Architectural Engineering, Kyungnam University, Korea
[2]Graduate, [3]Professor, School of Architecture & Civil Engineering, Kyungpook National University, Korea

Abstract- *Resource levelling minimizes resource fluctuations by postpone the earliest start time (EST) of non-critical activities with corresponding floats. Float consumption for resource leveling may reduces the project completion probability. This paper presents a method to minimize the resource fluctuations with minimum impact of float consumption. A case study is presented to verify the validity and usability of the method.*

I. Introduction

The purpose of the resource leveling in a construction project is to reduce the project completion time (PCT) and the project completion cost (PPC) by reducing the hire, release and re-hire of resources (i.e., labor, equipment). Existing resource leveling studies have adopted a method of minimizing resource fluctuations by synchronizing the resource accumulation graph with the resource requirements (Essa, 1989; Senouci & Eldin 2004) and by making it closer to the bell-shape (Mattila and Abraham 1998; Yeniocak 2013).

Previous studies have achieved resource leveling by delaying the start time of activity within the float range (Keane and Caletka 2015). This resource leveling method does not affect the project completion time because it uses the float that exists in non-critical activities. However, the consumption of float due to the start time delay of activity increases the criticality index of the non-critical activities. The increase in the criticality index reduces the probability of project success due to the uncertainties of the construction project and unexpected risks. Therefore, scheduling for a successful project should ensure flexibility and sustainability of the employment status to cope with uncertainty.

In this study, we propose a resource leveling method that identifies the activities with little effect on the probability of project success, uses them for resource leveling, and identifes the start time combination of each activity considering the ratio of critical activities.

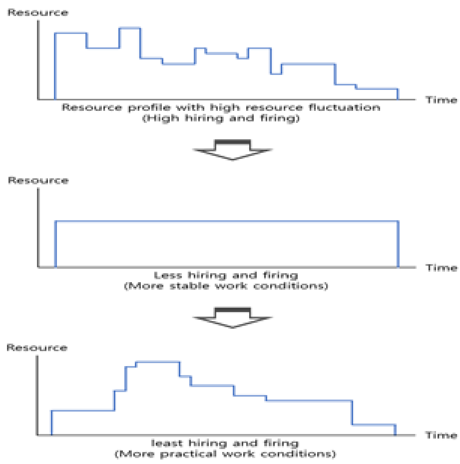

Figure 1. Resource accumulation graph

II. Methodology

The methodology minimizes the impact of float consumption and explores the activity start time combination to identify the optimal resource leveling plan. This system consists of the following four modules. (1) invoke schedule information in conjunction with the MS project, (2) implement a fitness function to achieve resource leveling considering the criticality index ratio, (3) to find the optimal activity start time combination, and (4) implemented as software integrated into MATLAB (ver. 2015b)
The detailed calculation steps are described as follows:

Step 1. Call up schedule data (activity ID, predecessor list, successor list, number of resources per day, activity duration, cost) from MS project.
Step 2. perform CPM operation.
Step 3. Store early start time, early finish time, late start time, and late finish time for each activity in the matrix.
Step 4. Calculate the project completion time (PCT).
Step 5. Identify non-critical activities.
Step 6. Define GA parameters [population size, crossing rate, mutation rate].
Step 7. Set GA end rule.
Step 8. Define the objective function [Release and Re-Hire index (RRH), weight (w1, w2)].
Step 9. Storage the critical activity.
Step 10. Sets the limit of the criticality index (CI).
Step 11. Identify critical activities.
Step 12. Replace the fitness function with the modified function.
Step 13. Define the limits of the main activity ratios.
Step 14. Create an initial population.
Step 15. Perform selection / intersection / mutation operations and compute chromosomal fitness values.
Step 16. Presents the calculation result.

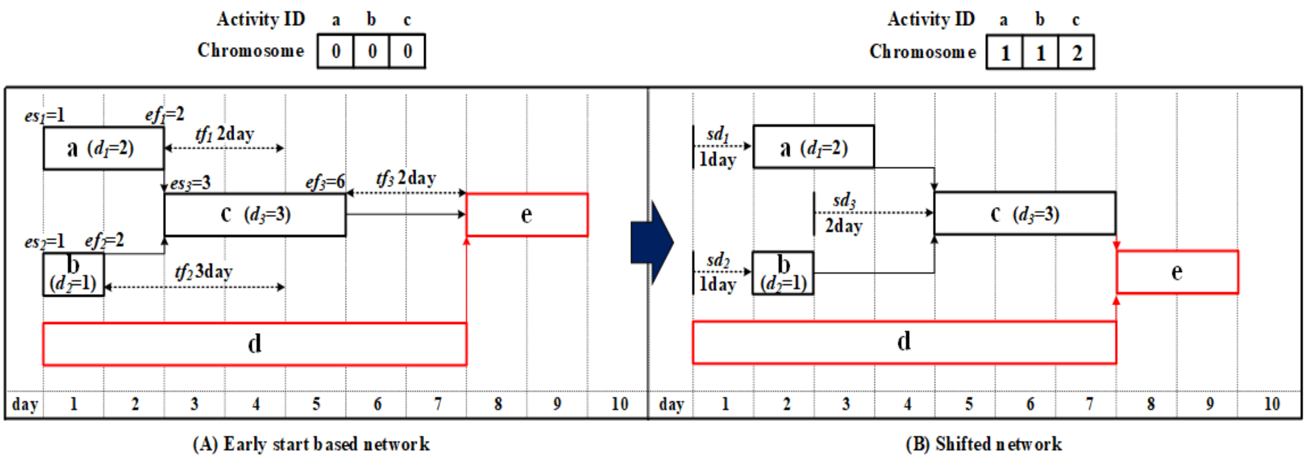

Figure 2. Chromosome & Example

Resource leveling is achieved by adjusting the start time of non-critical activities. The start time of the critical activities, maintains the original start time determined by the CPM operation. The chromosomes input for the GA operation are a set of days deliberately delayed from the originally scheduled earliest start time (es) of non-critical activities. Fig. 2 illustrates a network that is varied by gene expression and input gene values. The gene phenotype (e.g. [0, 0, 0]) in Fig.1 (A) means that the earliest start time of the non-critical activities (e.g. a, b, c) is equal to the originally scheduled time. On the other hand, the gene phenotype (e.g. [1, 1, 2]) in Fig.1 (B) shows that the earliest start time of non-critical activities (e.g. a, b, c) indicates deliberately delayed by 1, 1, and 2 days.

As the initial population is initialized with the near optimal solution, the GA search time is shortened and the reliability is improved. The genes of the early-age group are the set of shifted dates (sd), and these shifted dates are chosen considering the criticality index (CI), which is the probability of becoming the main process. Critical activities can change, because activity duration is volatile. Therefore, if a stochastic CPM calculation is performed to identify the main activity for each simulation run, a CI (e.g. a value between 0 and 100) is calculated. CI close to 100 is likely to be the main activity, and consuming float for these activities will reduce the project completion probability. Conversely, if the CI is close to 0, the probability of becoming a non-critical activity increases, and consuming the float of these activities has a relatively small impact on the project completion probability. Therefore, in order to reduce the effect of float consumption when performing resource leveling, the start time of activities with a high CI move to low probability, while the start time of activities with a low CI move to high probability. For example, if the float and CI of the activities are shown in Table 1, the activities with 0 (e.g. A, C, F, J, P and S) float are on the critical path, while the non-critical activities with some float (e.g. B, D, E, G, H, I, K, L, M, N, O, Q, R and T) are not on the critical path. Only the start time shifts of these non-critical activities are considered for resource leveling. The CI of D, G, H, and R of the non-critical activities are less than 10%, and they have less impact on the project completion probability than the other non-critical activities (e.g. B, E, K, L, M, N, O, Q, T). Thus, this methodology creates a population by preferentially adjusting the start times of D, G, H, and R activities.

Table 1. Criticality index and float

Activity ID	Total float (day)	Criticality index (%)
A	0	86.63
B	6	10.31
C	0	53.74
D	7	9.60
E	3	44.17
F	0	53.00
G	7	9.60
H	7	1.20
I	7	6.00
J	0	50.94
K	3	17.08
L	4	34.60
M	3	22.23
N	4	10.77
O	4	28.68
P	0	76.83
Q	4	26.20
R	6	2.97
S	0	78.57
T	4	26.20

III. Case Study

Using the network of Hegazy et al. (1999) (Fig. 3), verified the performance and effectiveness of this methodology. The project completion time (PCT) of this network is 32 days, and the critical path is A → C → F → J → P → S. The critical activities are B, D, E, G, H, I, K, L, M, N, O, Q, R and T and their float are [6, 7, 7, 3, 4, 3, 4, 4, 4, 6, 4]. Their start time is used to achieve resource leveling by moving within the allowable time range.

The system searched for the combination of the start time shift of non-critical activities as [6,7,3,0,2,2,3,0,3,0,0,2,0,0]. Cumulative resource graphs before resource leveling are shown by solid lines in Fig. 4, and it can be seen that hire, release, and re-hire are frequent occurrences. The cumulative resource graph of the resource leveling result of the methodology is shown in the dotted line in Fig. 4. This confirmed that optimum resource leveling options with a criticality index of 60% in the bell-shape can be determined.

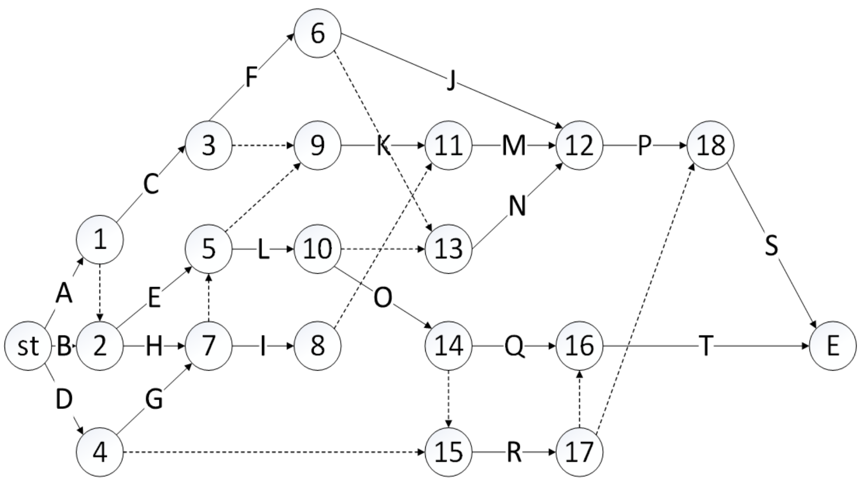

Figure 3. Case project network information

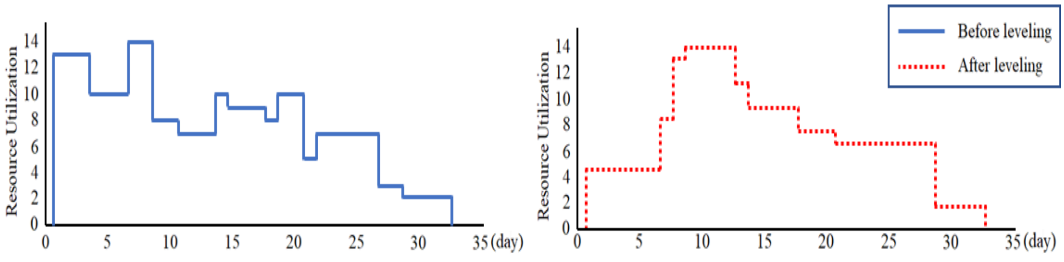

Figure 4. Resource profiles obtained before/after leveling

Table 2. Criticality index and float

Activity ID	Total float (day)	Shifting date	Remaining float (day)	CP & close-CP
A	0	0	0	*
B	6	**6**	0	*
C	0	0	0	*
D	7	**7**	0	*
E	3	**3**	0	*
F	0	0	0	*
G	7	**0**	7	
H	7	**2**	5	
I	7	**2**	5	
J	0	0	0	*
K	3	**3**	0	*
L	4	**0**	4	
M	3	**3**	0	*
N	4	**0**	4	
O	4	**0**	4	
P	0	0	0	*
Q	4	**2**	2	*
R	6	**0**	6	
S	0	0	0	*
T	4	**0**	4	

IV. Conclusion

This study presents the implemented a methodology that considers the ratio of critical activity index, and verified the effectiveness by case study. This methodology identifies activities that have little impact on project success probability and regard as a priority of resource leveling, and regard as a priority of resource leveling, and confirmed practicality through resource leveling case study.

This work was supported by the National Research Foundation of Korea(NRF) grant funded by the Korea government(MSIP) (NRF-2016R1D1A1B03933080).

References

1. Easa, S. M. (1989). Resource leveling in construction by optimization. Journal of construction engineering and management, 115(2), 302-316.
2. Hegazy, T. (1999). Optimization of resource allocation and leveling using genetic algorithms. Journal of construction engineering and management, 125(3), 167-175.
3. Keane, P. J., & Caletka, A. F. (2015). Delay analysis in construction contracts. John Wiley & Sons, New York.
4. Mattila, K. G., & Abraham, D. M. (1998). Resource leveling of linear schedules using integer linear programming. Journal of Construction Engineering and Management, 124(3), 232-244.
5. Senouci, A. B., & Eldin, N. N. (2004). Use of genetic algorithms in resource scheduling of construction projects. Journal of Construction Engineering and Management, 130(6), 869-877.
6. Yeniocak, H. Ü. S. E. Y. İ . N. (2013). An efficient branch and bound algorithm for the resource leveling problem Ph.D. dissertation, Middle East Technical University.

International Conference on Business, Finance and Economics 2018

ISBN	978-81-933584-5-0
Website	www.coreconferences.com
Received	15 – January – 2018
Article ID	CoreConferences011

VOL	01
eMail	mail@coreconferences.com
Accepted	10 - February – 2018
eAID	CoreConferences.2018.011

Distortions in Trade Statistics Revisited: Data and Empirical Issues

Sho Haneda[1], Akihiro Yogata[2], Naohiko Ijiri[3]
[1]School of Social Welfare, Tokyo University of Social Welfare
[2]Graduate School of Economics, Nihon University
[3]College of Economics, Nihon University

Abstract: *This paper aims to quantify distortions due to "data updating problem" in trade statistics that might cause biases in econometric analyses and policy evaluation. Using the UN Comtrade database over the period of 2005-2015, three main results are clarified. Firstly, the paper finds differences between old and updated data regarding the number of transactions as well as trade values. Secondly, the degree of distortions significantly differs among countries, even within OECD countries. Finally, estimation results indicate that the coefficient on independent variables can be changed because of the data updating problem in econometric analyses. As a policy implication, it should be noted that a replication of econometric results of previous studies requires exactly the same data. Thus, it may be required that UN Comtrade and other statistic offices keep old data in their website.*

JEL Classifications: F13, F14, F23

Key words: Trade statistics, Distortions, Data updating, UN Comtrade, HS classification

1. Introduction

Quality and availability of trade data have been crucial for economists and policy makers, especially in econometric analyses policy evaluation. A variety of trade statistics are published and can be freely downloaded in order to conduct empirical studies. However, previous studies basically use the "snapshot" of trade statistics in their researches. In this research, trade data obtained from the United Nations (herein UN) Comrade are employed to check the biases caused by the problem of data updating. The data updating problem refers to the issue such that the values of the first released data differ drastically from those of updated data. In order to fill the gap, this paper intends to quantify the distortions in trade statistics by comparing old and updated data in UN Comtrade. The aims of this study is to quantify distortions in official trade data published by international organizations. The rest of this paper is organized as follows. The section 2 introduces the methodology for a data manipulation

2. Methodology

This section explains the methodology for constructing databases that can identify the biases in trade statistics due to the updating problem.

2-1 Explanation of HS System

The trade data are reported from member countries to the UN according to the rule of International Merchandise Trade

Statistics: Concepts and Definitions (hereinafter IMTSCD). However, the statistical reports submitted by some countries should be modified because reporting system of these countries tends to differ from that of IMTSCD. To publish trade statistics of member countries, the UN basically revises the reported data in accordance with their rule.

Trade values are reported in two manners, which are Free On Board (FOB) for export values as well as Cost, Insurance and Freight (CIF) for import values. The former only includes the value of transactions while the latter additionally contains the cost of insurance and transportations.

Trade data are published based on Harmonised Commodity Description and Coding System (HS), Standard International Trade Classification (SITC) and Broad Economic Categories (BEC) classifications. Since the HS has more than 5,000 product IDs, this paper employ the HS classification for checking distortions. The HS system was developed by World Custom Organization (herein WCO). The classification has been updated every five years so far. It is organized by 4 levels, which are Section, Chapter, Heading and Subheading. The 6-digit level HS system is internationally common while each country has own schedule beyond 6-digit.

2-2 Data Coverage

a) Country

In this paper, 10 reporter countries and all partner are included. Since the period of data collection is from April 2017 to October 2017, this study only has a relatively small number of transactions.

b) Product

The research is based on HS 6-digit level and all products are covered.

c) Period

As we only obtained the data for 10 countries, target periods are 2005-2015.

d) Classification

As it is mentioned that the HS classification has been revising its codes every five years, this paper covers the following versions: HS1996, 6-digits HS2002, 6-digits HS2007, 6-digits, HS2012, 6-digits and HS2017, 6-digits.

2-3 Calculation Method

In order to investigate the distortions in trade reports due to the data updating problem, the paper calculates three types of variables (see table 1). Firstly, it defines the transaction 3 as the **REVEALED transaction** since trade value exists only in the updated data. Secondly, the paper uses the transaction 2 as the data for the **HIDDEN transaction** because it only appears in the old data. Finally, the transaction 4 is included in the **REVISED transaction** as both old and updated data have it while trade values differ between them.

Table 1: Definitions of each variable

Transactions	Flow	Reporter	Partner	Period	HS code	Trade value (Old data)	Trade value (Updated data data)
1	Export	Japan	UK	2014	871310	107,469	107,469
2	Export	Japan	UK	2014	871320	5,523	N/A
3	Import	Japan	UK	2014	831790	N/A	112,563
4	Import	Japan	UK	2014	871310	112,325	201,252

Note: These are defined by authors.

3. Stylized Facts: Distortions in Trade Statistics

This section summarises the characteristics of our results using UN Comtrade database. Main findings are threefold. Firstly, the paper finds the gap between first released data and updated data regarding the number of transactions. Secondly, the degree of the difference significantly differs among countries, even within developed economies. Thirdly, REVISED transactions may be the main source of biases in econometric analyses. Finally, the value of total trade seems not to change substantially after the updates.

4. Econometric Analysis

In order to achieve the purpose, this paper uses two types of dependent variables in the empirical analysis. The one is the value of exports and imports in old data and the other is those in updated data. The paper employs these variables to conduct our empirical analysis.

There are two steps in this section. Firstly, the paper estimates the gravity equation of international trade by Ordinary Least Square (OLS) with robust standard errors. Secondly, this study checks the similarity of coefficients from different OLS regressions, which are regression for old data and that for new data, using the Chi-squared test.

In the first stage of the empirical section, the baseline specification is:

$$lnTrade_{ijklt} = \beta_1 lnGDP_{jt} + \beta_2 lnDISTANCE_{ij} + \beta_3 Contiguity_{ij} + \beta_4 LANGUAGE_{ij} + \beta_5 COLONY_{ij} + \beta_6 COMColony_{ij} + \varepsilon_{ijt} \quad (1)$$

where *i, j, k, l* and *t* denote reporter, partner, trade flow, product and year respectively. In addition, *Trade* and *DISTANCE* are defined as value of trade as well as physical distance between two countries. *Contiguity* is a dummy variable for country-pairs that have a common border. *LANGUAGE* is equal to 1 if a country-pair shares the same language and 0 otherwise. *Colony* and *COMColony* are dummy variable for county-pairs which had a colonial relationship between them and that for country-pairs which have a common coloniser. Finally, ε is the error term.

As we explained above, one of our aims is to test the difference between old and new trade data. In order to examine the similarity (or difference) of coefficients from them, the paper uses *suest* command and Chi-squared test in STATA. This study checks the similarity using REVISED transactions for each exporter in order to quantify the bias caused by data updating issues. The results are summarised in table C for exports and D for imports.

Main findings are twofold. Firstly, it is clarified that there might be the difference in the coefficients between the results from old data and those from new data. Secondly, the degree of the variance depends on trade flow (export and import), reporter, and independent variables.

5 Concluding Remarks

This paper finds that the data updating problem exists, even for OECD countries. Also, the issue can cause the biases in the quantitative analysis.

As a policy implication, it should be noted that replication of the results of previous studies needs exactly the same data. Thus, it might be required that UN Comtrade and other statistic centres keep old data in their website. Furthermore, an international harmonisation of data collection and revision methods in the world need to be considered for the TRUE policy evaluation.

Further studies can target other economic variables such as FDI, income, employments, etc. In addition, the ranking of the quality of statistics of each country may be important for future research.

Main References

1. Beja, E. L. (2008). Estimating Trade Mis-invoicing from China: 2000–2005'. *China and World Economy*, 16, 1, 82–92.

2. Buehn, A. and Eichler, S. (2011). Trade Misinvoicing: The Dark Side of World Trade. *The World Economy*, 2011, 1263-1287.
3. Fisman, R. and Wei, S.-J. (2004). Tax Rates and Tax Evasion: Evidence from ''Missing Imports'' in China. *Journal of Political Economy,* 112, 2, 471–96.
4. Fisman, R. and Wei, S.-J. (2007). The Smuggling of Art, and the Art of Smuggling: Uncovering the Illicit Trade in Cultural Property and Antiques. *NBER Working Paper No. 13446.*
5. IMF (1993). A Guide to Direction of Trade Statistics (Washington, DC: IMF).
6. Kellenberg, D and Levinson, A. (2016). MISREPORTING TRADE: TARIFF EVASION, CORRUPTION, AND AUDITING STANDARDS. *NBER Working Paper No. 22593*
7. Kumakura M. (2011). The Characteristics and Usage of UN Comtrade. *IDE JETRO Research report 2010-2-03*.

Appendix

Table A: Target countries and date of updates

Country	Year	Publication Note	First Publication Date	Last Publication Date
Brazil	2007	Full revision	2008.03.03	2017.05.23
	2008	Full revision	2009.04.20	2017.05.23
	2009	Full revision	2010.01.15	2017.05.23
	2010	Full revision	2011.02.02	2017.05.16
	2011	Full revision	2012.02.01	2017.05.23
	2012	Full revision	2013.02.07	2017.05.23
	2013	Full revision	2014.01.17	2017.05.24
	2014	Full revision	2015.01.21	2017.05.24
	2015	Full revision	2016.02.24	2017.05.25
Canada	2014	Full revision	2015.02.12	2017.04.26
	2015	Full revision	2016.02.23	2017.06.27
China	2014	Full revision	2015.05.07	2017.06.28
	2015	Full revision	2016.05.25	2017.06.29
Estonia	2015	Full revision	2016.02.13	2017.09.06
Finland	2005	Full revision	2006.05.24	2017.03.02
Malta	2015	Full revision	2016.06.28	2017.05.15
Mexico	2015	Full revision	2016.03.01	2017.10.06
Netherlands	2015	Full revision	2016.05.20	2017.09.13
Rep. of Korea	2015	Full revision	2016.09.23	2017.05.08
Sweden	2015	Full revision	2016.03.17	2017.05.09

Source: UN, Comtrade.

Table B: The change in the value of total trade

		The value of trade (billion US dollar)			Total changes in the value of trade (billion US dollar)					
Country	Year	Export	Import	Total trade	Export	(%)	Import	(%)	Total trade	(%)
Brazil	2007	161	121	281	-0.006	0.00%	0.002	0.00%	-0.004	0.00%
	2008	153	135	288	**4.766**	**3.12%**	-0.201	-0.15%	**4.565**	**1.58%**
	2009	153	128	281	0.001	0.00%	0.008	0.01%	0.008	0.00%
	2010	202	182	384	**4.542**	**2.25%**	1.224	0.67%	**5.766**	**1.50%**
	2011	256	226	482	-0.068	-0.03%	0.020	0.01%	-0.048	-0.01%
	2012	243	223	466	-0.019	-0.01%	0.408	0.18%	0.388	0.08%
	2013	242	240	482	**4.145**	**1.71%**	0.860	0.36%	**5.005**	**1.04%**
	2014	225	229	454	0.067	0.03%	0.005	0.00%	0.072	0.02%
	2015	191	171	363	**2.450**	**1.28%**	0.684	0.40%	3.134	0.86%
Canada	2014	475	463	938	1.602	0.34%	0.087	0.02%	1.689	0.18%
	2015	409	420	828	0.081	0.02%	0.601	0.14%	0.682	0.08%
China	2014	2,342	1,959	4,302	-0.016	0.00%	1.142	0.06%	1.126	0.03%
	2015	2,273	1,680	3,953	-8.415	-0.37%	-2.194	-0.13%	-10.608	-0.27%
Estonia	2015	14	16	30	0.006	0.04%	-0.005	-0.03%	0.001	0.00%
Finland	2005	65	58	124	0.013	0.02%	0.002	0.00%	0.015	0.01%
Malta	2015	4	7	11	**1.335**	**34.09%**	**0.995**	**14.66%**	**2.330**	**21.77%**
Mexico	2015	381	395	776	-0.095	-0.02%	-0.029	-0.01%	-0.124	-0.02%
Netherlands	2015	474	425	899	0.027	0.01%	0.005	0.00%	0.033	0.00%
Rep. of Korea	2015	527	436	963	-0.079	-0.02%	-0.024	-0.01%	-0.103	-0.01%
Sweden	2015	140	138	278	-0.138	-0.10%	0.267	0.19%	0.129	0.05%

Source: UN Comtrade.

Note: Total change in the value of trade is defined as the following: The sum of the value of REVEALED trade - The sum of the value of HIDDEN trade + the sum of the value of REVISED trade.

Table C: The similarity of coefficients for exports

Export							
		Variable					
Country	**Year**	**GDP**	**Distance**	**Contiguity**	**ommon language**	**Colony**	**Common colony**
Brazil	2007						
	2008						
	2009				***		
	2010	***	***				
	2011	***	***	***	***	***	
	2012				***		
	2013				***		
	2014						
	2015				***		
Canada	2014		***	***		**	
	2015		*				
China	2014		***		***		
	2015	***	***	**	***		
Estonia	2015						
Finland	2005						
Malta	2015		**			***	
Mexico	2015					**	
Netherlands	2015		**	*			
Rep. of Korea	2015		**				
Sweden	2015	***		***	**	**	

Note: ***, ** and * denote that the equality of coefficients can be rejected by Chi-squared test at 1%, 5% and 10% level of significance respectively.

Table D: The similarity of coefficients for imports

Import							
		Variable					
Country	**Year**	**GDP**	**Distance**	**Contiguity**	**Common language**	**Colony**	**Common colony**
Brazil	2007	***	**		***	***	
	2008		***	***			
	2009	**	**	***	***		
	2010	***	***	***	***	***	
	2011	***	*	*	*		
	2012	**					
	2013	***					
	2014						
	2015						
Canada	2014						
	2015						
China	2014	***				***	
	2015	*					
Estonia	2015					***	
Finland	2005						
Malta	2015	***	***		***	***	***
Mexico	2015						
Netherlands	2015	***				***	
Rep. of Korea	2015						
Sweden	2015				**	**	

Note: ***, ** and * denote that the equality of coefficients can be rejected by Chi-squared test at 1%, 5% and 10% level of significance respectively.

CORE CONFERENCES

International Conference on Education, Transportation and Disaster Management 2018

ISBN	978-81-933584-5-0
Website	www.coreconferences.com
Received	18 – January – 2018
Article ID	CoreConferences012

VOL	01
eMail	mail@coreconferences.com
Accepted	05 - February – 2018
eAID	CoreConferences.2018.012

Introducing ACTOR as a Learning Framework - Merging Cultural Heritage Assessments with Risk Reduction and Disaster Recovery

Ann Kristina Bojsen[1]

[1]Associate Professor at the Bachelor´s Degree Programme in Emergency and Risk Management, Metropolitan University College, Copenhagen, Denmark

Abstract: *There is a general professional consensus that vulnerability and risk assessments are crucial tasks in any serious attempt to substantially reduce disaster losses and enhance the reconciliation or recovery in the post event phase. However, cultural heritage is often considered as an overarching element that should be assessed, rather than a permanent key component of the assessments. Research in disaster management noticeably illustrates how cultural heritage is increasingly at risk from disasters caused by natural and human-made hazards, as well as the effects of climate change. Still, disaster risk reduction interventions tend to overlook the importance of incorporating cultural heritage, as an independent and highly valuable component in order to increase the risk reduction. Furthermore, there is a lack of methodological expansion in order to merge disaster assessment and cultural heritage. These limitations serve as motivation for the introduction of the ACTOR framework (Assessing Cultural Threats, Obstacles and Resilience) ACTOR aims at merging cultural heritage assessments with risk reduction and disaster recovery, and provide disaster management students with a learning framework that considers how different impacts of cultural heritage affect disaster risk reduction, and how disasters and risk influence cultural heritage. The ambition of ACTOR is to outline a conceptual framework for cultural heritage in relation to disaster risk reduction interventions, and to introduce a methodological contribution to the field of disaster management education and training that places cultural heritage at the center of disaster risk reduction.*

International Conference on Education, Transportation and Disaster Management 2018

ISBN	978-81-933584-5-0		**VOL**	01
Website	www.coreconferences.com		**eMail**	mail@coreconferences.com
Received	08 – January – 2018		**Accepted**	12 - February – 2018
Article ID	CoreConferences013		**eAID**	CoreConferences.2018.013

Disaster Education in Japan: Tagajo High School in Miyagi Prefecture

Akiko Iizuka[1]

[1]Utsunomiya University, Center for International Exchange, Utsunmoiya-City, Tochigi, Japan

Abstract: *Disaster education is widely acknowledged and practiced in Japan, a disaster-prone country. However, many high schools do not offer disaster education in formal coursework, except for Maiko High School in Hyogo Prefecture and Tagajo High School in Miyagi Prefecture. This study examines a case from Tagajo High School, which began to offer the "Disaster Science Course" in 2016, five years after the 2011 Tōhoku earthquake and tsunami. Although Tagajo High School made a lot of efforts to implement the course, this paper discusses the approach and challenges the school encountered, which are relevant to anyone involved in high school education, as well as general disaster education in Japan.*

CORE CONFERENCES

International Conference on Education, Transportation and Disaster Management 2018

ISBN	978-81-933584-5-0		**VOL**	01
Website	www.coreconferences.com		**eMail**	mail@coreconferences.com
Received	20 – January – 2018		**Accepted**	05 - February – 2018
Article ID	CoreConferences014		**eAID**	CoreConferences.2018.014

Redistribution Problem of Relief Supply after a Disaster Occurrence

Etsuko Nishimura[1], Kentaro Uchida[2]
[1]Graduate School of Maritime Sciences, [2]Undergraduate Student,
Faculty of Maritime Sciences, Kobe University, Japan

Abstract- *The great earthquakes have occurred in various places of Japan after an interval of several years. After the disaster occurred, it seems that some shelters have oversupplied relief commodities, others have lacked them. Since some survivors cannot stay at shelters for some private reasons, they must stay at their home even if the lifeline stops. This paper proposes a methodology to redistribute the oversupply at shelters and relief supply at local distribution center to the shelters and other locations such as elderly care homes lacked relief commodities around one week from the disaster occurrence as the planning horizon. From the computational results, regardless of the balance between total volume of relief oversupplied and total volume of relief lacked, our approach can find the locations with or without relief supply.*

I. Introduction

The great earthquakes have occurred in various places of Japan after an interval of several years, and the mudslide disasters also have occurred about every rainy season for the past several years. The Japan government and municipality tackle kinds of countermeasures against disasters, in order to implement the disaster reduction. Some issues about relief supply after the disaster occurrence immediately were sometimes reported in the mass media. Especially related to emergency logistics, although relief arrives at local distribution centers, the survivors at the evacuation shelters cannot receive its relief timely. And after the disaster occurred around one week, it seems that some shelters have oversupplied relief commodities, others have lacked them. However, in the initial phase after the disaster occurred immediately, it is difficult to understand the scale and extent of the disaster. Then the government and municipality consider the strategic planning such as facility location and stock pre-position etc. and the pre-disaster operation before the disaster occurrence. In this phase, it is seemed that enough volume of relief must be sent to the disaster area regardless of commodities what survivors need at that time. Additionally, since some survivors cannot stay at shelters for some private reasons, they must stay at their home even if the lifeline (electricity, gas or water supply) stops. Those survivors cannot receive relief supply or they have low priority for relief supply in most cases, because they do not stay at the shelters. Then we investigate the survivors at locations except evacuation shelters, such as their own homes, special support schools and more. From our investigation, we also consider the problem for the target locations including the elderly care homes that will increase from now on.

Therefore, this study consider to redistribute the oversupply at shelters and relief supply at local distribution center to the shelters and other locations lacked relief commodities for the time being able to understand oversupply or shortage of relief supply around one week from the disaster occurrence as the planning horizon. We propose the approach for the vehicle routing problem and the redistribution problem for relief supply, in order to find feasible solution effectively.

II. Literature Review

Various natural disasters occur all over the world, academic researches address those challenges for emergency logistics. Sheu [1] define the process of planning, managing and controlling the flows of resources among locations to meet the urgent needs of the affected people under emergency condition as the emergency logistics. And Caunhye et al. [2] reviews the papers published at journal papers and conference proceedings about emergency logistics that searched by keywords such as disaster, emergency, humanitarian logistics and optimization. The literature can be classified into two main categories: (a) Facility location and (b) Relief distribution and casualty transportation. Most facility location optimization models in emergency logistics combine the process of location with stock pre-positioning or relief distribution. Their surveyed models about facility location are found to be single-period, since they are used for pre-disaster planning. Relief distribution models are used for post-disaster planning and are mostly multi-period, due to the large amount of uncertainty involved in post-disaster environments. From Caunhye et al. [2] observation, in most cases of resource allocation and commodity flow models, the objective function includes the transportation cost and sum of unsatisfied demand, the decision making includes the vehicle routing and unmet demands. Sheu [3] considers the emergency logistics distribution approach for quick response to urgent relief in affected area during a three-day crucial rescue period. His proposed approach involves mechanisms including group-based relief distribution and relief supply. Opit and Nakade [4] consider a single distribution center, multiple disaster areas, multi-items and multi-periods. They consider the distribution problem to maximize the expected value of total relief supplies delivered to each area as objective function. Yi and Kumar [5] proposed the meta-heuristics of ant colony optimization for disaster relief activities in order to consider the route construction in real time situation. They consider the objective aims at minimizing the weighted sum of unsatisfied demand and unserved wounded people waiting at demand nodes.

Although most studies consider relief supply and resource allocation for the evacuation shelters, however they do not consider those issues for survivors at locations except shelters. Therefore, we consider the relief redistribution problem for survivors at shelters and other locations such as elderly care homes.

III. Problem Description

The redistribution problem of relief supply (RPRS) is defined on a graph $G = (N, A)$ with N is a node set representing the vehicle depot, distribution centers, evacuation shelters and elderly care homes, and A is the arc set. Fig.1 shows the locations and routes for relief transportation in the target area as an example. In this example, two vehicles are assigned to 16 locations as vehicle depot "0" and other locations 1 to 15. If total oversupply at locations does not exceed total shortage at locations, it is assumed that there are some locations where are not serviced. Indeed, the vehicle depot is not always but often the same locations as distribution center. Therefore, it is assumed that the vehicle depot is given as the different location of distribution center. Both locations are same or not, can be controlled by the way to give location data.
From this example, one vehicle leaves from a vehicle depot "0", and then it visits the distribution center "1", elderly care homes "13" and "14", evacuation shelters with shortages "5" and "6" in turn, and then it goes back to the vehicle depot. Another vehicle leaves from a vehicle depot "0", and then it visits the evacuation shelter with oversupply "4", elderly care homes "10", "9" and "7", evacuation shelters with oversupply "3", elderly care home "12", evacuation shelter with oversupply "2", elderly care home "15" in turn, and then it goes back to the vehicle depot. It is considered that the working time limit for each vehicle and handling operation at each location are set. Additionally, under such a situation as total shortage of relief supplies is more than total oversupply, it can be interpreted locations 8 and 11 where the dotted line shown in Fig.1 is connected to, are no serviced to relief transportation.

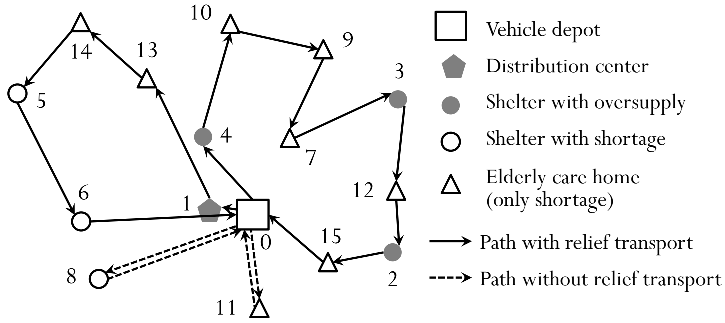

Figure 1. Concept of this problem.

IV. Problem Formulations

Its minimizes weighted total travel distances for relief transportation, and weighted total travel distances from oversupply points to shortage points for relief transportation, and weighted shuttle service distance without relief transportation as the objective function value. It is assumed that there is a homogeneous fleet of vehicles and each point is serviced by each one vehicle. Each vehicle has the maximum capacity to be loaded and the working time limit without considering the overtime work.

This problem RPRS will be formulated as follows:

[RPRS] Minimize $$\alpha \sum_{i\in N}\sum_{j\in N} C_{ij} \max\{0, \sum_{k\in V} x_{ijk} - z_j M\} +$$

$$\beta\left(\sum_{i\in N\setminus\{0\}} C_{i0}\max\{0,\sum_{k\in V} x_{i0k}-(z_i-1)M\}+\sum_{i\in N\setminus\{0\}} C_{0i}\max\{0,\sum_{k\in V} x_{0ik}-(z_i-1)M\}\right. \quad (1)$$

Subject to

$$\sum_{j\in N} x_{ijk} = y_{ik} \qquad \forall i\in N, k\in V \quad (2)$$

$$\sum_{i\in N} x_{ijk} = y_{jk} \qquad \forall j\in N, k\in V \quad (3)$$

$$\sum_{k\in V} y_{ik}\begin{cases}\le |N|-1 & \forall i\in\{0\}\\ =1 & \forall i\in N\setminus\{0\}\end{cases} \quad (4)$$

$$\sum_{j\in N} x_{ijk}-\sum_{j\in N} x_{jik}=0 \qquad \forall j\in N, k\in V \quad (5)$$

$$z_i=(1-\frac{\max\{S_i-D_i,0\}}{S_i-D_i})\times\max\{0,\sum_{k\in V}(x_{0ik}+(x_{i0k}-1)M)\} \qquad \forall i\in N\setminus\{0\} \quad (6)$$

$$u_{ik}-u_{jk}+1\le N(1-x_{ijk}) \qquad \forall i,j\in N\setminus\{0\}, k\in V \quad (7)$$

$$u_{jk}-u_{ik}-1\le N(1-x_{ijk}) \qquad \forall i,j\in N\setminus\{0\}, k\in V \quad (8)$$

$$y_{ik}\le u_{ik}\le Ny_{ik} \qquad \forall i\in N\setminus\{0\}, k\in V \quad (9)$$

$$w_{jk}=0 \qquad \forall j\in\{0\}, k\in V \quad (10)$$

$$w_{jk}\ge\sum_{i\in N}(w_{ik}+S_j-D_j)\times\max\{0,x_{ijk}-z_jM\} \qquad \forall j\in N\setminus\{0\}, k\in V \quad (11)$$

$$w_{jk}\le\sum_{i\in N}(w_{ik}+S_j-D_j)\times\max\{0,x_{ijk}-z_jM\} \qquad \forall j\in N\setminus\{0\}, k\in V \quad (12)$$

$$w_{ik}\le CAP^k \qquad \forall i\in N\setminus\{0\}, k\in V \quad (13)$$

$$b_0=0 \quad (14)$$

$$a_j\ge b_0+T_{0j}+H_j-(1-\sum_{k\in V} x_{0jk})M \qquad \forall j\in N\setminus\{0\} \quad (15)$$

$$a_j\ge b_i+T_{ij}+H_j-(1-\sum_{k\in V} x_{ijk})M \qquad \forall i,j\in N\setminus\{0\} \quad (16)$$

$$a_{N+1}\ge b_i+T_{i0}+H_i-(1-\sum_{k\in V} x_{i0k})M \qquad \forall i\in N\setminus\{0\} \quad (17)$$

$$b_i=\max\{0,a_i\} \qquad \forall i\in N\cup\{|N|+1\} \quad (18)$$

$$b_{N+1}\le TL_k \qquad \forall k\in V \quad (19)$$

$$x_{ijk}=\{0,1\} \qquad \forall i,j\in N, k\in V \quad (20)$$

$$y_{ik}=\{0,1\} \qquad \forall i\in N, k\in V \quad (21)$$

$$z_i=\{0,1\} \qquad \forall i\in N\setminus\{0\} \quad (22)$$

$$u_{ik}, w_{ik}\ge 0 \qquad \forall i\in N\setminus\{0\}, k\in V \quad (23)$$

$$a_i, b_i\ge 0 \qquad \forall i\in N\cup\{|N|+1\} \quad (24)$$

where $N(\in N^C\cup N^S\cup N^H\cup\{0\})$ represents the set of locations that consistes of distribution centers, evacuation shelters, eldely care homes and a vehicle depot; V is set of vehicles; N^C is set of distribution centers where the relief are stored at the time of pre-disaster and post-disaster; N^S is set of evacuation shelters with over-supplied or shortage; N^H is set of elderly care homes with shortage only; C_{ij} is the distances between location i and j (Note that $C_{ii}=\infty$); T_{ij} is traveling time between locations i and j; H_i is handling time spent by vanning or devenning relief supplies at location i; TL_k is working time limit for vehicle k; S_i is volume of oversupply relief at location i (this means that available volume supplied from location i to other locations); D_i is volume of lack-relief at location i (this means that available volume demanded from other locations to location i); CAP^k is maximum capacity which the relief can be loaded on vehicle k; α and β are the weights for travel distance with or without relief transportation, respectively; x_{ijk} is 1 if vehicle k moves between locations i and j, 0 otherwise (0-1 decision variables); y_{ik} is 1 if vehicle k visits to location i, 0 otherwise (0-1 decision variables); z_i is 1 if relief is not transported at location i by any vehicle, 0 otherwise (0-1 decision variables); u_{ik} is order of visiting to location i by vehicle k; w_{ik} is relief volume loaded on vehicle k at location i; a_i and b_i are arrival time and leaving time by any vehicle at location i, respectively.

The objective function (1) minimizes weighted total travel distances from oversupply locations to shortage locations for relief transportation, and weighted shuttle service distance without relief transportation. Constraint sets (2) and (3) show the relationship between variables x_{ijk} and y_{ik}, x_{ijk} and y_{jk}. Constraint set (4) ensure that a vehicle must visit each location except the vehicle depot exactly once. Constraint set (5) guarantee that the number of times arriving is same as the number of times leaving by a vehicle at each location. Constraint set (6) shows that variable zi is defined by variables x_{0ik} and x_{i0k}. z_i is set to 1 if both variables x_{0ik} and x_{i0k} equal to 1, 0 otherwise. Constraint sets (7) and (8) mean that a sub-tour visited only points except the vehicle depot "0" is forbidden. Constraint set (9) guarantee that variable u_{ik} is greater than and equal to 0 if y_{ik} equals to 1, and u_{ik} equals to 0 otherwise. Constraint sets (10) to

(12) define the volume of relief loaded on each vehicle which visits just before location j except the vehicle depot “0”. Constraint set (13) guarantees that each vehicle must service as its maximum capacity not exceeded. Constraint set (14) defines the time when any vehicle leaves from the vehicle depot “0” is 0. Constraint sets (15) to (17) define that the time a_j when vehicle k arrives to location j by the arrival time a_i at location i where its vehicle visited just before location j and variable x_{ijk}. Constraint set (18) defines the time when each vehicle arrives at each location. Constraint set (19) guarrantees that each vehicle must service its assigned workload within its working time limit.

V. Solution Procedure

It will be proposed the heuristic algorithm used Genetic Algorithm (GA), in order to find feasible solution effectively. In this section, it is explained that the chromosome representation and its interpretation. Table I shows the attribute information of each location in the example of Fig.1. Location 1 is a distribution center “D”, locations 2 to 7 are evacuation shelters, locations 8 to 15 are elderly care homes. Relief can be supplied from a distribution center to other locations, is classified in oversupply category in table I. An evacuation shelter with oversupply or shortage is included, and an elderly care home with shortage only is included as the target location of this problem. Although oversupply or shortage volume of each location depends on its location capacity or its serious damage size, it is seems that the relief for fifty persons with minimum unit size “1” can be supplied in an elderly care home. Volume of relief supplied to other locations is given and multiplied several times as the above unit size.

Table II shows the chromosome representation of the example shown in Fig.1 and the balance with oversupply and shortage (S_i - D_i) at location i. The visiting order and location number from the left side are shown in table II. Table III shows the vehicle number assigned as not exceed the vehicle capacity “10”, and order of visiting to each location. In this example, vehicle-1 visits 0, 4, 10, 9, 7, 3, 12, 2, 15 in turn and then goes back to 0, and vehicle-2 visits 0, 1, 13, 14, 5, 6 in turn and then goes back to 0. Locations 8 and 11 are not serviced to relief supply. Note that travel distances with shuttle service from a vehicle depot are included. The more locations without relief transportation are, the larger the objective function value becomes.

Table I Attribute Information for Each Location

Location (i)	1	2	3	4	5	6	7	8	9	10	11	12	13	14	15
Facility type	D	Evacuation shelters						Elderly care homes							
Volume of oversupply	10	5	5	5	0	0	0	0	0	0	0	0	0	0	0
Volume of shortage	0	0	0	0	3	3	3	1	1	1	1	1	1	1	1

Table II Chromosome Representation

Order of visiting	1	2	3	4	5	6	7	8	9	10	11	12	13	14	15
Location No.	4	1	10	9	7	13	14	5	6	8	11	3	12	2	15
Balance between oversupply and	5	10	-1	-1	-3	-1	-1	-3	-3	-3	-1	5	-1	5	-1

Table III Way to Find Feasible Solution as Vehicle Dispatch and Routes

k: Vehicle number

	Location No.	4	1	10	9	7	13	14	5	6	8	11	3	12	2	15
$k = 1$	Num. of relief loaded on	5	15x	4	3	0	-1x	-1x	-3x	-3x	-3x	-1	5	4	9	8
	Location where a vehicle	**4**	**-**	**10**	**9**	**7**	**-**	**-**	**-**	**-**	**-**	**-**	**3**	**12**	**2**	**15**
$k = 2$	Num. of relief loaded on		10				9	8	5	2	-	-				
	Location where a vehicle	**-**	**1**	**-**	**-**	**-**	**13**	**14**	**5**	**6**	**-**	**-**	**-**	**-**	**-**	**-**
$k = 3$	Num. of relief loaded on										-3					
No	Location where a vehicle	No distribute to relevant location →									**8**					
$k = 4$	Num. of relief loaded on											-1				
No	Location where a vehicle	No distribute to relevant location →										**11**				

Vehicle-1 : 0 – 4 – 10 – 9 – 7 – 3 – 12 – 2 – 15 – 0, Vehicle-2 : 0 – 1 – 13 – 14 – 5 – 6 – 0

Locations 8 and 11 are not serviced to relief supply. Note that travel distances with shuttle service from a vehicle depot are included. The more locations without relief transportation are, the larger the objective function becomes.

VI. Computational Experiments

There is our campus "Graduate School of Maritime Sciences, Kobe University" in Higashinada area of Kobe city, Japan. Indeed, there are one vehicle depot, one distribution center, 35 evacuation shelters and 36 elder care homes in this area. Then in order to conduct computational experiments, it is assumed that 25 evacuation shelters and 24 elder care homes are randomly selected among the above Kobe data, and the relief commodity has to be redistributed to those locations at that time.

Table IV shows the computational results as total travel distances (objective function), total travel distances with relief transportation, dummy distances for shuttle service without relief transportation, and number of locations without relief supply.

Case studies #1 to #10 show the results in the case that total volume of relief oversupplied is less than total volume of relief lacked. Case studies #11 to #20 show the results in the case that total volume of relief oversupplied is greater than total volume of relief lacked. Case studies #21 to #30 show the results in the case that total volume of relief oversupplied is greater than total volume of relief lacked. And the weights of dummy distances in cases #21 to #30 are heavier than those of dummy distances in cases #11 to #20. As shown in #1 to #10, if total volume of relief oversupplied is less than total volume of relief lacked, some locations are not serviced to relief supply and this approach can find the locations with no relief supply. However, as shown in #11 to #20, even if total volume of relief oversupplied is greater than total volume of relief lacked, and if the weight of travel distances with relief transportation is same as that of dummy distances for shuttle service without relief transportation, this approach find some locations where no relief is supplied. Therefore, the weight of dummy distances without relief supply transportation is set to large value. Then if total volume of relief oversupplied is greater than total volume of relief lacked, all locations are serviced to relief supply, shown in case #21 to #30. In our future works, we investigate more information of a real situation, and it needs to find the type of service priority and to consider how to give it to the locations.

Table IV Computational Results

Case study	Location data #	Balance between total volume of relief oversupplied and lacked	Weights of α and β	Total travel distances (km)	Total travel distance with relief transportation (km)	Dummy distance for shuttle service without relief transportation (km)	Number of locations without relief supply
1	1	Total volume of relief oversupplied < Total volume of relief lacked	$\alpha = 1,\ \beta = 1$	81.86	61.26	20.60	4
2	2			89.47	71.87	17.60	5
3	3			79.11	64.11	15.00	4
4	4			91.92	74.52	17.40	5
5	5			93.46	74.66	18.80	5
6	6			84.94	61.54	23.40	5
7	7			81.83	65.64	16.20	5
8	8			98.09	77.29	20.80	4
9	9			81.36	63.16	18.20	4
10	10			84.69	65.29	19.40	4
11	1	Total volume of relief oversupplied > Total volume of relief lacked	$\alpha = 1,\ \beta = 1$	84.80	84.80	0.00	0
12	2			85.92	85.82	0.00	0
13	3			81.21	81.21	0.00	0
14	4			89.76	89.76	0.00	0
15	5			84.31	80.51	3.80	1
16	6			86.22	86.22	0.00	0
17	7			80.97	80.97	0.00	0
18	8			77.58	77.58	0.00	0
19	9			88.22	88.22	0.00	0
20	10			82.78	76.78	6.00	2
21	1	Total volume of relief oversupplied > Total volume of relief lacked	$\alpha = 1,\ \beta = 10$	84.80	84.80	0.00	0
22	2			80.90	80.90	0.00	0
23	3			84.38	84.38	0.00	0
24	4			88.20	88.20	0.00	0
25	5			73.52	73.52	0.00	0
26	6			83.55	83.55	0.00	0
27	7			89.87	89.57	0.00	0
28	8			83.86	83.86	0.00	0
29	9			74.95	74.95	0.00	0
30	10			80.35	80.35	0.00	0

VII. CONCLUSION

After the disaster occurred around one week, it seems that some shelters have oversupplied relief commodities, others have lacked them. As some survivors cannot stay at shelters for some private reason, they must stay at their home even if the lifeline stops. This study consider to redistribute the oversupply at shelters and relief supply at local distribution center to the shelters and other locations as elderly care home lacked relief commodities. From the computational results, regardless of the balance between total volume of relief oversupplied and total volume of relief lacked, it is clear that our approach can find the locations with or without relief supply. In our future works, it will need to find the types of service priority to locations and also consider the issues in real situation.

References

1. Sheu, J.B., "Challenges of emergency logistics management", Transportation Research Part E, Vol.43, pp.655-659, 2007.
2. Caunhye, A.M., Nie, X., Pokharel, S., "Optimization models in emergency logistics: A literature review", Socio-Economic Planning Sciences, Vol.46, pp.4- 13, 2012.
3. Sheu, J.B., "An emergency logistics distribution approach for quick response to urgent relief demand in disasters", Transportation Research Part- E, Vol.43, pp.687-709, 2007.
4. Opit, P.F., Nakade, K., "Distribution model of disaster relief supplies by considering route availability", Journal of Japan Industrial Management Association, Vol. 66, pp.154-160, 2015.
5. Yi, W., Kumar, A., "Ant colony optimization for disaster relief operations", Transportation Research Part E, Vol.43, pp.660-672, 2007.

CORE CONFERENCES

International Conference on Education, Transportation and Disaster Management 2018

ISBN	978-81-933584-5-0
Website	www.coreconferences.com
Received	08 – January – 2018
Article ID	CoreConferences015

VOL	01
eMail	mail@coreconferences.com
Accepted	12 - February – 2018
eAID	CoreConferences.2018.015

Pedestrian Conflict Risk Model at Unsignalized Locations on a Community Street

Hyunmi Lee[1], Jeong Ah Jang[2]

[1,2]Transportation Research Institute, Ajou University, Suwon, Republic of Korea

Abstract: *Crossing a street at unsignalized location can be dangerous to pedestrians, especially the elderly. This paper evaluate the pedestrian-vehicle collision risk on specific roads to identify that the degree of Pedestrian safety requires pedestrian intervention such as road improvement. First, age was a significant variable in that older people tend to be at greater risk than the non-elder people. There was an insignificant difference between the PSM of approaching vehicles that were traveling at speeds less than 30 km/h and those traveling at speeds in the range of 30-50 km/h. Interestingly, conflicts when the speed of the vehicles exceeded 50 km/h, the risk of conflict risk was higher than it was for vehicles traveling at speeds below 30km/h. The ratio of conflict risk for crossing gradient topography road was about 21.7 times greater than that for the non-gradient topography area. Regarding safety facilities, the 30 km/h speed limit sign influenced the risk situation of conflict. The ratio of conflict risk for a road with the safety facility was about 0.395 times lower than that for an unmarked road.*

I. Introduction

Crossing a street at an unsignalized location can be dangerous to pedestrians, especially elderly people. The safety of pedestrian crossings requires interventions that include improvement of road safety facilities and assessment of the risk of collisions between pedestrians and vehicles. Such interventions are necessary to identify areas in which there is a risk of conflict between pedestrians and vehicles so that improvements can be made to avoid these conflicts. There are insufficient safety measures for non-signal areas of roadways, and there is a lack of research on the analysis of the risk of pedestrian-motor vehicle conflicts, especially in Korea. Models are needed in order to delve into the factors that influence the risk of such conflicts. Therefore, the purpose of this study was to identify situations that involved the risk of conflicts on roads without traffic signals and analyze the factors that affect pedestrians' ability to cross such roads safely. After initially reviewing the previous research, we developed a statistical model that can be used to explain the relationship between the possible risk of pedestrians' possible conflicts with vehicles and the factors that affect that possibility.

A. Literature Review

Researchers have investigated how pedestrians' demographic characteristics influence their crossing behavior. Ref. [1] analyzed the effect of pedestrians' ages on determining when to cross the road via a simulation technique in a virtual environment. Ref. [2] presented the pedestrian speed was influence in pedestrian behavior and analyzed pedestrians' gap acceptance behavior in the mid-block section without regulation. Studies have been conducted to determine the effect of a vehicle's velocity and the effect of the condition of the street on the occurrence crashes between vehicles and pedestrians. Ref. [3] provided an analysis of the relationship between the speed of a vehicle and the severity of the pedestrian injuries and the risk of death. Ref. [4] addressed the effects of environmental features, such as the availability of crossing facilities, the volume of traffic, and roadway geometry, on pedestrians' crossing behavior to determine the relationship between safety facilities on the road and pedestrians' safety in crossing the road. Ref. [5] provided the effect of the construction of traffic facilities on pedestrians' crossing behavior. Ref. [6] indicated that the purpose of constructing a pedestrian crossing was to avoid pedestrians' conflicts with vehicles and allow pedestrians to cross the road safely.

Several studies have been conducted that used various statistical models to estimate the impact of risk factors on the severity of crashes between vehicles and pedestrians at intersections. Ref. [7] used the Probit model to determine the risk factors that affect the severity of crashes at intersections in Singapore. Ref. [8] used a Bayesian hierarchical binomial logistic model to identify the significant factors that affect the severity of crashes at signalized intersections in Singapore. Ref. [9] used a logit model to examine the factors that affected crashes at intersections in Greensboro, North Carolina. Ref. [10] used Multi-level, Mixed effect Poisson models to determine the correlation of locations. Ref. [11] analyzed the risk factors associated with intersection crashes using logistic regression models. Ref. [12] identified the important factors that affect the severity of pedestrians' injuries in collisions with vehicles by using a mixed logit model. Ref. [13] applied a decision model and a motion model to simulate the interaction process between pedestrians and vehicles at uncontrolled, mid-block crosswalks. Although many studies have investigated the causes of and cures for crashes between people and vehicles at intersections, research related to determining the factors that contribute to crashes between pedestrians and vehicles on local streets without traffic signals is relatively rare. In this study, logistic regression and the Pedestrian Safety Margin index were used to model the significant factors that affect the risk of conflicts between vehicles and pedestrians at crosswalks with no traffic signals. Logistic regression is a reliable statistical approach for estimating the relationship between the response and explanatory variables in the traffic conflict field, as in [14][15]. The potential risk factors of crashes contain pedestrians' characteristics, the speed of vehicles, the features of the roads, and the features of any associated facilities in an actual situation. A study of the dangerous factors that affect the severity of pedestrian-vehicle conflicts in South Korea will lead to a better understanding of traffic safety issues.

II. Methods

B. Pedestrian Safety Margin

Pedestrian Safety Margin (PSM) has been defined in different ways in earlier papers [1] [16], and, in this research, we used the concept of the difference between the time at which a pedestrian crosses the street at a specific conflict point and the time at which the next vehicle arrived at that point [17]. PSM, which quantifies the degree of conflict between a vehicle and a pedestrian, was defined as shown in Fig.1. PSM is closely related to personal attributes, such as age or gender, the size of the group of pedestrians who are crossing the street, whether or not the pedestrians are vulnerable [18], how decisions are made about whether to cross the street or wait [19], and the average time delay until the next crossing opportunity.

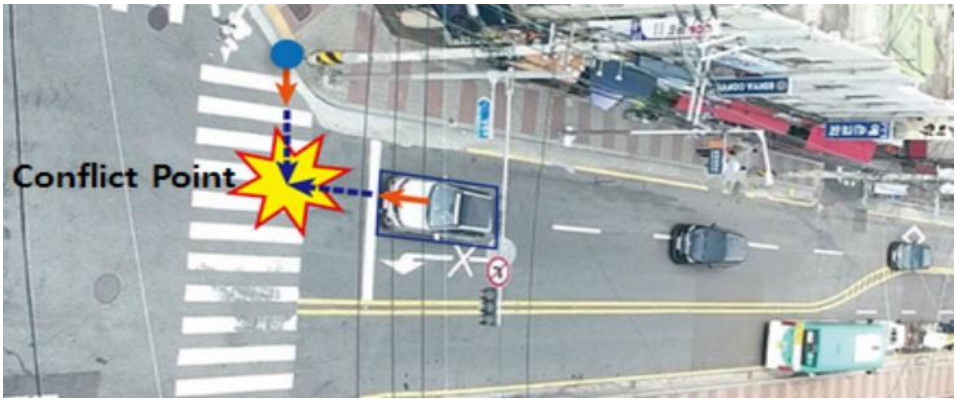

Figure 1. Concept of pedestrian safety margin

In this research, PSM is used as a measure to determine whether or not the risk of conflict exists. Normally, when providing warning of danger, the distance required to stop based on the speed of the vehicle is a crucial factor. The minimum time required for the driver to stop is based on the distance between the car and the pedestrian, the reaction time of the driver after perceiving the possibility of a collision, and the distance required to stop the vehicle with maximum braking. In this case, the speed at which the vehicle is traveling, the driver's perceived response time, and the friction coefficient of the roadway are important variables. In general, the driver's perceived response time is calculated by combining the risk factor judgment time of 1.5 seconds and 1 second required to activate braking. Therefore, in this study, we also analyzed the thresholds for more dangerous situations in which the PSM was less than 2.5 seconds.

C. Data Collection

Cross-sectional data were collected from different six locations at two sites, one in Suwon and one in Jeungpyeong, Republic of Korea. Both of the sites that were selected were local community streets that were identified as silver zones or school zones and had reported frequent traffic accidents. All collection points shown in Fig.2 are two-lane roads with traffic in both directions.

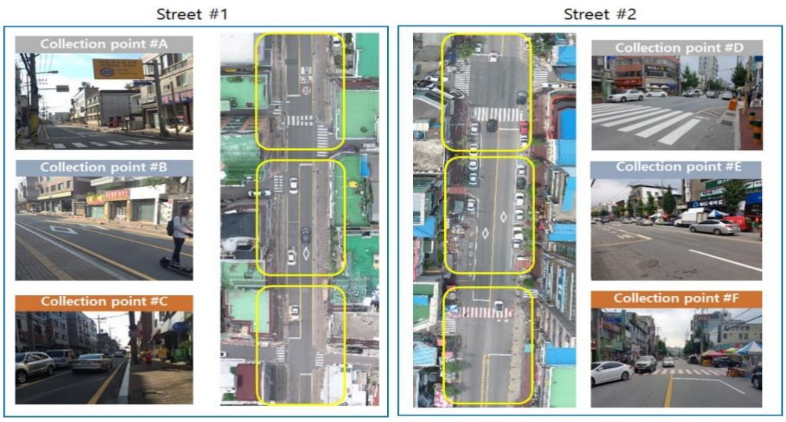

Figure 2. Survey location

The data were comprised of demographic characteristics, vehicle information, and video-recorded street information. The data required for modeling were extracted from these three sources of data, and they were used to calculate PSM, the speeds of the vehicles, the speeds at which pedestrians crossed the roadway. Based on the research method in reference [2], demographic characteristics, including age and gender, were assessed visually at research location. We made sure that the pedestrians were unaware that we were collecting data so that their behaviors would not be affected. We defined and collected indicators to assess the risk of pedestrian-vehicle conflicts, as in Table I, and the feature of the data collection point is revealed in Table II.

Table I Descriptive of the variable

Variables	Type	Unit or Code
Age	Discrete	0: Non-Elders, 1: Elders
Gender	Discrete	0: Women, 1: Men
Pedestrian platoon	Discrete	0: Single, 1: more than one
Jaywalking	Discrete	0: No, 1: Yes
Danger status	Discrete	0: No, 1: Yes
Pedestrian speed	Continuous	m/s
Vehicle speed	Continuous	Km/h
Pedestrian Safety Margin(PSM)	Continuous	Time in sec

Table II Survey area feature

		Feature of data collection point		Vehicle-related		Number of jaywalking	
Collection point		Facility	Topography	Average traffic per hour	Vehicle speed(km/h)	Elderly(%)	Non-Elderly(%)
Street #1	A	30 km/h speed limit sign +Unsignalized marked crosswalk	Flat	537	28.6±10.2	117(99.2)	185(91.0)
	B	No facility	Flat	639	39.9±12.2	171(100)	134(100)
	C	No facility	Gradient	611	40.1±20.8	66(100)	5(100)
Street #2	D	Unsignalized marked crosswalk	Flat	626	23.8±8.4	75(54.3)	41(33.9)
	E	No facility	Flat	567	30.1±9.8	34(100)	8(100)
	F	Unsignalized marked crosswalk	Flat	563	28.9±14.2	56(56.6)	2(28.6)
Summary				590	32.1±13.9	519(82.9)	375(78.5)

D. Logistic Regression Analysis

Logistic regression analysis can be used to illustrate the relationship between the binary response variable and the related factors, and this method was used to estimate the significance of the risk factors that influence traffic accidents. In this study, the response variable was defined if PSM is less than 2.5 sec considered as conflict risk status(Y=1) and if PSM over than 2.5 sec as non-danger status (Y=0). The probability of conflict risk is based on a linear combination function, as shown by equation (1).

$$logit(P) = ln\left(\frac{P}{1-P}\right) = \beta_0 + \beta_1 x_1 + \cdots + \beta_i x_i \quad (1)$$

where P is the probability of conflict risk, x is the explanatory variable, and beta is the coefficient of variables. The odds ratio (OR) illustrates the comparison of the risk status among different levels. The likelihood of the conflict risk status is defined as the probability of a conflict risk state divided by the probability of a non-danger conflict status.

III. Results

E. Descriptive Data

There were 1,104 conflict risk cases that were available for analysis, 17.7% of the total number of crossings occurred; 626 (56.7%) were elderly people, and 478 (46.3%) were non-elderly people. Table III shows the basic statistical information that was collected. The elderly people crossing speed was about 12.3% smaller than the non-elderly. PSM was calculated based on the analysis of the data of 1,104 pedestrian-vehicle conflicts. The results showed that there was a difference between the PSM of the elderly pedestrians and the non-elderly people. PSM is related to the speed of the vehicle, and the effects of the factors that could contribute to the risk of a collision were shown by the odds ratio against the reference level.

Table III Descriptive Statistics

		Number of conflict events			Pedestrian Safety Margin (sec)		Pedestrian crossing speed(m/s)	
Collection point		Total(%)	Elderly(%)	Non-Elderly(%)	Elderly(%)	Non-Elderly(%)	Elderly (Mean±StD)	Non-Elderly (Mean±StD)
Street #1	A	321(29.1)	118(36.8)	203(63.2)	3.93	4.39	1.44±0.41	1.61±0.39
	B	305(27.6)	171(56.1)	134(43.9)	3.63	3.96	1.48±0.44	1.52±0.46
	C	71(27.4)	66(93.0)	5(7.0)	1.54	1.78	1.37±0.45	1.45±0.48
Street #2	D	259(23.5)	138(53.3)	121(46.7)	3.79	3.83	1.27±0.40	1.42±0.37
	E	42(3.8)	34(81.0)	8(19.0)	3.41	3.71	1.48±0.47	1.55±0.48
	F	106(9.6)	99(93.4)	7(6.6)	3.24	3.27	1.05±0.21	1.04±0.24
Summary		1,104(100)	626(56.7)	478(43.3)	3.33	4.04	1.35±0.42	1.53±0.42

F. The Effect of Age and the Velocity of the Vehicle

This model shows the influence of age and the speed of the vehicle speed on the risk of conflict. The speed of the vehicle is a continuous variable that first must be categorized for convenient interpretation of the analysis, and, in this study, it was categorized into three groups, i.e., less than30 km/hr, 30-50 km/hr, and more than 50 km/hr. The descriptive statistics of the model are illustrated in Table IV, and the model shows that two variables, i.e., age and vehicle speed, are significantly influenced in the pedestrian safe road crossing. The probability of unsafe crossing increase when the elderly cross the road than the non-elderly does. The ratio of conflict risk for elderly people crossing is about 3.1 times higher than for non-elderly people. In terms of vehicle speed, the vehicle with less than 30km/h speed was used as reference, the ratio of conflict risk for vehicle with over than 50km/h speed is about 2.9 times higher than vehicle approaching with 30km/h, the difference between of vehicle speed 30~50km/h and less than 30km/h was found as insignificant in this model though.

Table IV Estimated coefficients

		B	S.E	t(p)	p-value	Exp(B)	95% Confidence Interval
Elderly		1.132	0.198	32.565***	0.000	3.101	2.102-4.573
Vehicle speed	30 km <= Speed < 50 km	-0.020	0.181	0.012	0.912	0.980	0.687-1.398
	50 km <= Speed	1.078	0.295	13.387***	0.000	2.919	1.650-5.237
Intercept		-2.519	0.188	178.639***	0.000	0.081	

Probability (Unsafe crossing) = -2.519 + 1.132(Elderly) + 1.078(Vehicle speed >= 50 km/h) (2)

The risk associated with elderly people crossing the road is higher than that of those less than age 55 as in Ref [20], and age had a positive correlation with PSM. In case of a collision with a pedestrian, the speed of the vehicle is one of the most important parameters that affect the result of the accident, and reference [3] identified the speed of the vehicle as the most influential factor. The velocity of an approaching vehicle is the important factor that affects the risk of injuries to pedestrians in a collision, so we must consider safety measures, such as marked crosswalks when there is no traffic signal or speed limit signs to determine whether these measures can cause drivers to decrease the speed of their vehicles.

G. The Effect of Age, Road Facility, and Geometrical Features

The model aims to determine the effect of age, road facility, and geometrical features on the risk of conflict. Road facility variables are categorized into three groups, i.e., 1) non-facility zone, 2) unsignalized crosswalk zone, and 3) unsignalized crosswalk zone with a vehicle speed limit sign. The geometry feature is categorized into two groups regarding whether gradient topography or not. The descriptive statistics of the model are illustrated in Table V, and the model shows that two variables, i.e., age and gradient topography, have a significant positive influence on the probability of conflict risk with a vehicle.

Table V Estimated coefficients

		B	S.E	t(p)	p-value	Exp(B)	95% Confidence Interval
Elderly		0.657	0.216	9.256***	0.002	1.930	1.264 - 2.947
Gradient topography		3.076	0.346	78.943***	0.000	21.682	10.999 - 42.741
Safety facility	Unsignalized crosswalk	-0.241	0.221	1.187	0.276	0.786	0.509 - 1.212
	30 km/h speed limit sign + Unsignalized crosswalk	-0.928	0.290	10.235***	0.001	0.395	0.224 - 0.698
Intercept		-2.183	0.215	103.389***	0.000	0.113	

Probability (unsafe crossing) = -2.183 + 0.657(Elderly) + 3.076(Gradient topography) - 0.928(Speed limit sign) (3)

Compared to the non-elderly people, the probability of unsafe crossing is greater when elderly people cross the road. The ratio of conflict risk for elderly people crossing the road is about 1.93 times higher than the risk for non-elderly people, and the ratio of conflict risk of crossing at gradient topography road is about 21.7 times than non-gradient topography area. In terms of safety facility varible, no facility zone was used as reference. The vehicle speed limit sign showing 30 km/hr had an influence on the pedestrians being able to cross the road safely, and the ratio of conflict risk for a road with a speed limit sign at unsignalized crosswalk was about 0.395 times lower than no facility at an unmarked road. However, the effect of an unsignalized crosswalk was found to be insignificant in this model, so it can be concluded that a marked road without a signal does not have a positive effect on safe crossings.

IV. Conclusions

The aim of the present research was to identify the effect of age, vehicle speed, and road environmental factors on the risk of pedestrians' colliding with vehicles on the safety improvement of unsignalized roads by measuring the risk of conflict between pedestrians and vehicles. We acquired data using video equipment in order to extract the pedestrians' characteristics, and we extracted the secondary data to acquire the speed of an approaching car and the PSM between the pedestrian and the vehicle. Critical thresholds were classified for cases in which the PSM was less than 2.5 seconds. A total of 1,104 data with PSM were collected, and a logistic regression model was used to demonstrate the risk factors that affect the risk of conflict with a vehicle when pedestrians cross a local street that does not have any traffic signals. First, age was a significant variable in that older people tend to be at greater risk than the non-elder people, and this result was similar to that in [21]. There was an insignificant difference between the PSM of approaching vehicles that were traveling at speeds less than 30 km/h and those traveling at speeds in the range of 30-50 km/h. Interestingly, conflicts when the speed of the vehicles exceeded 50 km/h, the risk of conflict risk was higher than it was for vehicles traveling at speeds below 30km/h. The ratio of conflict risk for crossing gradient topography road was about 21.7 times greater than that for the non-gradient topography area. Regarding safety facilities, the 30 km/h speed limit sign influenced the risk situation of conflict. The ratio of conflict risk for a road with the safety facility was about 0.395 times lower than that for an unmarked road. However, the effect of a marked crosswalk without a traffic signal was found to be insignificant, so the result showed that a marked road without a signal has no effect on safe crossings.

References

1. R. Lobjois and V. Cavallo, "Age-related differences in street-crossing decisions: The effects of vehicle speed and time constraints on gap selection in an estimation task," Accident Analysis & Prevention, vol.36(5), pp.934-943, September 2007.
2. K. B. Raghuram and V. Perumal, "Pedestrians' gap acceptance behavior at mid-block location," International Journal of Engineering and Technology, vol.4(2), pp. 158, April 2012.

3. S. Oikawa, Y. Matsui, T. Doi, and T. Sakurai, "Relation between vehicle travel velocity and pedestrian injury risk in different age groups for the design of a pedestrian detection system," Safety science, vol.82, pp.361-367, September 2016.
4. K. B. Raghuram, and P. Vedagiri. "Modelling pedestrian road crossing behaviour under mixed traffic condition," European transport vol.55(3), pp. 1-17, 2013.
5. U. Gupta, G. Tiwari, N. Chatterjee and J. Fazio, "Case study of pedestrian risk behavior and survival analysis," Proceedings of the Eastern Asia Society for Transportation Studies, Eastern Asia Society for Transportation Studies, vol.7, 2009. [The 8th International Conference of Eastern Asia Society for Transportation Studies, 2009].
6. P. Onelcin and Y. Alver, "Illegal crossing behavior of pedestrians at signalized intersections: factors affecting the gap acceptance," Transportation research part F: traffic psychology and behavior, vol.31, pp.124-132, May 2015.
7. R. Tay and S. M. Rifaat, "Factors contributing to the severity of intersection crashes," Journal of Advanced Transportation, vol.41(3), pp.245-265, September 2007.
8. H. Huang, H. C. Chin and Md. M. Haque, "Severity of driver injury and vehicle damage in traffic crashes at intersections: a Bayesian hierarchical analysis," Accident Analysis & Prevention, vol.40(1), pp.45-54, January 2008.
9. K. Obeng, "Injury severity, vehicle safety features, and intersection crashes," Traffic injury prevention vol.9(3), pp.268-276, November 2007.
10. D. A. Quistberg, E. J. Howard, B. E. Ebel, A. V. Moudon, B. E. Saelens and P. M. Hurvitz, "Multilevel models for evaluating the risk of pedestrian–motor vehicle collisions at intersections and mid-blocks," Accident Analysis & Prevention, vol.84, pp.99-111, November 2015.
11. H. Chen, L. Cao and D. B. Logan, "Analysis of risk factors affecting the severity of intersection crashes by logistic regression," Traffic injury prevention, vol.13(3), pp.300-307, February 2012.
12. K. Haleem, P. Alluri and A. Gan, "Analyzing pedestrian crash injury severity at signalized and non-signalized locations," Accident Analysis & Prevention, vil.81, pp.14-23, August 2015.
13. P. Chen, C. Wu and S. Zhu, "Interaction between vehicles and pedestrians at uncontrolled mid-block crosswalks," Safety science. vol.82, pp. 68-76, 2016.
14. R. Harb, E. Radwan, X. Yan, A. Pande, M. Abdel-Aty, "Freeway work-zone crash analysis and risk identification using multiple and conditional logistic regression," Journal of Transportation Engineering, vol. 134(5), pp.203-214, 2008.
15. A. S. Al-Ghamdi, "Using logistic regression to estimate the influence of accident factors on accident severity," Accident Analysis & Prevention, vol.34(6), pp. 729-741, 2002.
16. Hydén, C., and L. Linderholm, "The Swedish traffic-conflicts technique," International Calibration Study of Traffic Conflict Techniques. Springer, Berlin, Heidelberg, 1984, pp.133-139.
17. X. Chu and M. R. Baltes, "Pedestrian mid-block crossing difficulty," National Center for Transit Research, Center for Urban Transportation Research, University of South Florida, 2001.
18. C. M. Dipietro and L. E. King, "Pedestrian gap-acceptance," Highway Research Record, vol.308, 1970.
19. R. R. Oudejans, C. F. Michaels, B. V. Dort and E. J. P. Frissens "To cross or not to cross: The effect of locomotion on street-crossing behavior," Ecological psychology, vol.8(3), pp. 259-267, 1996.
20. J. A. Oxley, E. Ihsen, B. N. Filder, J. L. Charlton and RO. H. Day, "Crossing roads safely: an experimental study of age differences in gap selection by pedestrians," Accident Analysis & Prevention, vol.37(5), pp.962-971, 2005.
21. H. Zhao, G. Yang, F. Zhu, X Jin, P. Begeman and Z. Yin et al., "An investigation on the head injuries of adult pedestrians by passenger cars in China," Traffic Inj. Prev. 14, pp.712–717, 2013.

International Conference on Architecture and Civil Engineering 2018

ISBN	978-81-933584-5-0		**VOL**	01
Website	www.coreconferences.com		**eMail**	mail@coreconferences.com
Received	08 – January – 2018		**Accepted**	12 - February – 2018
Article ID	CoreConferences017		**eAID**	CoreConferences.2018.017

Suggestion of Management Method of Ready-Mixed Concrete (RMC) Pouring Centred on Construction Site

Yije Kim[1]

Abstract: *In construction sites, ready-mixed concrete (RMC) is one of the most important materials that should be unloaded and placed on the site within the standard time (60 ~ 90 minutes) immediately after shipment from RMC plants due to the characteristics of the material. In addition, longer waiting time and pouring time during concrete pouring process affects the quality of RMC significantly. Therefore, the time-based delivery management for fluent supply and demands is the most important issue in RMC placement plan. For this reason, optimization research has been carried out on the RMC vehicle tracking and RMC delivery management algorithms. However, they were more of RMC companies centered truck dispatching and pouring management, and there were few studies on construction site centered RMC installation planning and management. Moreover, the information from RMC truck invoices and the time information of RCM truck, such as plant departure time, on-site arrival time, and turnover time, are limitedly considered in RMC placement planning and quality control. Therefore, the purpose of this study is to derive the necessary parameters for field-oriented RMC management process using information from the invoice and RMC management process used at the construction site. Especially, the necessity of the management of pouring time using the pouring location, pouring volume, and RMC material property retrieved from planning and ordering stage is suggested and proved through on-site verification. Through this, it is anticipated that it will be possible to secure the RMC quality by enabling RMC pouring planning centered on the construction site.*

International Conference on Architecture and Civil Engineering 2018

ISBN	978-81-933584-5-0		**VOL**	01
Website	www.coreconferences.com		**eMail**	mail@coreconferences.com
Received	20 – January – 2018		**Accepted**	05 - February – 2018
Article ID	CoreConferences018		**eAID**	CoreConferences.2018.018

Research on the Development Level Evaluation of Regional Construction Industrialization: A Case Study in Jiangsu, China

Ping Liu[1]
[1]Department of Construction and Real Estate, Southeast University, Nanjing 210096, China

Abstract: *In recent years, there have been concerns raised about construction industrialization in China, which have initiated a wave of policy change in both governmental and industrial organizations in order to change the mode of conventional construction. However, the current development level of regional construction industrialization (RCI) in China has not been well-characterized. This study screened preliminary index systems in five dimensions: technical, economic, sustainable, enterprise development and development environment. Based on the data gathered from the questionnaire surveys and subsequently analyzed, twenty-two critical evaluation indicators were identified. Analytic Hierarchy Process (AHP) was then employed to determine the weighting of each indicator. The evaluation method of the development level was formulated on the basis of the evaluation criteria. Jiangsu Province was used as an example in this study, with the development level of this province being comprehensively examined using a combination of the index system and evaluation method. The results show that Jiangsu has a relatively high RCI development level. The data from analysis scores of five dimensions and twenty-two indicators show that the index system is feasible, with evaluation results being consistent with actual practice. These findings provide a good practical reference for making decisions about how best to guide the development of RCI.*